MECHANICS OF SOIL EROSION FROM OVERLAND FLOW GENERATED BY SIMULATED RAINFALL

By

Mustafa Kilinc and Everett V. Richardson

September 1973

HYDROLOGY PAPERS
COLORADO STATE UNIVERSITY
Fort Collins, Colorado

63

MECHANICS OF SOIL EROSION FROM OVERLAND FLOW GENERATED BY SIMULATED RAINFALL

By

Mustafa Kilinc*

and

Everett V. Richardson**

HYDROLOGY PAPERS
COLORADO STATE UNIVERSITY
FORT COLLINS, COLORADO

September 1973 No. 63

*Post-Doctoral Research Associate, Department of Civil Engineering, Colorado State University, Fort Collins, Colorado.
**Professor of Civil Engineering, Colorado State University, Fort Collins, Colorado.

TABLE OF CONTENTS

ABSTRACT

MECHANICS OF SOIL EROSION FROM OVERLAND FLOW
GENERATED BY SIMULATED RAINFALL

The mechanics of soil erosion from overland flow generated by simulated rainfall are studied experimentally and analytically. The experiments were conducted in a 4' deep, 5' wide and 16' long flume at the Colorado State University Engineering Research Center. Twenty-four runs were made over bare (without vegetation) sandy soil, using six different slopes (5.7 to 40 percent) and four different rainfall intensities (1.25 to 4.60 in. per hour).

Flow under rainfall conditions cannot be strictly called laminar, but neither is it turbulent. The Reynolds number $(q_o X/\nu)$ range (0 to 130) was small in these experiments. The flow was influenced by viscosity, and perturbations were damped. However, flow subjected to a continuous series of perturbations, such as raindrop impact appears turbulent and may be called agitated laminar flow. Froude numbers ranged from 0.5 to 5.4. The majority of the flows were supercritical.

Momentum and continuity equations for steady, spatially varied overland flow under rainfall were derived, and boundary shear stress, τ_o , was calculated from the momentum equation with a numerical approximation. The stream power was then related to sediment yield as a transport model. A longitudinal mean local velocity equation for steady spatially varied overland flow in terms of friction slope, rainfall excess, length of run, viscosity, and gravitational acceleration was also derived and tested. Predicted velocities with this equation were comparable to the velocities measured in the experimental runs. Dimensional analysis was performed on all variables, and the data were analyzed by computer, using a nonlinear multiple regression method. Prediction equations were developed from these methods of analysis, and models were tested. It was concluded that sediment transport models from dimensional analysis, data analysis, and analytical approaches are similar. Velocity, slope, and rainfall intensities were found to be the most important variables affecting soil erosion. In sediment-transport prediction equations, the slope and Reynolds number proved to be dominant parameters.

Sediment yield from overland flow for laboratory conditions can be predicted by the equations developed in this study. For field conditions, the equations can be used as first approximations of soil loss due to overland flow. The numerical constant of the prediction equations would need to be modified for different soil conditions.

ACKNOWLEDGMENTS

The material in this paper is based on the Ph.D. dissertation submitted by M. Kilinc to Colorado State University in partial fulfillment of the requirements for the degree of Doctor of Philosophy. The research leading to the dissertation was financially sponsored by the Colorado State University Experiment Station and the Government of Turkey. This financial support is gratefully acknowledged by both writers. The research leading to this paper has been conducted within the Civil Engineering Department, Engineering Research Center, Colorado State Univesity.

INTRODUCTION

Paramount among man's ecological concerns are the conservation, development, and use of soil and water resources, including the control of soil erosion. Loss of surface soil through erosion means decreased soil fertility as well as reduced storage in reservoirs and reduced capacity of rivers to carry flood flows because of sedimentation. This study deals with soil erosion - the removal or detachment and transportation of soil particles from their environment by water, more particularly sheet erosion of the soil by overland flow. Sheet erosion results from two processes, detatchment and transport, and from two agents, rainfall and overland flow (flowing surface water).

The process begins when raindrops hit the earth's surface; they detach soil particles by their impact and transport them by splash. The diameter of the raindrops, their distribution, their velocity, and their total mass or kinetic energy at impact determine the detaching capacity of rainfall. The available detached particles, the rainfall excess, and the slope of overland surface determine its transporting capacity. Unless the soil surface is covered by vegetation, rainfall alone can detach and transport tremendous quantities of soil downslope.

Most eroded particles, however, are moved downslope by overland flow, which occurs when there is no more surface storage capacity and the rainfall intensity exceeds the infiltration rate of the soil. The detaching and transporting capacity of overland flow depends on surface slope, velocity, and depth of flow, that is, the shear stress or tractive force on the soil boundary. Physicochemical properties, especially the cohesiveness of soil particles, determine the degree of detachability of the soil. The cohesiveness and dispersion of soil components are determined by the silt-plus-clay and organic-matter content of the soil. The smaller the silt-plus-clay percentage, the greater the dispersion; the less the cohesion, the greater the erosion. Size distribution, diameter and shape of soil grains, availability of detached particles, and slope of surface all influence transportability.

In this study, "erosion" refers to the removal of soil particles by overland flow resulting from rainfall; because of the noncohesiveness of the sandy soil used, the soil detaching-and-transporting capacity of raindrop impact was ignored. The behavior of sediment transportation by streams has been of interest to engineers for many years. However, apart from a few papers, notably Ellison (1947), Meyer and Monke(1965), and Meyer (1971), little comprehensive work has been done to show the basic mechanics of soil erosion resulting from overland flow generated by rainfall. Yet the mechanics of soil erosion is an important study.

Although research in the field provided equations for conservation technicians, these, were not designed to meet the present need for a mathematical model to simulate soil erosion as a dynamic process. Ellison (1947) analyzed separately each factor and component of erosion by water. Meyer and Wischmeier (1969) simulated the process of soil erosion by a mathematical model using various component subprocesses such as soil detachment by rainfall, transport by rainfall, detachment by runoff, transport by runoff, and their interaction. They evaluated the four subprocesses for successive slope-length increments. They thus simulated soil erosion as a dynamic process and described soil movement at all locations along a slope at any given time. Meyer (1971), referring to this method as a new approach, maintained: "The development of a mathematical model for simulating the process of soil erosion by water promises to afford greater precision in soil-loss evaluations on upland areas."

Although geologists, agronomists, and hydraulic engineers have given attention to problems of erosion and sedimentation, much of their work has little practical application to the sheet erosion problem. For example, geologists have attempted to study sedimentation in relation to a parent material and soil characteristics with a large time scale; agronomists have studied soil properties in relation to erosion, but have made little effort to relate erosion to hydraulics, since most of their research has studied erosion qualitatively. Because they already had a sufficiently complex problem with stream erosion, hydraulic engineers have displayed little interest in soil erosion. The problem requires the comprehensiveness of an interdisciplinary approach; thus, it requires the cooperation of geologists, agronomists, watershed managers, and engineers.

Since the phenomenon of soil erosion is complex, a purely theoretical approach is impractical; a simulated model where factors can be controlled or altered is desired. For that reason, this study used both empirical data and analysis. The experimental results were obtained from an outdoor physical model with given and limited variables.

The research, conducted at Colorado State University's rainfall-runoff facility, used simulated rainfall upon a sandy soil in a plywood flume to investigate land slopes up to 40 percent and rainfall intensities up to 4.6 in. per hour. In this research, the discharge, velocity, depth of flow, and rate of sedimentation were measured for each slope and intensity of rainfall. Analysis of the experimental data led to the formulation of an equation to predict soil loss from a single, short-duration storm, an equation that can be applied in the field. Since the theoretical reasoning of the study is supported by statistical results, the formula appears to be useful.

Up to now no study has been conducted on slopes reaching up to 40 percent; the value of selecting such a steep slope is its usefulness in the study of the upland areas of a watershed. Developing an equation to predict soil loss offers a practical way to calculate expected soil loss and improve soil conservation practices.

OVERLAND FLOW HYDRAULICS

Overland flow is that part of the surface runoff which flows in a thin sheet over the land surface toward stream channels. Hydrologists have long sought a more sophisticated method of predicting overland runoff to determine rainfall- runoff relationships. They are also interested in calculating the water-surface profile of overland flow, especially under the action of rainfall. Because overland flow is unsteady and spatially varied, predicting it by means of a hydraulic procedure is difficult. Flow depths may vary with rate of flow and nature of surface; and flow may be laminar, turbulent, or both. The impact of roll waves and raindrops on the sheet of flowing water also contributes to the unsteadiness of overland flow (Robertson, et al., 1964). The flow is unsteady and nonuniform, the fluid treated as incompressible and viscous. Further assumptions are unidirectional, two-dimensional flow with constant intensity of rainfall and constant infiltration. Two equations can be developed for overland flow, one based on the principle of conservation of mass and the other on the principle of conservation of momentum.

The continuity equation is

$$\frac{\partial h}{\partial t} + \frac{\partial (\bar{u}h)}{\partial x} = q_o \quad \text{or} \quad \frac{\partial h}{\partial t} + \bar{u}\,\frac{\partial h}{\partial x} + h\,\frac{\partial \bar{u}}{\partial x} = q_o, \qquad (1)$$

and the momentum equation is

$$\frac{\partial \bar{u}}{\partial t} + \bar{u}\,\frac{\partial \bar{u}}{\partial x} + g\,\frac{\partial h}{\partial x} = g\,(S_o - S_f) - \frac{q_o}{h}\,(\bar{u} - v), \qquad (2)$$

in which

q_o = inflow rate or rainfall excess (L/t) [1/],
g = the acceleration of gravity (L/t^2),
S_o = the bottom slope (L/L),
S_f = the friction slope (L/L), defined by an appropriate relation such as Darcy-Weisbach, Chézy or Manning's Equation,
$\bar{u}$ = mean local velocity component in x direction (L/t),
h = depth of flow (L),
v = the x component of the velocity of the lateral inflow (L/t), and
x and t = space and time coordinates, respectively.

These two nonlinear partial differential equations for gradually varied unsteady flow were first derived by de St. Venant, the late 19th century French mathematician.

Although there is no standard method of obtaining overland flow, all equations use the same principles. They differ in their coordinate systems, symbols, assumptions, definitions, evaluation of terms, and general form depending on the investigator's area of interest.

The following derivation of the momentum and continuity equations for overland flow under rainfall is made for a control volume of the fixed Cartesian Coordinate System (Fig. 1); the derivation gives results similar to those presented by Chen and Chow (1968). Steady, spatially varied, unidirectional, two-dimensional flow; uniform, constant infiltration and rainfall intensity; and momentum and velocity correction coefficients of unity are assumed. From Newton's Second Law of Motion ($\bar{F} = M\bar{a}$, where $\bar{F}$ is a vector force, $\bar{a}$ is a vector acceleration, - is vector sign, and M is mass) at equilibrium condition, the summation of the forces acting on the control volume in the direction of flow must equal the change in momentum flux within the control volume. All forces are taken in x direction.

Momentum flux at section one is

$$\rho\bar{u}^2 h \quad \text{or} \quad \rho q\bar{u}\ ,$$

in which

ρ = mass density of water (Ft^2/L^4), and
q = unit discharge (L^3/tL).

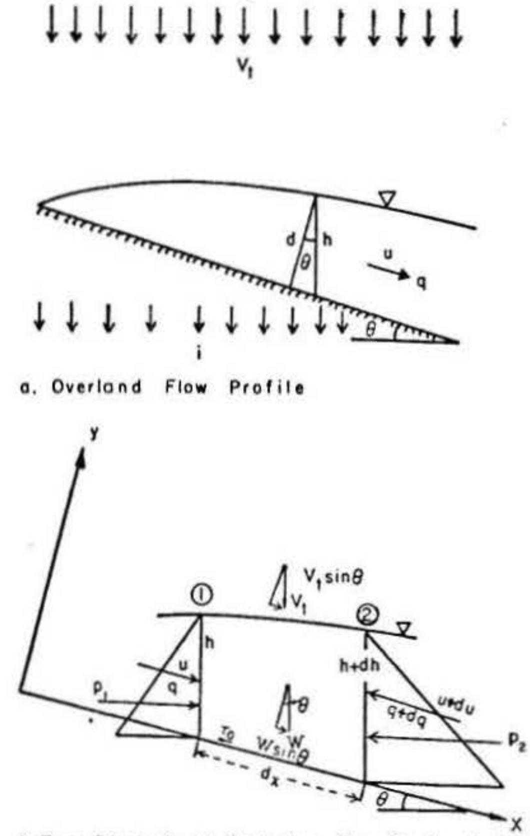

Fig. 1. Overland flow on an inclined surface under rainfall and infiltration.

Momentum flux at section two is

$$\rho(\bar{u} + d\bar{u}^2)\ (h + dh)\ , \quad \text{or} \quad \rho(q + dq)\ (\bar{u} + d\bar{u}),$$

and addition of momentum by rainfall in x direction on control volume is

$$\rho r V_t \sin\theta\ dx\ ,$$

in which

r = rainfall intensity (L/t),
V_t = terminal velocity of raindrop (L/t),
θ = an angle of inclination (degrees), and
dx = the distance increment (L).

The net change of momentum flux on control volume in the direction of x with the dx increment is

$$\rho(q + dq)\ (\bar{u} + d\bar{u}) - \rho q\bar{u} - \rho r V_t \sin\theta\ dx.$$

After simplifying, and ignoring the second order differentials,

$$dM = \rho\bar{u}dq + \rho q d\bar{u} - \rho r V_t \sin\theta\ dx\ , \qquad (3)$$

in which dM represents the net change of momentum flux (F)

The forces acting on the control volume are pressure, gravity, and skew. Although pressure distribution is assumed to be hydrostatic, the over pressure head h* due to raindrop impact, is also included in pressure force evaluation. Over pressure head, h* was first defined by Chen (1962) and later by Grace and Eagleson (1965) as:

$$h^* = \frac{\beta_r \, rV_t \cos^2 \theta}{g} , \tag{4}$$

in which

- β_r = the momentum correction factor for the terminal drops (β_r is assumed unity here), and
- h^* = the over pressure head due to raindrop impact (L).

The pressure force in x direction at section one is

$$\tfrac{1}{2} \rho g \, (h \cos \theta + h^*)^2 .$$

The pressure force at section two is

$$\tfrac{1}{2} \rho g \, [(h + dh) \cos \theta + h^*]^2 .$$

The net pressure on the control volume, after simplifying and ignoring all small terms, is

$$(\rho g \cos^2 \theta \, hdh + \rho gh^* dh).$$

The gravity force is simply a weight component of the control volume in the x direction that can be expressed as

$$\rho gh \sin \theta \, dx$$

The shear force (drag on the bottom) is

$$\tau_o dx ,$$

in which τ_o represents the average boundary shear stress (F/L^2). Equating the change of momentum to the summation of all forces in the x direction (as positive) will yield:

$$\rho \bar{u} dq + \rho q d\bar{u} - \rho r V_t \sin \theta \, dx = \rho gh \sin \theta \, dx$$
$$- \rho g \cos^2 \theta \, hdh - \rho gh^* dh - \tau_o dx . \tag{5}$$

Dividing this equation by dx,

$$\rho \left(\bar{u} \frac{dq}{dx} + q \frac{d\bar{u}}{dx}\right) - \rho r V_t \sin \theta = \rho gh \sin \theta$$
$$- \rho g \left(\cos^2 \theta \, h \frac{dh}{dx} + h^* \frac{dh}{dx}\right) - \tau_o . \tag{6}$$

Rearranging,

$$\rho \frac{d(\bar{u}q)}{dx} - \rho r V_t \sin \theta = \rho gh \sin \theta$$
$$- \rho g \frac{dh}{dx} (h \cos^2 \theta + h^*) - \tau_o . \tag{7}$$

The final form of the momentum equation then becomes

$$\rho \frac{d(\bar{u}^2 h)}{dx} - \rho r V_t \sin \theta = \rho gh \sin \theta$$
$$- \rho g \frac{d}{dx} (\tfrac{1}{2} h^2 \cos^2 \theta + hh^*) - \tau_o . \tag{8}$$

For incompressible steady flow, the continuity equation in the vector integral form is

$$\iint_{c.s.} \bar{V} \cdot d\bar{A} = 0 , \tag{9}$$

in which

- $\bar{V}$ = the vector fluid velocity,
- $d\bar{A}$ = the vector differential area on the control surface, ($|dA| \, \bar{n}$), and
- c.s.= the control surface.

After summing, the inflows through c.s. are equal to outflow through c.s. , which yields

$$\bar{u}h + (r - I) \, dx = (\bar{u} + d\bar{u}) \, (h + dh) , \tag{10}$$

in which I = the infiltration rate (L/t). Simplifying and rearranging this equation reduces it to

$$\bar{u} \frac{dh}{dx} + h \frac{d\bar{u}}{dx} = r - I . \tag{11}$$

Further rearranging, and substituting $q_o = r - I$, makes the continuity equation

$$\frac{d(\bar{u}h)}{dx} = q_o \quad \text{or} \quad \frac{d(q)}{dx} = q_o . \tag{12}$$

The problem of overland flow is not only to derive the governing equations, but also to solve them for velocity and depth with respect to time and space coordinates. A major difficulty in solving the equations is to express the friction function under rainfall impact. (In kinematic-wave approximation, S_o , slope of surface, is assumed equal to S_f , friction slope.) The problem is complex; in order to arrive at an analytical solution, one must simplify. Hence, the characteristics method and the finite-difference method have been widely used. Even the numerical solutions of equations require certain simplifications and assumptions before they can be put into the form of numerical analysis. Woolhiser and Liggett (1967, p. 754) described the problem as follows:

> . . . there is no general analytic solution to this system of equations. Analytic solutions have been restricted to limited regions of the solution domain or to special cases where suitable simplifications could be made. Numerical and graphical solutions have been obtained for some special cases. Unfortunately, graphical techniques are prohibitively slow, and many of the finite difference schemes have exhibited convergence problems.

Existing overland flow equations (shallow water equations) may be used not only for rainfall-runoff relations, routing problems, and flow profile calculations, but also for sediment transport and erosion problems. Velocity and depth profiles can be used to evaluate the overland flow process. The tractive force approach can be related to overland flow characteristics to evaluate the rate of sediment transport over land surface. Tractive force and stream power can also be found by examining length of overland flow in relation to erosion as determined by the overland flow equation and its analysis.

Mathematical models describing velocity profiles use certain assumptions for steady, spatially varied overland flow, with and without raindrop impact. Recent studies by Yoon and Wenzel (1971) and by Kisisel (1971) show that raindrop impact retards the surface velocity of the flow and increases resistance to flow. At present, there is no way to express theoretically this velocity profile and friction factor (friction slope). The following analysis attempts to express velocity, depth, and boundary shear in terms of rainfall excess, distance, and slope.

Vertical Velocity Profile

This model, assuming that there is no raindrop impact and that laminar flow velocity profiles are similar along the overland distance, shows the velocity profile of overland flow in the vertical direction as a second-degree curve of the form presented in Fig. 2a.

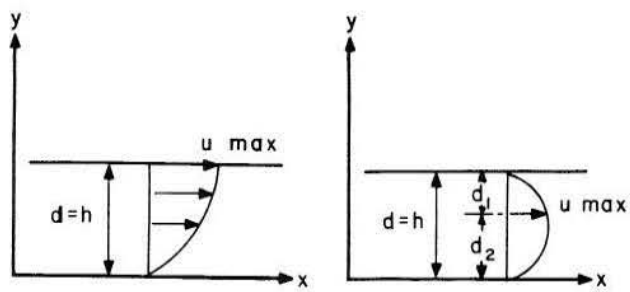

a. Velocity profile without raindrop impact.

b. Velocity profile with raindrop impact.

Fig. 2. Velocity profiles

The velocity profile model is

$$u = \alpha\, y + \beta\, y^2 , \qquad (13)$$

in which α and β = constants.

The constants of Eq. (13) can be determined by employing the boundary and initial conditions (B.C., I.C.), which are

$$u = 0 \quad \text{when} \quad y = 0$$

$$u = u_{max} \quad \text{when} \quad y = h \qquad \text{B.C.}$$

and

$$\frac{du}{dy} = 0 \quad \text{when} \quad y = h \qquad \text{I.C.}$$

Applying these conditions, Eq. (13) leads to these results:

$$0 = 0 + 0$$

$$u_{max} = \alpha h + \beta h^2 \qquad (14)$$

$$\frac{du}{dy} = \alpha + 2\beta y \rightarrow 0 = \alpha + 2\beta h. \qquad (15)$$

Solving for α and β yields

$$\alpha = \frac{2u_{max}}{h} \qquad (16)$$

and

$$\beta = -\frac{u_{max}}{h^2} \qquad (17)$$

Substituting these values into Eq. (13) yields the vertical velocity profile for laminar overland flow, which is

$$u = \frac{2u_{max}}{h}\, y - \frac{u_{max}}{h^2}\, y^2 . \qquad (18)$$

Unit discharge and mean velocity can be determined as follows:

$$q = \bar{u}h = \int_0^h u dy. \qquad (19)$$

Substituting the equation for u, yields

$$q = \int_0^h \left(\frac{2u_{max}}{h}\, y - \frac{u_{max}}{h^2}\, y^2 \right) dy , \qquad (20)$$

and then by differentiating

$$q = \int_0^h \left(\frac{2u_{max}}{2h}\, y^2 - \frac{u_{max}}{3h^2}\, y^3 \right) , \qquad (21)$$

The following is obtained:

$$q = u_{max}\, h - \frac{u_{max}\, h}{3} = u_{max}\, h\, (1 - \tfrac{1}{3}) = \tfrac{2}{3}\, u_{max}\, h \qquad (22)$$

equating gives

$$q = \frac{2}{3}\, u_{max}\, h = \bar{u}\, h \qquad (23)$$

Solving for $\bar{u}$ yields

$$\bar{u} = \frac{2}{3}\, u_{max} \qquad (24)$$

This relation can also be obtained by any calculus using parabolic-curve properties. For further analysis, differentiation of u is required, and is as follows:

$$\frac{du}{dy} = \frac{2u_{max}}{h} - \frac{2u_{max}}{h^2}\, y \qquad (25)$$

when $y = o$

$$\frac{du}{dy} = \frac{2u_{max}}{h} \quad \text{or} \quad \frac{du}{dy} = \frac{3\bar{u}}{h} . \qquad (26)$$

Longitudinal Mean Velocity Profile ($\bar{u} = f(x)$)

Mean velocity profile (Fig. 3) as a function of overland flow distance, X, can be obtained by assuming

$$\tau_o = \gamma\, d\, S_f , \qquad (27)$$

and

$$\gamma \; d \; S_f = \mu \left(\frac{du}{dy}\right)\Big|_{y=0} , \tag{28}$$

in which

γ = the specific weight of water (F/L^3)

μ = the dynamic viscosity of water $(F - t/L^2)$, and

d = the normal depth of flow (L).

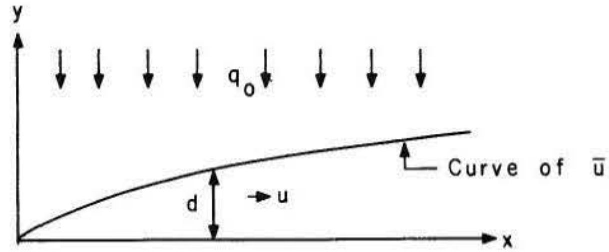

Fig. 3. Overland flow profile.

The right side of the equation is the Newtonian definition of shear stress; the left side of the equation comes from the boundary-shear stress relation for steady uniform flow. When $y = 0$, $\frac{du}{dy} = \frac{3\bar{u}}{h}$; substituting these values of $\frac{du}{dy}$ into Eq. (28) yields

$$\gamma \; d \; S_f = \mu \; \frac{3\bar{u}}{h} . \tag{29}$$

If we assume $h = d$ and substitute $\mu = \rho\nu$ and $\gamma = \rho g$, the equation becomes

$$\rho \; g \; d \; S_f = \rho\nu \; \frac{3\bar{u}}{d} , \tag{30}$$

in which ν = the kinematic viscosity of water (L^2/t). Solving for $\bar{u}$ from the above equation gives

$$\bar{u} = \frac{g \; S_f d^2}{3\nu} . \tag{31}$$

If the continuity equation is applied,

$$q = q_o X = \bar{u} d , \tag{32}$$

where X = the length of surface (distance) (L). Solving for d from the above relation yields

$$d = \frac{q_o X}{\bar{u}} . \tag{33}$$

Substituting this relation into Eq. (31) gives

$$\bar{u} = \frac{g \; S_f}{3\nu} \left(\frac{q_o X}{\bar{u}}\right)^2 . \tag{34}$$

If the terms are rearranged,

$$\bar{u}^3 = \frac{g \; S_f}{3\nu} \; q_o^{\;2} \; X^2 , \tag{35}$$

taking the cube root gives the mean velocity profile of overland flow as a function of distance, friction slope, rainfall excess, and known constants. The final relation is

$$\bar{u} = \left(\frac{g}{3\nu}\right)^{1/3} S_f^{\;1/3} \; q_o^{\;2/3} \; X^{2/3} \tag{36}$$

or

$$\bar{u} = \left(\frac{g}{3\nu}\right)^{1/3} S_f^{\;1/3} \; q^{2/3} . \tag{37}$$

To solve this equation, S_f must be evaluated. For a short segment of overland, and ignoring raindrop impact on shallow flow, S_f may be assumed equal to S_o.

Mean Velocity Profile of Retarded Overland Flow

If similar analysis is conducted for the velocity profile, where the surface velocity is retarded by rainfall drops, assuming $d_1 = h/3$ and $d_2 = dh/3$ in Fig. 2b, the mean velocity profile of overland flow will be (where d_1 is the affected depth of flow and d_2 is the unaffected depth of flow in feet)

$$\bar{u} = \left(\frac{g}{4\nu}\right)^{1/3} S_f^{\;1/3} \; q_o^{\;2/3} \; X^{2/3} . \tag{38}$$

The only difference between Eq. (36) and Eq. (23) is the presence of (4) instead of (3).

Mean Depth of Overland Flow

Using the continuity equation and Eqs. (33) and (36) provides the mean depth for unretarded flow as follows:

$$d = \frac{q_o X}{\left(\frac{g}{3\nu}\right)^{1/3} S_f^{\;1/3} \; q_o^{\;1/3} \; X^{1/3}} . \tag{39}$$

Simplifying yields

$$d = \left(\frac{3\nu}{g}\right)^{1/3} S_f^{\;-(1/3)} \; q_o^{\;1/3} \; X^{1/3} . \tag{40}$$

Friction Slope, S_f , and Friction factor, f

Solving Eq. (31) for S_f in terms of depth and velocity of flow, and using Darcy-Weisbach relation and uniform-flow friction-slope assumption yields

$$S_f = \frac{3\nu\bar{u}}{gd^2} . \tag{41}$$

The friction factor, f , will be:

$$f = \frac{8gd^3 S_f}{q^2} = \frac{3gdS_f}{\bar{u}^2} , \tag{42}$$

where f is the Darcy-Weisbach friction coefficient. Recent studies by Li (1972), Kisisel (1971), and Yoon and Wenzel (1971) show that raindrop impact on flow increases the friction factor and, as a result, the friction slope, S_f , and the boundary shear, τ_o. Li (1972) measured boundary shear, τ_o , under simulated rainfall in the CSU hydraulics laboratory and calculated friction factors, f , for given rainfall intensities and slopes. He obtained the following empirical relation from nonlinear regression analysis:

$$f = \frac{27.162\ r^{.407} + 24}{Re}\ , \tag{43}$$

where Re is the Reynolds number. The above relationship is for a smooth bed; if this equation is to be used for our case, the constant, 24, should be changed. The friction slope under raindrop impact will be different from the friction slope of uniform-flow assumption. The friction slope modified by raindrop impact, S_f^* , was given by Chen and Chow (1968) as follows:

$$S_f^* = \frac{h^*}{h \cos\theta}\ \frac{\partial h}{\partial x} \cos\theta + S_f \tag{44}$$

where S_f^* is the modified friction slope due to raindrop impact (L/L). Using the Darcy-Weisbach formula, friction slope, S_f , in terms of f , $\bar{u}$, and d, is

$$S_f = \frac{f}{8g}\ \frac{\bar{u}^2}{h \cos\theta}\ . \tag{45}$$

The modified friction slope due to raindrop impact in terms of modified friction factor becomes

$$S_f^* = \frac{f^*}{8g}\ \frac{\bar{u}^2}{h \cos\theta}\ , \tag{46}$$

where f^* = modified friction coefficient due to raindrop impact. Equating Eqs. (44) and (46) and solving for f^* will yield

$$f^* = \frac{h^*}{\bar{u}^2}\ \frac{\partial h}{\partial x} \cos\theta + \frac{f}{8g}\ . \tag{47}$$

For laminar uniform flow, the friction factor, f , is given as

$$f = \frac{C}{Re}\ , \tag{48}$$

where C = constant (as a special case, C = 24 for overland flow and Reynolds number is in the form of $Re = \frac{uh \cos\theta}{\nu} = \frac{q}{\nu} = \frac{q_o X}{\nu}$).

The following relationships of friction factors are given by Chen and Chow (1968). For turbulent flow on smooth surfaces, the friction factor is

$$\frac{1}{\sqrt{f}} = 2 \log_{10} Re \sqrt{f} + 0.404\ \ . \tag{49}$$

For turbulent flow on rough surfaces, the friction factor is

$$\frac{1}{\sqrt{f}} = 2 \log_{10} \frac{2h \cos\theta}{k} + 1.74\ , \tag{50}$$

where k is the roughness size of the surface texture. It may be used as $k = d_{84}$, where d_{84} is diameter of sediment of which 84 percent is finer than this diameter. Chen and Chow (1968) commented that the assumption that 500 is the lower critical Reynolds number for flow without rainfall and 200 with rainfall is arbitrary. They expressed the critical Reynolds number, Re , (defined as rainfall excess times length of runs divided by kinematic viscosity), explicitly in terms of relative roughness by equating Eqs. (48) and (50) for f :

$$R_c = C\ (2 \log_{10} \frac{2h \cos\theta}{k} + 1.74)^2\ , \tag{51}$$

where R_c = critical Reynolds number. According to Eq. (51), the Reynolds number of the present study falls in the laminar-flow category.

<u>Average Boundary Shear Stress and Stream Power of Overland Flow</u>

Substituting Eq. (40) into Eq. (27) gives the boundary shear as

$$\tau_o = (3g^2 \rho^3 \nu)^{1/3}\ S_f^{2/3}\ q_o^{1/3}\ X^{1/3}\ . \tag{52}$$

The product of Eqs. (36) and (52) yields the following relation for stream power:

$$P_s = \tau_o\ \bar{u} = \rho g\ S_f\ q_o\ X = \gamma\ S_f\ q\ , \tag{53}$$

where P_s = the stream power of flow (F/L-t).

In sediment transport, evaluation of boundary shear, τ_o , and stream power, P_s , is important. Since analytical solution for τ_o or P_s is impossible because friction slope, S_f , and friction factor f , are unknown, and since sediment transport is closely related to τ_o or P_s , these should be evaluated either experimentally or numerically or both. Calculation of S_f or f can be done only for uniform flow; hence there is no way of finding f and S_f analytically for spatially varied flow, except through simplifications and restrictive assumptions. Moreover, raindrop impact further complicates the problem.

Shear stress, τ_o , can be measured directly in flumes without sediment transport, but it cannot be measured in overland flow with sediment transport. In this study, τ_o will be approximated by solving the momentum equation (8) numerically. Solving for τ_o , Eq. (8) yields:

$$\tau_o = \rho\ g\ h \sin\theta - \rho\ g \frac{d}{dx} \left[\tfrac{1}{2}\ h^2 \cos^2\theta + hh^*\right] - \rho\ \frac{d(\bar{u}^2 h)}{dx} + \rho\ r\ V_t \sin\theta\ . \tag{54}$$

Substituting the value of h^*, $\frac{d(\bar{u}h)}{dx} = q_o$, $q = q_o X$, $H = q_o X/\bar{u}$ and $\frac{dh}{dx} = \frac{d(q_o X/\bar{u})}{dx}$ into Eq. (54) will yield the final form of τ_o as follows:

$$\tau_o = \frac{\gamma q}{\bar{u}} \sin\theta + \rho\ r\ V_t \sin\theta - \frac{\gamma q}{\bar{u}^2} \cos^2\theta - \frac{\rho\ r\ V_t \cos^2\theta}{\bar{u}} + \frac{\gamma X q}{\bar{u}^3}\ \frac{d\bar{u}}{dx} \cos\theta + \frac{\rho\ X\ r\ V_t \cos^2\theta}{\bar{u}^2}\ \frac{d\bar{u}}{dx} - \rho\ \bar{u} q_o - \rho\ q \frac{d\bar{u}}{dx}\ . \tag{55}$$

Equation (55) can be solved by numerical approximation using $\frac{du}{dx}$ obtained from the graph or, for short increment, with the following relationship:

$$\frac{d\bar{u}}{dx} \equiv \frac{\Delta\bar{u}}{\Delta x} \cong \frac{\bar{u}_{i-1} - \bar{u}_i}{x_{i-1} - x_i} \qquad (56)$$

in which i = the increment or step number. To solve Eq. (55), the following calculations were made: experimental values of $\bar{u}$ were plotted versus x, and best polynomial curve fit was done with computer analysis of data. From these curves $\frac{\Delta\bar{u}}{\Delta x}$ was obtained for Δx = 1 foot. Terminal velocity of raindrop, required in Eq. (55), was calculated by using the equation derived by Chow and Harbaugh (1965), namely:

$$V_t = (4\gamma\, d_r^3 \;/\; 3\rho_a\, C_d\, d_1^2)^{\frac{1}{2}}, \qquad (57)$$

where

- d_r = the mean diameter of raindrop (L) (Holland, 1969),
- ρ_a = the mass density of air (ft^2/L^4) (assumed $0.0024\ lb/sec^2/ft^4$),
- C_d = the drag coefficient of air (0.4 for hemisphere),
- d_1 = the diameter of the transformed hemisphere, which is geometrically equal to 1.25 d_r (L).

V_t was found to equal 16.5 feet per second for the present study. The remaining terms needed in Eq. (55) were obtained from experimental data. Substituting the values of the terms into Eq. (55), τ_o was calculated for each run at the end of flow. This data will be presented in a following section. This method allowed the values of τ_o to include effect of raindrop impact on friction factor, f, and friction slope, S_f, without determining them.

SOIL EROSION BY WATER

Ellison (1947), one of the first investigators to make comprehensive studies of soil erosion, defined it as "a process of detachment and transportation of soil materials by erosive agents." Although current analyses are more mathematical, Ellison's definitions and approaches are still valid. He divided soil erosion into four processes--detachment and transport of soil by rainfall and detachment and transport of soil by overland flow--he then studied each independently. Meyer and Monke (1965) and Meyer (1971) applied these categories and studied them furhter.

Although rainfall and runoff erosion may be studied separately, erosion is usually the result of the combined effect of raindrop impact (splash) first and subsequent runoff (overland flow). Water erosion occurs in three stages: sheet, rill, and gully. Sheet erosion was defined by the Soil Conservation Society of America in 1952 as "removal of a fairly uniform layer of soil or material from the land surface by the action of rainfall and runoff." The rill or microchannel stage begins after runoff occurs (when removal of soil is caused by raindrop splash only, it is uniform). During the "rill erosion" stage, the runoff creates more and deeper microchannels. Gullies start to form when concentration and channelization of runoff increase.

The basic factors affecting soil erosion are climate, topography, soil, vegetation, and the human factor. Baver (Soil Physics, 1965) summarizes these factors as follows:

$$\text{Erosion} = \phi\,(C_1, T, V, S, H)$$

in which

- C_1 = the climatic factors,
- T = the topographic factors,
- V = the vegetative factors,
- S = the soil factors, and
- H = the human factor.

FACTORS AFFECTING SOIL EROSION DUE TO WATER
(AFTER BAVER, 1965, p. 431)

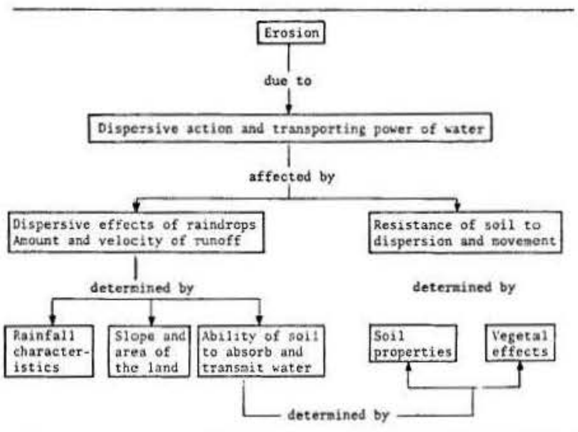

Any of these factors can create a rainfall erosion problem. The two most important influences, slope and rainfall, affect bare soil more than vegetated soil. The following discussion deals with each group of factors in turn.

Of the major climatic factors (rainfall, wind, temperature, snow), rainfall is obviously the most important. Wind erosion, because it is an entirely different field, will not be discussed here, nor will temperature, because its effect is dependent on so many other factors (variability of soil moisture, compactness, and permeability; and change of viscosity, which affects suspension in runoff).

Wischmeier (1959) found that the rainstorm parameter most highly correlated with soil loss from fallow ground was a product term: kinetic energy of the storm times maximum 30-minute rainfall intensity. This product is called "rainfall-erosion index." The rainfall-erosion index explained 72 to 97 percent of the variation in individual-storm erosion from tilled continuous fallow ground on each of six widely scattered soils (Smith and Wischmeier, 1962). Kinetic energy is a function of the combination of drop velocities and rainfall amount. The maximum 30-minute intensity is an indication of the excess rainfall available for runoff.

Erosion is a problem on bare soil wherever the topography is even slightly rolling. Thus, slope is the main topographical feature with which erosion study is concerned. To illustrate: Zingg (1940) found that on slopes of less than 10 percent, erosion approximately doubled as slope increased twofold.

Much work has been done under both field and simulated rainfall conditions to evaluate the effect of magnitude and length of slope on erosion, but little has been done to evaluate that of the curvature of slope. The effect of degree of slope on soil loss was studied under sprinklers by Duley and Hays (1932), Neal (1938), Borst and Woodburn (1940), and Zingg (1940). Borst and Woodburn (1940) found soil loss under artificial rainfall proportional to $S_o^{1.30}$, in which S_o is in percent. Neal (1938) found soil loss proportional to $S_o^{.7}r^{1.2}$, in which r represents intensity of rain in in. per hour.

The major soil factors affecting erosion and runoff are the texture, structure, permeability, compactness, and infiltration capacity of the soil profile. Erodibility, detachability, and transportability of the soil determine the rate and amount of soil erosion. Under the same hydraulic, climatic, topographic, and vegetative conditions, different types of soil have the potential for different erodibility and soil loss. The studies cited in the preceding paragraph showed that a silty clay loam eroded more on the flatter slopes than did a sandy soil, while the same loam eroded less on steeper slopes than did a sandy soil.

Soil scientists have long been interested in obtaining an index of the erodibility of soils by measuring some physical properties of soil. One of the first to attempt to do so was Middleton (1930), who measured the physical properties of soils from various experimental stations and made correlation analyses between these properties and amount of erosion measured in the field. His "dispersion ratio" and "erosion ratio" are the erosion indices which relate erosion to the physical characteristics of soil. The dispersion ratio is obtained by dividing the amount of silt and clay in a sediment sample by the total quantity of silt-plus-clay present in the soil (found by suspending the soil in pure water). The erosion ratio equals the dispersion ratio divided by the colloid-moisture equivalent ratio.[1/] The greater its dispersion and erosion ratio, the more easily a soil can be dispersed and eroded. The colloid-moisture equivalent ratio can also be used to express the relative permeability of the soil. The erosion ratio was obtained by assuming that erosion should increase directly with the dispersion ratio and inversely with the colloid-moisture equivalent ratio. These criteria enable the researcher to classify soils according to degree of erodibility. If the dispersion ratio is greater than ten and the erosion ratio is greater than fifteen, the soil is erodible; if the dispersion ratio is less than ten and the erosion ratio is less than fifteen, the soil is nonerodible.

The greatest protection against soil erosion is plant cover, this affects both the infiltration rate and the susceptibility of soil to erosion. The most effective cover is well-managed, dense sod; however, crop pattern and rotation control erosion without limiting productivity.

Baver (1965) classified the major effects of vegetation on runoff and erosion as follows: interception of rainfall by plants; decrease in both the velocity of runoff and the cutting action of water by the vegetative cover; increasing granulation of soil by roots; increased soil porosity because of vegetative growth; and plant transpiration of water leading to subsequent drying out of the soil. The most important effects of vegetative cover on erosion are the obsorption or dissipation of raindrop impact and the reduction of overland flow velocity and tractive force by increasing the hydraulic roughness and decreasing the effective slope.

Soil erosion control measures are protective and curative. Protective measures prevent erosion; curative measures reduce or regulate erosion after it starts. Erosion control measures may be structural designs, vegetative cover, or legislative or administrative actions. Engineering measures designed to reduce runoff and erosion are usually preventive and include such measures as contour tillage, diversion, waterways, ponds and reservoirs, check dams, and gully control structures. One basic conservation practice used by farmers is that of grass-lined waterways; one of the oldest and best mechanical erosion control practices is terracing, which decreases the length and degree of slope. Other mechanical structures control grading and gullies, store water, prevent floods, store sediment, control water level, provide drainage and irrigation, and protect streambanks. Vegetative practices such as strip cropping, crop rotation, residue management, stubble-mulch farming, grass seeding, and tree planting are curative measures designed to prevent runoff and insure soil stability. Legislative and administrative erosion-control measures such as zoning, rotational grazing, taxing, and fining violators are the most effective means of initiating and financing technical and vegetative measures, and often determine their success.

Both raindrops and overland flow are major erosive agents. Overland flow tends to channelize and make rills and gullies, whereas splash erosion tends to remove soil particles from the surface as a uniform sheet layer. Ellison (1944) considered splash erosion the initial phase of the water erosion process. Soil erosion by splash is a function of drop size, drop velocity, and rainfall intensity, expressed by Ellison (1945) as

$$E = K\, V_t^{4.33}\, d_r^{1.07}\, r^{0.65} , \qquad (58)$$

in which

- E = the relative amount of soil splashed in grams during a 30-minute period,
- K = a constant of soil,
- V_t = velocity of raindrops in feet per second,
- d_r = diameter of raindrops in millimeters, and
- r = in. depth of rainfall per hour.

The study of rainfall momentum and energy in relation to erosion requires knowledge of the determining factors: raindrop mass, size, size distribution, shape, velocity, and direction (Smith and Wischmeier, 1960). Neal and Baver (1937) attempted to measure momentum of rainfall directly by the use of torsion balances but were unsuccessful. Laws and Parsons (1943) first investigated the diameter of drop and distribution by size in natural rain with respect to erosion; they

[1/] The colloid-moisture equivalent ratio is obtained as follows: colloid percentage of soil, i.e., particles finer than .001 mm diameter, divided by moisture equivalent, which was defined by Briggs and McLane (1907) as the percentage of water retained by a sample of soil one centimeter deep which has been saturated with water and drained under a centrifugal force of 1000 times gravity for 30 minutes.

measured drop size by the flour method, using a calibration curve. Median (midpoint of the total volume) drop size, d_{r50}, usually describes the drop-size distribution. Laws and Parson (1943) described the relationship of median drop size to intensity by the equation

$$d_{r50} = 2.23r^{0.182} . \quad (59)$$

It is understood Laws (1941) studied the fall velocity of raindrops using photographic equipment to measure drop velocity. In natural rain, air turbulence can either increase or decrease drop velocity. Neither the magnitude of air turbulence during rainfall nor the effect of drop velocity has been studied. Wind also has an appreciable effect on drop velocity. The kinetic energy of rainfall is important in erosion studies, since erosion is a work process and much of the energy required to accomplish this work is derived from the falling raindrops.

Chow and Harbaugh (1965) designed a rainfall simulator for laboratory study and derived theoretical relationships to obtain drop size and terminal velocity. These equations include rainfall drop size

$$d_r = 2.4 \; (\bar{\sigma} \; d_t)^{1/3} \quad (d_r \text{ is expressed in in.}) , \quad (60)$$

in which

$\bar{\sigma}$ = the surface tension of water in contact with air (F/L) (Average value is $5x10^{-3}$ lb/ft),
d_t = the inside diameter of the producer tube in in. (L).

$$d_r = 61.0 \; (\sigma \; d_t)^{1/3} \quad (d_r \text{ is expressed in millimeters}) . \quad (61)$$

Drop terminal velocity in feet per second was given before in Eq. (57):

$$V_t = (4 \; \gamma \; d_r^{\;3}/3 \; \rho_a C_d \; d_1^{\;2})^{1/2} .$$

Drop velocity at given distance for a known terminal velocity is

$$V_x = V_t [1 - \exp(-2gX/V_t^{\;2})]^{1/2} , \quad (62)$$

where V_x = terminal velocity of drop at X distance (L/t) .

The raindrop impact-splash process shows high detachment capacity but low transport capacity, while sheet and microchannel flow evidence low detachment capacity and high transport capacity.

The transportability of a soil particle in overland flow will depend largely on soil particle size, distribution, density, and shape, and soil compactness. The transporting capacity of surface flow will depend on the velocity of surface flow or velocity head, $u^2/2g$; the depth of flow; the capacity of the flow to suspend soil materials, as this will limit the soil content of the flow; slope; and roughness (irregularities) of the soil surface.

The mechanics of soil erosion by rainfall and overland flow was studied experimentally by Meyer and Monke (1964). They performed a multiple regression analysis on the data. The equation resulting which best fits runoff erosion was

$$E = C_{1sd} \; L_s^{\;1.9} \; S_o^{\;3.5} \; d_r^{\;0.5} , \quad (63)$$

in which C_{1sd} = constant for L_s , S_o and d_r. Meyer and Wischmeier (1969) simulated the process of soil erosion by water in a mathematical soil-erosion model. They assumed that the velocity of flow in small upland rills is approximately proportional to $S_o^{\;1/3} q^{1/3}/n^{2/3}$, the tractive force is proportional to u^2 , and the carrying capacity of flowing water is proportional to u^5 . Any change in S_o , q , and n may greatly affect the erosion rates. The resistance of a soil to the erosive forces of rainfall and runoff depends on such soil properties as particle, size, shape, density, cohesiveness, and aggregate strength plus the soil macrostructure (cloddiness) that affects detachability from the soil mass and transportability by runoff.

Musgrave (1947) suggested the following mathematical relation as a first approximation for sheet erosion:

$$E = K \; S_o^{\;1.35} \; L_s^{\;0.35} \; r_{30}^{\;1.75} , \quad (64)$$

in which

E = erosion loss in tons per acre,
S_o = slope in percent,
L_s = length of slope in feet, and
r_{30} = the maximum annual 30-minute rainfall in in. per hour.

It is usually impossible to observe shallow surface flow (sheet erosion) acting alone to detach thin sheets of soil from the broad surface of a field, because irregularities of the surface, together with the effects of other roughness in the soil's structural properties, cause minor rills (microchannels) to form, and once these rills have formed, they continue deepening to end as gullies. The significant erosion caused by the flowing surface water will occur within these channels.

Sediment Transport Model of Overland Flow

Stream-erosion and sediment-transportation equations may be modified and used in land erosion, because the mechanics of stream channel erosion and land erosion are complementary. From the hydraulic standpoint, understanding the mechanism of stream-channel erosion and land erosion is both a necessity and a great aid in understanding land erosion.

Early sediment-transport equations were developed by such investigators as Du Boys (1879), Schoklitsch (1935), MacDougall (1934), Kalinske (1947), Meyer-Peter and Muller (1948), Einstein (1950), Laursen (1958), Colby (1964), and Bagnold (1966). They generally related the sediment discharge (bedload) to tractive forces, stream power, slope, flow rate, roughness, and particle properties. Any bedload transport equation for alluvial channels using tractive force or stream-power methods may be modified for overland flow and used as a transport equation for land erosion.

Huff and Kruger (1967) adapted Bagnold's equation (1966) for overland flow under rainfall. The transport equation for sheet flow is:

$$q_{si} = e_g \frac{(P_s + P_r - P_c)}{\tan \alpha} \qquad (65)$$

(for the immersed weight of material transported),

or

$$Q_s = \left(\frac{\rho_s}{\rho_s - \rho}\right) q_s \qquad (66)$$

(for dry mass of material in transport),

in which

Q_s = dry mass of material in transport $(M/L^2\text{-}t)$,
$\tan \alpha$ = the coefficient of solid friction,
ρ_s = density of soil particles (Ft^2/L^4) ,
P_r = stream power due to rainfall $(F/L\text{-}t)$,
P_c = critical stream power to initiate the motion, and
e_g = the efficiency of transfer of stress from liquid to solids.

The value of P_s is given by

$$P_s = \rho\, g\, S_o\, q , \qquad (67)$$

and the power input to the flow from rainfall is

$$P_r = K_r\, r\, (1 - e^{-0.481(r)^{1/4}})^2 , \qquad (68)$$

in which

K_r = a constant, and
r = rainfall intensity in mm per hour.

Smerdon and Beasley (1961) plotted critical tractive force as a function of dispersion ratio; in this case the value of critical tractive power can be obtained using the relationships between tractive force and streampower.

Meyer and Wischmeier (1969) used the following mathematical models to evaluate each component of the sub-process of soil erosion.

(1) Soil detachment by rainfall, D_r :

$$D_r = S_{Dr}\, A_i\, r^2 , \qquad (69)$$

(2) Transport by rainfall, T_r :

$$T_r = S_{Tr}\, S_o\, r , \qquad (70)$$

(3) Detachment by runoff, D_F :

$$D_F = S_{DF}\, A_i\, q^{2/3}\, S_o^{2/3} , \qquad (71)$$

(4) Soil transport by runoff, T_F :

$$T_F = S_{TF}\, q^{5/3}\, S_o^{5/3} , \qquad (72)$$

in which A_i = the area of the increment, and

S_{Dr} , S_{Tr} , S_{DF} and S_{TF} = the soil coefficients.

The following models can be used for sediment discharge resulting from overland flow:

$$q_s = K_n\, (\tau_o - \tau_c)^n \qquad (73)$$

and

$$q_s = K_m\, ((\tau_o - \tau_c)\, \bar{u}\,)^m , \qquad (74)$$

in which

q_s = sediment discharge (F/tL) ,
K_n and K_m = constants representing soil and roughness properties, and
n and m = coefficients to be found experimentally.

Equation (73), which uses the tractive-force concept, is one of the earliest models for sediment transport by streamflow.

Equation (74) is similar to Eq. (65), which uses the stream power concept. In Eq. (65), stream powers that result from flow and from rainfall are separated. If τ_o is calculated for overland flow generated by rainfall, rainfall effect will be taken into account. It is not necessary, therefore, to calculate separately stream powers resulting from flow and from rainfall. In the present study, calculated τ_o combines both effects. These two models will be tested with experimental data, and predicted values of sediment discharge will be compared with measured values in a later section.

Langhaar (1967) defined dimensional analysis as a treatment of the general forms of equations that describe natural phenomena. It has been used in all fields of engineering, especially in fluid mechanics and hydraulics. Usually natural phenomena are complex. Therefore, dimensional analysis reduces and groups variables. It can easily identify the significant variables involved in any problem and can determine the relationship between an independent and a dependent variable. Too, dimensional analysis contributes to both analytical and mathematical analysis of a problem relative to a given general mathematical model. In the preface of his book, Langhaar (1967) noted that:

> The application of dimensional analysis to any particular phenomenon is based on the assumption that certain variables, which are named, are the independent variables of the problem, and that all variables, other than these and the dependent variable, are redundant or irrelevant. This initial step--the naming of the variables--often requires a philosophic insight into natural phenomena...The second step in the dimensional analysis of a problem is the formation of a complete set of dimensionless products of variables.

If the dimensionless groups obtained are not meaningful, dividing or multiplying dimensionless groups together may elicit meaningful groups. Dimensionless groups can be related to each other linearly or nonlinearly. The exponents of a dimensionless product represent the solution of a certain set of homogeneous linear algebraic equations.

The purpose of dimensional analysis is to deduce information about a phenomenon from a single premise, which is that the phenomenon can be described by a dimensionally correct equation among certain variables. Reducing the number of variables in a problem greatly amplifies the information obtainable from a few experiments.

Sediment discharge by means of overland flow is a function of the hydraulic properties of flow, the physical properties of soil, and surface characteristics. In the present analysis, sediemnt transport as a result of erosion under simulated rainfall is assumed to be related to the following variables:

$$q_s = (C_s,\ u,\ I,\ r,\ q_o,\ d,\ d_{50},\ X,\ S_o,\ p$$
$$d_b,\ \mu,\ \nu,\ g,\ \rho,\ \rho_s,\ \Delta\gamma,\ \bar{\sigma}) \ , \qquad (75)$$

Elimination of some of the variables is possible since (1) some are closely related to others, (2) some are redundant, and (3) some have relatively less effect than others on sediment discharge. For example, $\mu = \rho\ \nu$; therefore μ is unnecessary. In the equation $\gamma = \rho\ \nu$, and since Eq. (75) has ρ_s and ρ , $\Delta\gamma$ can be eliminated. Bulk density, d_b , is related to porosity in percent by $P = (1 - d_b/dp)\ 100$, in which d_p represents particle density equal to 2.65 gm/cm^3. The advantage of retaining porosity is its dimensionlessness.

Nordin and Richardson (1971) defined sediment concentration as the ratio by weight or volume of the sediment discharge to the total discharge of the water-sediment mixture. Therefore, if q_s, u, and d are used in Eq. (75), C_s can be eliminated because the dimensionless form of sediment discharge will be sediment concentration. That is $q_s = C_s q\gamma$ constant. All the independent variables related to sediment discharge, consequently, will have the same correlation as sediment concentration. After the dependent variables are eliminated, Eq. (75) reduces to:

$$q_s = \emptyset\ (u,\ q_o,\ d,\ d_{50},\ X,\ \nu,\ g,\ \rho,\ \rho_s,\ S_o,\ P). \quad (76)$$

Dimensionless groups of variables depend upon the selection of repeated variables. If these are changed each time, different groupings can be obtained. Selection of these repeated variables will be based on representation of flow, geometry, and sediment characteristics in consideration of the physical phenomenon of sediment transport. In the following analysis, different sets of variables will be selected as repeated variables, and the results of the dimensionless form of equations will be shown.

When ν , ρ and d_{50} are selected as repeating variables, Eq. (76) will be expressed as

$$\frac{q_s d_{50}^3}{\rho\ \nu^3} = \emptyset\left(\frac{ud_{50}}{\nu},\ \frac{q_o d_{50}}{\nu},\ \frac{d}{d_{50}},\ \frac{X}{d_{50}},\ \frac{gd^3{}_{50}}{\nu^2},\ \frac{\rho_s}{\rho},\ S_o,\ P\right) \qquad (77)$$

If this equation is expressed in terms of known, common dimensionless numbers, and if meaningless or less important groups are eliminated, then Eq. (77) reduces to:

$$C_s = \emptyset\left(Re_{d_{50}},\ Re_{q_o},\ \frac{d}{d_{50}},\ S_o,\ P\right)\ , \qquad (78)$$

in which

C_s = a dimensionless form of sediment discharge,

$Re_{d_{50}}$ = the particle Reynolds number,

Re_{q_o} = rainfall-particle Reynolds number, and

d/d_{50} = roughness properties.

If ν , ρ , and d are repeated and some of the parameters are eliminated and rearranged, the following equation is obtained:

$$C_s = \emptyset\left(Re,\ Re_{q_o},\ \text{roughness},\ S_o,\ P\right)\ . \qquad (79)$$

When ν , ρ and X are repeated, a relationship similar to that in the previous equations will be obtained; the Reynolds number, however, will assume a different form:

$$C_s = \emptyset\left(\frac{uX}{\nu},\ \frac{q_o X}{\nu},\ \frac{d}{X},\ \frac{d_{50}}{X},\ \frac{gX^3}{\nu^2},\ \frac{\rho_s}{\rho},\ S_o,\ P\right) \qquad (80)$$

Eliminating unimportant variables and rearranging terms results in

$$C_s = \left(Re_X,\ Re_{q_o},\ \text{roughness},\ S_o,\ P\right)\ , \qquad (81)$$

in which Re_X is the Reynolds number in terms of distance.

Repeating ν , ρ , and u will give the dimensionless relation

$$C_s = \emptyset\left(\frac{q_o}{u},\ \frac{ud}{\nu},\ \frac{ud_{50}}{\nu},\ \frac{uX}{\nu},\ \frac{g\nu}{u^3},\ \frac{\rho_s}{\rho},\ S_o,\ P\right). \quad (82)$$

Rearranging and eliminating insignificant groups from this equation gives

$$C_s = \emptyset\left(Re,\ Re_{d_{50}},\ Re_X,\ \frac{q_o}{u},\ S_o,\ P\right). \qquad (83)$$

Thus, three different forms of the Reynolds number are obtained in Eq. (83).

Finally, if u , d , and ρ are used as repeated variables, Eq. (75) will take the form of the dimensionless relation,

$$\frac{q_s}{\rho u^3} = \emptyset\left(\frac{q_o}{u},\ \frac{d_{50}}{d},\ \frac{X}{d},\ S_o,\ P,\ \frac{ud}{\nu},\ \frac{u}{\sqrt{dg}},\ \frac{\rho_s}{\rho}\right), \qquad (84)$$

or

$$\frac{q_s}{\rho u^3} = \emptyset\ (Re,\ Fr,\ S_o,\ P,\ \text{roughness}) \qquad (85)$$

If $q_s/\rho u^2$ is multiplied by the square of the Froude number, the sediment concentration C_s will result. That is:

$$\frac{q_s}{\rho u^3} \times \frac{u^2}{dg} = \frac{q_s}{\rho gud} = C_s\ . \qquad (86)$$

Thus

$$C_s = \phi\ (Re,\ Fr,\ S_o,\ P,\ S_f) \qquad (87)$$

In Eq. (88), sediment concentration is a function of the Reynolds number, Froude number, slope, porosity, and roughness of surface.

It will be easily seen from the dimensionless relationships of sediment discharge, as in Eqs. (78, 79, 83, and 85), that most of the dimensionless groups and especially the Reynolds number, are repeated in a slightly different form.

Thus, the more variables are simplified and eliminated, the more compact the form of the dimensionless relation of sediment discharge to sediment concentration. The Froude number, Fr , can be eliminated from Eq. (87) if it is relatively constant for the conditions being studied. After groups are eliminated and parameters rearranged, Eq. (87) assumes the form of

$$C_s = \phi\left(Re,\ S_o,\ P,\ \frac{d_{50}}{d}\right) . \qquad (88)$$

Sediment discharge and sediment concentration have the same physical significance, with the Reynolds number, Re , slope, and roughness as the most important parameters affecting them.

The local velocity of overland flow is a function of rainfall, slope, gravity, and surface characteristics. That is:

$$u = \phi\ (q_o,\ d,\ d_{50},\ X,\ S_o,\ \nu,\ g,\ P) . \qquad (89)$$

Designating ν , g , and d as repeated variables results in the following dimensionless relation:

$$\frac{u}{\sqrt{dg}} = \phi\left(\frac{q_o d}{\nu},\ \frac{d_{50}}{d},\ \frac{X}{d},\ S_o,\ P\right) . \qquad (90)$$

If the dimensionless groups are replaced with known common parameters, then

$$Fr = \phi\left(Re,\ S_o,\ P,\ \frac{d_{50}}{d},\ \frac{X}{d}\right) . \qquad (91)$$

The dimensionless form of velocity gives a relation similar to that given for sediment discharge or sediment concentration. The same parameters, such as Reynolds number, slope, and roughness, appeared in Eq. (88) and Eq. (91). If Eq. (91) is rearranged, more meaningful results can be obtained. For example, the first group Froude number, Fr , can be divided by slope, S_o , and the result will be $\frac{u}{\sqrt{dgS_o}}$. This is simply $\frac{u}{\sqrt{\tau_o/\rho}} = \frac{u}{u_*}$, in which u is velocity and u_* is shear velocity. If X/d is eliminated and Eq. (91) rearranged, the relation $u/u_* = \phi\ (Re,\ S_o,\ P,\ D_{50}/d)$ can be found. Squaring the first term gives

$$\frac{u^2}{(\tau_o/\rho)} = \phi\left(Re,\ S_o,\ P,\ \frac{d_{50}}{d}\right) \qquad (92)$$

in which P and d_{50}/d represent porosity and roughness of surface.

Using the $\tau_o = f\ \rho\ u^2/8$ relation in which f is the Darcy-Weisbach resistance coefficient gives

$$f = \frac{8(\tau_o/\rho)}{u^2} ,\ \text{or}\ \frac{8}{f} = \frac{u^2}{(\tau_o/\rho)} . \qquad (93)$$

Substituting 8/f for $u^2/(\tau_o/\rho)$ in Eq. (92) , results in:

$\frac{8}{f} = \phi\ (Re,\ S_o\ ,\ \text{roughness})$; or the general dimensionless form of the friction factor can be written as

$$\frac{1}{f} = \phi\ (Re,\ S_o,\ \text{roughness}) . \qquad (94)$$

Equation (94) is the general form for the reciprocal of f ; the Darcy-Weisbach friction factors, as a function of the Reynolds number; the slope; and the surface roughness characteristics.

EQUIPMENT AND EXPERIMENTAL PROCEDURES

The experiment was conducted at the rainfall-runoff facilities of the one-acre model watershed adjacent to the Engineering Research Center, Foothills Campus, Colorado State University, Fort Collins, Colorado. (See Holland, 1969 for a detailed description of the facilities).

The major controlled variables were intensity of rainfall and slope of soil surface. Infiltration and erodibility of surface were constant. Six bare slopes were tested with four different rainfall intensities (a total of 24 runs). In addition, four runs were made over a vegetated surface* (See Appendix).

Runoff was recorded continuously and sampled for sediment concentration every five to ten minutes during each hour-long run. Sediment concentration figures were obtained in parts per million and averaged for each run. Dye injections helped measure the average surface velocity. Bulk density soil samples were taken from the surface, and depth of flow with respect to overland distance was measured for each run, as were depth, surface area, and volume of rills.

The experiment was run in a plywood flume 4' high x 5' wide x 15' long, with an adjustable slope, filled with soil. The flume had a 4'-wide outlet which discharged into a collection tank. At the top of the flume was a four-wheeled carriage, leveled horizontally, able to move up and down, and equipped with a point-gage capable of reading to the nearest tenth of a foot with vernier. The point-gage was attached to the carriage and could be moved horizontally. Using the carriage and point gage, the elevation of any point on the flume could be determined.[1/]

Commercial sprinklers on 10' risers, placed 10' apart along the sides of the flume, simulated rainfall. The sprinkler head was mounted on top of the riser. A 7' section of 3/4" steel pipe joined the sprinkler

[1/] Measurements taken by the point-gage with the idea of measuring depth of flow at different sections of the land surface during rainfall proved unreliable, partly because of rainfall-impact depressions and partly because of the movable bed.

to the tire-pressure tap. Each nozzle was fitted with a control valve, and a series of valves was connected to one pressure manifold to provide simultaneous operation of a set of sprinklers (Holland, 1969). Figure 4 shows the elements of the sprinkler riser.

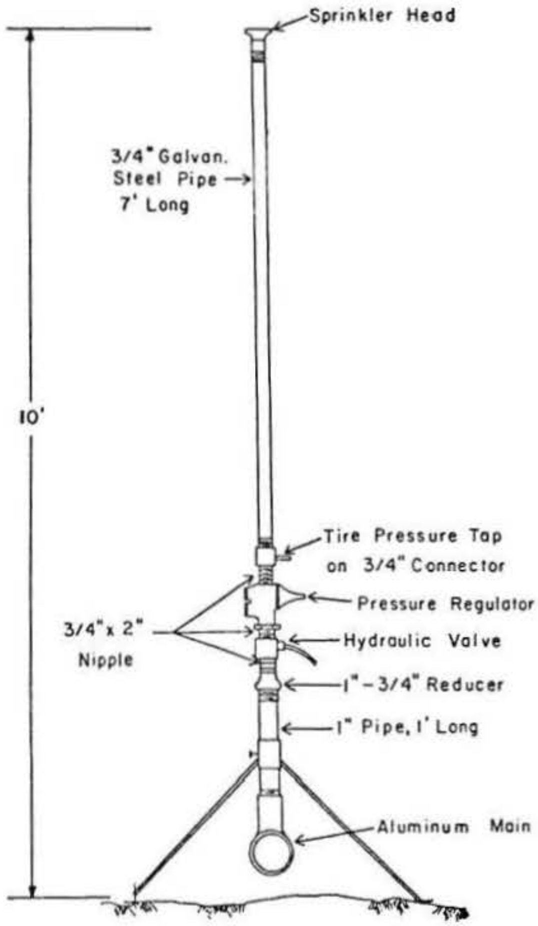

Fig. 4. Schematic of sprinkler riser for grid system (after Holland, 1969).

Four independent control valves were fixed to manipulate the pressure system of the sprinkler riser on the upstream part of the flume so that rainfall production for this experiment could be operated independently of the main control center.

To collect and store the total discharges, a collecting tank 6' in diameter and 3' high, calibrated for depth versus volume of water, was installed at the end of the flume. A floating-type stage recorder was attached to the tank to continuously record water level. It used an eight-hour chart with a mechanical clock drive (scale: 5" per foot; one division every 5 minutes).

The flume was filled with compacted sandy soil (90 percent sand and 10 percent silt-and-clay) which was leveled and smoothed before each run. The soil had a non-uniform size distribution with $d_{50} = .35$ millimeter, and with

$$\sigma = \frac{1}{2}\left(\frac{d_{84}}{d_{50}} + \frac{d_{50}}{d_{16}}\right) = \frac{1}{2}\left(\frac{1.0^{mm}}{.35^{m}} + \frac{.35^{m}}{.10^{m}}\right) = 3.2 \ . \qquad (95)$$

in which

d_{16} = the diameter of the sediment recorded for 16 percent of the samples having a diameter finer than this size,

d_{50} = the median diameter of the sediment recorded for 50 percent of the samples having a diameter finer than this size,

d_{84} = the diameter of the sediment recorded for 84 percent of the samples having a diameter finer than this size, and

σ = the gradation or size distribution index in which one and less represents uniform soil; if gradation is greater than one, soil is non-uniform.

Since porosity and bulk density are indicators of the compactness of soil surface, the following research was performed. Bulk density soil samples were dried in the oven and weighed. The bulk volume of the samples was determined from the sampling cup; then the weight of the sample was divided by the bulk volume to obtain the bulk density. The porosity of the soil samples was found from the bulk density by the equation:

$$\text{Bulk density, } d_b, = \frac{\text{weight of oven-dried soil}}{\text{undisturbed (bulk) volume of soil}},$$

and

$$\text{Porosity (\%)} = \left(1 - \frac{d_b}{d_p}\right) \times 100 \ , \qquad (96)$$

in which

d_b = the bulk density (F/L^3), and

d_p = the particle density (F/L^3).

Slopes of 5.7, 10, 15, 20, 30, and 40 percent were tested with four intensities of rainfall: 1.25, 2.25, 3.65, and 4.60 in. per hour. Slope was measured using an Engineers level and the point-gage on the movable carriage. Slope changes were made by tilting the flume and screeding the soil surface to the desired slope.

Overland-flow velocity was measured by injecting dye into the surface flow. A liquid dye (a combination of Rhodomine WT and food color) was applied to the ground surface at the upper end of the flume. As the dyed water started to flow, one observer watched the dye trace, while another kept a stop watch and note pad. As the dye front passed each successive four-foot downslope distance, the first observer signaled the second observer, who recorded the time. Increments of time provided the average velocity over each four-foot reach of slope. As the dye trace faded, it was reinforced with a new injection. The leading edge of the dye trace was used in timing its movement. These measurements were repeated every 10 to 15 minutes during every one-hour run. All values were averaged to obtain average point velocity at every 4' station along the 16' overland flow for each run. These values were assumed as mean velocities at that point.

Sediment samples were collected in bottles held by hand under the outflow. The total sediment discharge was measured as follows: after being dried, the sediment samples were weighed. The weight of the sediment was divided by the weight of the evaporated water. This ratio was multiplied by one million to obtain sediment concentration in parts per million.

All oven-dried sediment samples were analyzed for size distribution by sieve analysis. Samples of each run were separated into two to five time groups and sieved eight times to separate the sediment sample into nine diameter groups. Sieves used in the sieve analysis had the following diameters: 2000, 1000, 701, 500, 354, 250, 125, and 53 microns. The percentage by weight of each diameter group was calculated. The sieve analysis revealed that much of the sediment was coarse.

Runoff from all sprinklers was recorded continuously by the recorder attached to the collector tank. Runoff passing overland as a result of excess rainfall was discharged toward the collector tank through the outlet and channel. Chart recordings were converted into volume per time (cfs) by using the calibration curves. Records showed that discharge was constant, i.e., discharge increased by distance linearly. To calculate unit discharge at any x distance, the relation

$$q_x = q_o X \qquad (97)$$

was used, in which

- q_x = unit discharge at X distance in cfs/ft of width,
- q_o = rainfall excess in ft/sec, and
- X = the distance from the beginning of flow in ft.

Besides determining soil porosity and bulk density, and temperature of flow for every run, rill depth and length were measured and the number of rills counted. Also, pictures of the soil surface were taken before, during, and after each run.

PRESENTATION AND ANALYSIS OF DATA

Primary sources of data collected for each experiment or ("run"--defined as the experiment conducted with fixed slope and rainfall intensity) were slope, rainfall intensity, sediment concentration samples, tank water contents vs. time, surface flow velocity, rill geometry, and water temperature. From these experimental data, secondary data were calculated: sediment concentration, sediment discharge, water discharge, infiltration, rainfall excess, bulk density, mean local velocity of flow, mean depth of flow, sediment size distribution, friction factor, friction slope, tractive force, critical tractive force, stream power, Reynolds number, Froude number, rill mean depth, rill surface area, and rill volume. The primary and secondary data were reduced and summarized for each run (see tables and figures), and simple plots on Cartesian coordinates were made. Further, statistical analyses of the data were made using the computer; the results are shown, with brief discussion.

DATA REDUCTION AND TABULATION

Sediment Concentration

Sediment samples were collected every five to ten minutes during each run; their concentrations are shown in Table 1. The average concentration for each run is given in Table 2.

Water Discharge and Rainfall Excess

Total discharge was first recorded as the stage of flow versus time, then converted into volume versus time by using the calibration curves prepared before each run. Sediment discharge and water discharge were calculated and are tabulated for each run in Table 2. Water discharge data were constant with respect to time; that is, after a brief initial time the flow and erosion rates were steady, but spatially varied because with uniform constant rainfall and runoff, water discharge must increase with distance. It was assumed that water discharge increased with distance linearly. Thus, $q = q_o X$, and the rainfall excess becomes $q_o = dq/dx = q/X$. Rainfall excesses, q_o, are tabulated for each run in Table 2. The unit discharge at any distance, X, can be calculated by the relation $q_x = q_o X$. Rainfall intensity minus rainfall excess gives the infiltration; the results are summarized in Table 3. Because intensity of rain and rainfall excess were constant, infiltration was constant for each run. As shown in Table 3, water discharge (runoff) was calculated for distances of 3, 6, 12, and 16 feet, as cubic feet per second per foot of width, for given slope and intensity of rainfall.

Sediment Discharge

The data on sediment discharge were converted into several units for each run and tabulated for given slopes and intensities in Table 4. Sediment discharge was expressed in pounds per second per foot of width, pounds per hour, and tons per acre per day for each run, and also in. of surface soil per hour for each run. Sediment discharge and erosion rate may not change linearly with respect to distance because of the nonlinear change of velocity and boundary shear with respect to distance. The sediment-discharge data represent the total sediment removed from the 16-foot-long experiment flume.

Mean Local Velocity of Overland Flow

Velocities of overland flow were measured by dyeing the water. The time of travel between prescribed stations was recorded. This data was used to calculate point velocities for every three-foot station. As an example, let t_1 represent time of travel from zero to three feet and t_2 represent time of travel from three to six feet. Relating distance to time as follows gives

$$\frac{x_2 - x_1}{t_2 - t_1} = \frac{6 - 3}{t_2 - t_1} = \bar{u}_1 \qquad (98)$$

in which $\bar{u}_1$ represents the average velocity between three feet and six feet; this is called the point velocity at a three-foot distance (see the following sketch). Point velocities at 3, 6, 12 and 16 feet were calculated. Because the depth of flow was very shallow

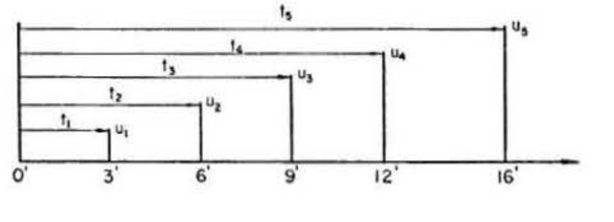

TABLE 1. INSTANTANEOUS SEDIMENT CONCENTRATION, C_i , FOR GIVEN SLOPE AND INTENSITY OF RAIN AT GIVEN TIME AND THE END OF FLOW

Rainfall Intensity	Slope 5.7%		10%		15%		20%		30%		40%	
	Time (minute)	ppm (C_s)	Time	ppm (C_s)	Time	ppm (C_s)	Time	ppm (C_s)	Time	ppm (C_s)	Time	ppm (C_s)
1.25	5	5840	2	11870	5	23293	3	25375	5	33169	5	36210
inch	10	6025	5	19137	10	24063	15	28306	10	38752	15	47405
per	17	6119	10	12088	22	24079	22	29273	15	35268	20	42995
hour	24	5150	22	13517	34	25219	30	28356	20	37288	25	49613
	30	5000	34	14499	48	26888	37	28077	30	38563	30	42328
	40	5210	48	14970	60	23119	45	29136	40	37426	35	42375
	50	5125	60	15300			53	30895	50	40676	40	42764
	60	5018					60	28454	60	48655	50	45494
											60	42159
2.25	3	6000	3	23957	1	50972	2	88651	1	97153	1	134116
inch	12	6220	5	30259	10	51119	5	106800	2	126927	3	167507
per	25	6830	15	32381	20	55523	10	104384	5	135994	5	157669
hour	35	7017	25	33852	30	57600	17	106164	10	202485	10	194965
	48	6623	38	33132	40	55021	25	116938	15	198095	15	206622
	60	6807	48	34253	50	60359	32	118252	20	206266	20	226616
			60	36191	60	66332	40	114127	25	191298	25	239299
							45	100217	30	202177	30	245598
							50	97086	35	18 8253	35	242672
							55	99577	40	186375	40	230562
							60	90607	45	169631	45	223164
									60	168272	60	222230
3.65	2	8150	1	35862	2	64422	2	162472	1	191585	1	301335
inch	5	7757	12	43942	5	97612	5	167874	3	247223	2	309511
per	12	8098	24	43386	7	90232	10	178098	6	244670	5	314449
hour	24	8333	36	43231	15	77000	15	169071	11	208079	8	326792
	36	7949	48	45217	23	77130	20	159010	15	204943	12	334913
	48	7847	60	48158	30	77273	25	149112	19	226705	15	326793
	60	8242			37	80526	30	140550	23	216512	20	311586
					45	80228	40	139246	27	218890	25	317103
					52	79218	50	138016	30	213970	30	307475
					60	75253	60	138217	40	213867	40	305912
									50	213574	50	304118
									60	213214	60	305000
4.60	1	12826	1	53353	1	112783	1	217804	1	243286	1	311831
inch	12	14690	10	50353	3	109328	4	219790	3	290012	2	343321
per	24	14315	20	52883	5	110579	8	211510	5	287342	3	368421
hour	36	14416	30	54444	10	115858	12	236201	7	280649	5	374000
	48	14818	40	53016	15	110726	17	198516	10	264346	8	387975
	60	15000	50	52238	20	109038	22	194961	15	259592	10	348421
			60	53866	25	106299	27	190272	20	245116	15	355395
					30	109590	30	190098	25	240386	20	344537
					35	108422	40	189217	30	238516	25	354565
					40	105567	50	191000	40	238000	30	369807
					45	107670	60	190516	50	238124	40	358716
					50	108000			60	237980	50	354896
					55	107700					60	354218
					60	107712						

TABLE 2. AVERAGED SEDIMENT CONCENTRATION, C_s , WATER DISCHARGE AND SEDIMENT DISCHARGE AND RAINFALL EXCESS FOR GIVEN SLOPE AND INTENSITY OF RAIN AT THE END OF OVERLAND FLOW

Run No.	Slope (%)	Intensity of rain (in/hr)	C_s (ppm)	q (cfs/ft of width)	q_s (lb/sec/ft of width)	q_o (ft/sec)
I	5.7	1.25	5436	.000279	.000096	.0000174375
II	5.7	2.25	6583	.0007171	.00030	.0000448187
III	5.7	3.65	8054	.001274	.00646	.000079625
IV	5.7	4.60	14344	.0016295	.001482	.0001018437
V	10.0	1.25	14483	.000316	.000294	.00001975
VI	10.0	2.25	32004	.000727	.001508	.0000454375
VII	10.0	3.65	43300	.001289	.00372	.0000805625
VIII	10.0	4.60	52279	.0016556	.00588	.000103475
IX	15.0	1.25	24434	.000332	.00548	.00002075
X	15.0	2.25	57418	.0007398	.002974	.0000462375
XI	15.0	3.65	79895	.0013023	.007138	.0000813938
XII	15.0	4.60	109234	.001683	.01288	.0001051875
XIII	20.0	1.25	28493	.000349	.000644	.0000218125
XIV	20.0	2.25	103891	.000741	.005686	.0000463125
XV	20.0	3.65	154167	.001306	.014904	.000081625
XVI	20.0	4.60	202717	.001696	.02666	.0001060
XVII	30.0	1.25	37975	.0003588	.000922	.000022425
XVIII	30.0	2.25	172744	.000745	.01015	.0000465625
XIX	30.0	3.65	217769	.001329	.022648	.0000830625
XX	30.0	4.60	255279	.001700	.03752	.00010625
XXI	40.0	1.25	44149	.0003659	.00134	.0000228687
XXII	40.0	2.25	207585	.000748	.013096	.00004675
XXIII	40.0	3.65	313749	.001335	.03700	.0000834575
XXIV	40.0	4.60	355885	.001702	.06508	.000106375

TABLE 3. INFILTRATION AND WATER DISCHARGE FOR GIVEN SLOPE AND INTENSITIES AT GIVEN DISTANCE

Run No.	Slope (%)	Intensity (ft/sec)	Infiltration, i (ft/sec)	q (cfs/ft) @ 3'	q (cfs/ft) @ 6'	q (cfs/ft) @ 12'	q (cfs/ft) @ 16'
I	5.7	.00002893	.0000114925	.00005230	.00010460	.00020925	.0002790
II	5.7	.0000520833	.0000072646	.000135	.000270	.000540	.0007171
III	5.7	.0000844907	.0000048657	.0002393	.0004785	.000957	.001274
IV	5.7	.0001064815	.0000046378	.000306	.000612	.001224	.0016295
V	10.0	.00002893	.00000918	.0000597	.0001194	.0002388	.000316
VI	10.0	.0000520833	.0000066458	.0001365	.000273	.000546	.000727
VII	10.0	.0000844907	.0000039282	.00024169	.0004834	.00096675	.001289
VIII	10.0	.0001064815	.0000030065	.0003104	.00062085	.0012417	.0016556
IX	15.0	.00002893	.00000818	.0000623	.0001246	.000249	.000332
X	15.0	.000052083	.0000058458	.0001387	.00027743	.00055415	.0007398
XI	15.0	.0000844907	.0000030969	.000244	.000488	.000977	.0013023
XII	15.0	.0001064815	.000001294	.00031556	.000631	.00126225	.001683
XIII	20.0	.00002893	.0000071175	.0000654	.0001308	.0002616	.000349
XIV	20.0	.0000520833	.0000057708	.0001389	.00027787	.00055575	.000741
XV	20.0	.0000844907	.0000028657	.00024488	.00048975	.0009795	.001306
XVI	20.0	.0001064815	.000004815	.000318	.000636	.001272	.001696
XVII	30.0	.00002893	.000006505	.0000672	.000134	.0002688	.0003588
XVIII	30.0	.0000520833	.0000055208	.0001398	.0002796	.0005592	.000745
XIX	30.0	.0000844907	.0000014282	.0002492	.0004984	.00099675	.001329
XX	30.0	.0001064815	.0000002315	.00031875	.0006375	.001275	.001700
XXI	40.0	.00002893	.0000060613	.0000686	.000137	.0002744	.0003659
XXII	40.0	.0000520833	.0000053333	.0001403	.0002805	.000561	.000748
XXIII	40.0	.0000844907	.0000010332	.0002503	.0005006	.001001	.001335
XXIV	40.0	.0001064815	.0000001065	.0003191	.000638	.0012765	.001702

TABLE 4. SEDIMENT DISCHARGE IN TERMS OF DIFFERENT UNITS

Run No.	q_s (lb/sec/ft of width)	q_s (lb/hr)	q_s (lb/hr/ft of width)	q_s (ton/hr/acre)	Erosion (in/hr)	Erosion (ft/hr)
I	.000096	1.728	.3456	.0435	.0028205	.0002350427
II	.00030	5.400	1.080	.1423	.0092307696	.0007692308
III	.000646	11.628	2.3256	.29163	.018923077	.001576923
IV	.001482	26.676	5.3352	.6615	.042923077	.003576923
V	.000294	5.292	1.0584	.1309	.0084923076	.0007076923
VI	.001508	27.144	5.4288	.6757	.0438461544	.0036538462
VII	.00372	66.960	13.392	1.780	.1153846152	.0096153846
VIII	.00588	105.84	21.168	2.845	.1846153848	.0153846154
IX	.000548	9.864	1.9728	.249	.0161538456	.0013461538
X	.002974	53.53	10.7060	1.316	.0853846152	.0071153846
XI	.007138	128.484	25.6968	3.200	.2076923076	.0173076923
XII	.01288	231.840	46.3680	5.760	.3738461544	.0311538462
XIII	.000644	11.592	2.3184	.292	.018923077	.0015769231
XIV	.005686	102.348	20.4696	2.51	.1629487176	.0135790598
XV	.014904	268.272	53.6544	6.544	.4246153848	.0353846154
XVI	.02666	479.88	95.976	11.810	.7661538456	.0638461538
XVII	.000922	16.596	3.3192	.3983	.0258461544	.0021538462
XVIII	.01015	182.70	36.5400	4.41	.2861538456	.0238461538
XIX	.022648	407.664	81.5328	9.766	.633717949	.052809829
XX	.03752	675.36	135.072	16.175	1.04953846	.0874615395
XXI	.001134	20.412	4.0824	.4766	.030923077	.002576923
XXII	.013096	235.728	47.1456	5.477	.355384615	.0296153846
XXIII	.03700	666.000	133.200	15.650	1.015384615	.0846153846
XXIV	.06508	1171.44	234.288	27.25	1.767948718	.1473290598

and the dye was thoroughly mixed with water, the measured-point velocities were assumed to represent mean overland-flow velocities at given distances. The results of velocity calculations are shown in Table 5. Mean point velocities for given slopes, intensities, and distances were the main sources of statistical analysis.

TABLE 5. LOCAL MEAN VELOCITY AND DEPTH OF FLOW FOR A GIVEN RUN AT A GIVEN DISTANCE

	Velocities, measured (ft/sec)				Depth, calculated (ft) on the basis of continuity			
Run No.	$\bar{u}$ at 3'	$\bar{u}$ at 6'	$\bar{u}$ at 12'	$\bar{u}$ at 16'	d at 3'	d at 6'	d at 12'	d at 16'
I	.05224	.0768	.1314	.17602	.001001	.001362	.00159	.001585047
II	.08620	.1367	.2172	.29820	.001566	.001975	.002486	.0024047619
III	.12636	.1875	.2842	.41981	.001894	.002552	.003367	.0030347
IV	.14862	.21618	.3476	.50321	.002059	.002831	.003521	.0032382
V	.06849	.099038	.17315	.22004	.000872	.0012056	.001379	.0014361
VI	.1267	.2066	.3203	.37083	.0010772	.0013214	.001705	.00196047
VII	.19006	.30219	.48049	.52252	.001272	.0016	.002012	.00246689
VIII	.2302	.3572	.5781	.61291	.0013484	.001738	.002148	.0027012
IX	.081167	.11732	.2052	.27404	.0007676	.001062	.001213	.0012115
X	.15016	.23875	.37962	.42323	.000924	.001162	.0014597	.00174798
XI	.22524	.35813	.5694	.63473	.001083	.001363	.001716	.002051738
XII	.27155	.42767	.6976	.74872	.001162	.001475	.001810	.00224784
XIII	.09238	.14688	.2335	.32034	.000708	.0008905	.0011203	.00108947
XIV	.1709	.27105	.42988	.47193	.000813	.001025	.0012928	.001570148
XV	.2564	.40665	.64495	.71794	.000955	.001204	.001519	.00181909
XVI	.3067	.49024	.79293	.82652	.001037	.0012973	.00160417	.002051977
XVII	.10772	.17084	.27096	.36484	.000624	.000784	.000992	.00098344
XVIII	.19928	.31606	.50127	.56472	.0007015	.0008846	.0011156	.0013192379
XIX	.2989	.47406	.75185	.84204	.0008337	.001051	.001326	.0015783098
XX	.3562	.57253	.91267	.94373	.0008948	.0011135	.001397	.001801363
XXI	.12012	.1905	.30215	.40398	.000571	.0007192	.000908	.00090574
XXII	.2222	.3524	.5526	.62442	.000631	.000796	.0010152	.0011979
XXIII	.34209	.5386	.8584	.92119	.0007317	.000929	.001166	.0014492
XXIV	.41667	.6625	1.008	1.0523	.0007658	.000963	.0012664	.00161741

Mean Local Depth of Overland Flow

Measuring depth was the most difficult problem in the overland-flow experiment, since there is no exact method yet in practice to measure depth of overland flow, especially with a movable bed, under simulated rainfall. The U. S. Geological Survey uses a point gage or hook gage attached to a carriage flow in both the laboratory and the field (Emmet, 1970). In the present experiment several methods were considered, such as manometers mounted on the sides of the box to measure piexometric head, a simple ruler placed in the flow, electric capacitance, and a chemical staff gage, but ultimately a point gage with carriage, such as that used by the Geological survey, was decided upon. But the point-gage flow depth had appreciably scattered and was not considered reliable. For this reason, the mean depth of flow with respect to distance was calculated from unit discharge and mean point-velocity data. Since unit discharge changed linearly with respect to distance for steady flow, unit discharge at any X distance was calculated using $q_x = q_o X$; depth of flow at any X distance was calculated using $d_x = q_x/u_x$; the results are found in Table 5.

Sediment Size Distribution

The results of sieve analyses of the original soil samples used are shown in Table 6. In Table 7 the d_{84} , d_{50} , d_{16} and σ of the transported sediment (the porosity and bulk density of the soil) are given for each run. Both the porosity in percent and the bulk density in pounds per cubic feet were found constant for each run. The range of σ was 2.5-4.5 (Table 7). This indicates that the transported silt distribution of the sediment varied with flow conditions. The σ of the original soil was

$$\sigma = \frac{1}{2}\left(\frac{1.00}{.350} + \frac{.350}{.1}\right) = 3.2 ,$$

indicating a nonuniform size distribution.

Table 6 shows that only about 1-1/2 percent of the original soil had a diameter larger than 2 millimeters and about 12 percent had a diameter finer than .053 millimeters (that is, fell in the silt-plus-clay range). The transported sediment had approximately 1-2 percent particles with a diameter larger than 2 millimeters and 5-16 percent finer than .053 millimeters.

Temperature, Viscosity, Reynolds Number, and Froude Number

Temperature of flow was measured for each run, and corresponding kinematic viscosities are recorded in Table 8. The Reynolds and Froude numbers were calculated at given distance for each run, using the steady-linear relationship of unit discharge and distance, and the following relations:

$$Re = \frac{qx}{\nu} , \tag{99}$$

$$Fr = \frac{u}{\sqrt{gd}} \tag{100}$$

Calculated values of the Reynolds number and the Froude number are listed in Table 8.

The critical Reynolds number, Re , was calculated for the last run only, using the data collected at the end of the flume to determine whether flow was laminar or turbulent on the basis of the criteria given by Eq. (51). The reason for calculating the Re of the last run only was that it would be the maximum Re and would be sufficient for finding the range of Re Sample calculation of Re for last run is

$$Re = 24\ (2 \log \frac{.72}{.50} + 1.74)^2 = 24 \times 4.2 = 101.8 .$$

Thus, the range of Re is 0 to 101.8 (Re = 0; no flow) , that is, laminar-flow range. Note that the Froude number of flow for almost all points is greater than one; therefore, it is called supercritical agitated laminar flow.

Friction Factor, f , and Friction Slope, S_f

If one uses the Darcy-Weisbach definition of friction coefficient and assumes that γ_o can be given by the steady state, uniform flow equation ($g\rho dS_f$) when S_f accounts for the acceleration effects. The equation reduces to

$$f = 8\ \frac{\tau_o}{\rho\bar{u}^2} \tag{101}$$

$$f = \frac{8\rho gdS_f}{\rho\bar{u}^2} = \frac{8gdS_f}{\bar{u}^2} = \frac{8gqS_f}{\bar{u}^3} . \tag{102}$$

From this equation, S_f can be solved for

$$S_f = f\ \frac{\bar{u}^2}{8gd} . \tag{103}$$

If f or S_f is known, calculation of either on the basis of the other is easy. In the case of steady uniform flow, $S_o = S_f$, then f will be:

$$f = \frac{gdS_o}{\bar{u}^2} , \tag{104}$$

and S_o will be

$$S_o = f\ \frac{\bar{u}^2}{8gh} . \tag{105}$$

To calculate friction slope the following relation may be used

$$S_f = \frac{3\nu}{g}\ \frac{\bar{u}}{d^2} = \frac{3\nu q}{gd^3} . \tag{106}$$

S_f was calculated at various distances for each run, using Eq. (106) (Table 9) and assuming no rainfall effect. The determined values of S_f were then used to calculate the friction factors, assuming no rainfall effect. The calculated f is shown in Table 9.

In Table 10 the values of f are given which were calculated using Eq. (43) (Li, 1972), but with a constant of 34 (Yoon and Wenzel, 1971) instead of 24. Using this value of f the friction slope, S_f , was calculated (Table 10). These values include the rainfall-impact effect.

TABLE 6. SIEVE ANALYSIS OF ORIGINAL SOIL USED FOR THE EXPERIMENT

Sieve diameter in micron	Net weight of sed.	Percentage of total	Percentage finer
2000	6.9	1.26	98.74
1000	80.0	14.56	84.18
701	56.0	10.19	73.99
500	49.8	9.1	64.89
354	54.3	9.88	55.01
250	62.5	11.38	43.63
125	94.0	17.11	26.52
53	81.3	14.80	11.72
53	64.5	11.74	

TABLE 7. THE d_{84}, d_{50}, d_{16}, AND σ OF TRANSPORTED SEDIMENT, d_b AND POROSITY, P, FOR A GIVEN RUN (d_{84} = 1.00, d_{50} = .35 or .325 AND d_{16} = .1 MM OF THE ORIGINAL SAMPLE)

Run No.	d_{84} (mm)	d_{50} (mm)	d_{16} (mm)	d_b Bulk density (lb/ft^3)	P Porosity (%)	σ (Dimensionless)
I	1.30	.49	.080	93.6	43	4.39
II	1.25	.50	.200	93.6	43	2.50
III	1.30	.49	.200	93.6	43	2.56
IV	1.20	.48	.150	93.6	43	2.85
V	1.00	.40	.100	93.6	43	3.25
VI	1.20	.40	.100	93.6	43	3.50
VII	1.20	.40	.130	93.6	43	3.04
VIII	1.25	.40	.130	93.6	43	3.10
IX	.90	.36	.130	93.6	43	2.63
X	1.00	.40	.150	93.6	43	2.58
XI	1.00	.40	.100	93.6	43	3.25
XII	1.00	.30	.100	93.6	43	3.17
XIII	.80	.30	.075	93.6	43	3.33
XIV	.90	.31	.100	93.6	43	3.00
XV	1.00	.30	.100	93.6	43	3.17
XVI	1.10	.25	.100	93.6	43	3.45
XVII	.65	.30	.060	93.6	43	3.39
XVIII	1.00	.30	.060	93.6	43	4.16
XIX	.80	.30	.055	93.6	43	4.06
XX	1.00	.30	.053	93.6	43	4.49
XXI	.65	.27	.040	93.6	43	4.58
XXII	.85	.27	.053	93.6	43	4.12
XXIII	.95	.27	.065	93.6	43	3.84
XXIV	1.00	.27	.053	93.6	43	4.40

TABLE 8. EXPERIMENTALLY CALCULATED REYNOLDS NUMBER, Re , FROUDE NUMBER, Fr , FOR A GIVEN RUN AND RAINFALL EXCESS AT A GIVEN DISTANCE

Run No.	Rainfall excess, q_o, (ft/sec)	Temp. (F^0)	Kin. Vis. $\nu \times 10^5$ (ft^2/sec)	Re @ 3'	Re @ 6'	Re @ 12'	Re @ 16'	Fr @ 6'	Fr @ 12'	Fr @ 16'
I	.0000174375	57.0	1.282	4.08	8.16	16.32	21.76	.581	.853	.779
II	.0000448187	48.2	1.430	9.44	18.88	37.76	50.15	1.077	1.286	1.071
III	.000079625	48.2	1.430	16.734	33.46	66.92	89.09	1.190	1.453	1.342
IV	.0001018437	50	1.410	21.7	43.40	86.81	115.57	1.401	1.598	1.558
V	.00001975	52.8	1.390	4.295	8.59	17.18	22.73	.735	1.052	1.023
VI	.0000454375	52.8	1.390	9.82	19.64	39.28	52.30	1.184	1.445	1.475
VII	.0000805625	52.8	1.390	17.39	34.78	69.55	92.73	1.568	1.888	1.853
VIII	.000103475	52.8	1.390	22.33	44.665	89.33	119.11	1.769	2.061	2.078
IX	.00002075	57	1.282	4.860	9.719	19.423	25.90	1.060	1.083	1.387
X	.0000462375	48.2	1.430	9.700	19.40	38.75	51.73	1.444	1.668	1.783
XI	.0000813938	55	1.312	18.600	37.195	74.466	99.26	2.160	2.513	2.469
XII	.0001051875	57	1.282	24.615	49.22	98.459	131.28	2.305	2.770	2.782
XIII	.0000218125	61	1.220	5.361	10.72	21.44	28.606	1.378	1.626	1.710
XIV	.0000463125	52.8	1.390	9.99	19.99	39.982	53.31	1.739	2.082	2.098
XV	.000081625	59	1.240	19.75	39.50	79.00	105.32	2.296	2.587	2.966
XVI	.00010600	57	1.282	24.805	49.61	99.22	132.29	2.435	3.098	3.215
XVII	.000022425	61	1.220	5.508	10.98	22.03	29.41	1.624	1.709	2.050
XVIII	.0000465625	57	1.282	10.90	21.81	43.03	58.11	2.370	2.612	2.739
XIX	.0000830625	61	1.220	20.43	40.85	91.70	108.93	3.176	3.545	3.735
XX	.000106250	57	1.282	24.863	49.73	99.454	132.61	3.517	3.916	3.918
XXI	.0000228687	61	1.220	5.65	11.23	22.49	29.94	2.400	3.207	2.365
XXII	.00004675	57	1.282	10.94	21.88	43.76	58.35	3.445	4.424	3.179
XXIII	.000083475	60.8	1.222	20.483	40.966	81.915	109.25	4.217	5.134	4.264
XXIV	.000106375	57	1.282	24.891	49.766	99.571	132.76	5.016	5.447	4.611

TABLE 9. FRICTION FACTOR, f , FRICTION SLOPE, S_f , BOUNDARY SHEAR, τ_o , AND CRITICAL TRACTIVE FORCE, τ_c , FOR A GIVEN RUN AT A GIVEN DISTANCE (WITHOUT RAINFALL EFFECT USING DARCY-WEISBACH FORMULA)

Run No.	S_f @ 3'	S_f @ 6'	S_f @ 12'	S_f @ 16'	f @ 3'	f @ 6'	f @ 12'	f @ 16'	τ_o @ 16'	τ_c @ 0'-16'
I	.062275	.04945	.06206	.08622	6.10	3.86	1.54	.833	.007361	.0061
II	.0468	.046685	.04583	.06981	2.88	1.443	.7195	.3633	.00814	.0062
III	.0469	.03835	.0334	.0652	1.406	.86017	.494	.19005	.00875	.0061
IV	.0460	.0354	.03683	.0641	1.081	.7022	.3378	.14577	.0093	.0060
V	.095476	.07224	.09655	.11386	4.549	3.008	1.1256	.72113	.00874	.0057
VI	.115544	.12525	.1165	.10292	1.988	.9171	.49233	.4190	.01444	.0057
VII	.133498	.13418	.134927	.10326	1.143	.56869	.28286	.27718	.0196	.0057
VIII	.14415	.13464	.14266	.10039	.8587	.45967	.21689	.23115	.02235	.0057
IX	.16446	.12422	.166576	.2234	5.10	3.379	1.2615	.7052	.013214	.0051
X	.23436	.23559	.237387	.18446	2.354	1.171	.58186	.4683	.02503	.0057
XI	.234717	.235655	.23636	.18605	1.2263	.61047	.3040	.2898	.02928	.0057
XII	.240187	.234786	.2543	.18417	.9255	.47365	.21845	.22632	.03247	.0048
XIII	.20945	.21059	.21146	.31003	5.022	2.499	1.244	.6359	.01638	.0047
XIV	.3348	.33409	.3331	.2527	2.25	1.1285	.56586	.5594	.03145	.0048
XV	.32478	.32409	.32292	.2612	1.1526	.57767	.2897	.26867	.03548	.0047
XVI	.340617	.34795	.368034	.2459	.9258	.4533	.21426	.24052	.0423	.0040
XVII	.31433	.31593	.312976	.46507	4.8485	2.422	1.2182	.61417	.02151	.0047
XVIII	.42857	.4275	.42624	.36164	1.8656	.9353	.4689	.4149	.03413	.0047
XIX	.513595	.512584	.51072	.41818	1.1779	.59031	.2961	.2713	.049073	.0047
XX	.5314	.551577	.55857	.36994	.9084	.4375	.21601	.2446	.05662	.0047
XXI	.38988	.38979	.38787	.57732	4.445	2.2258	1.1171	.5627	.0245	.00415
XXII	.74578	.741	.71434	.6081	2.3045	1.1558	.5995	.5282	.052985	.00415
XXIII	.787075	.7687	.77765	.57418	1.1709	.5997	.29634	.3009	.0663	.00415
XXIV	.86852	.8732	.7683	.50584	.8567	.4262	.2421	.27576	.07756	.00415

TABLE 10. FRICTION FACTOR, f , FRICTION SLOPE, S_f , AND BOUNDARY SHEAR, τ_o , FOR A GIVEN RUN AT A GIVEN DISTANCE (WITH RAINFALL EFFECT IN THE INDOOR LABORATORY; f IS CALCULATED BY EQUATION 2-43)

Run No.	f @ 3'	f @ 6'	f @ 12'	f @ 16'	S_f @ 3'	S_f @ 6'	S_f @ 12'	S_f @ 16'	τ_o @ 16'
I	15.815	7.9075	3.954	2.965	.1674	.1329	.1668	.225	.022253
II	7.6613	3.8306	1.915	1.442	.141117	.140699	.14107	.20699	.031060
III	4.793	2.397	1.1986	0.9004	.15685	.128187	.11162	.2029	.03842
IV	3.8959	1.9479	.924	0.7315	.16224	.12483	.1231	.22208	.044869
V	15.02	7.512	3.756	2.84	.31366	.23725	.317	.371698	.033309
VI	7.365	3.682	1.84	1.383	.42603	.11617	.42979	.376587	.046069
VII	4.613	2.306	1.153	.865	.50855	.5109	.5136	.37164	.057208
VIII	3.786	1.893	.9464	.7098	.5776	.5395	.57161	.3832	.06459
IX	13.277	6.639	3.322	2.491	.44236	.3340	.44766	.59942	.045315
X	7.456	3.728	1.866	1.398	.7063	.70992	.71516	.556132	.06066
XI	4.313	2.156	1.077	.808	.7843	.78757	.78993	.61592	.078855
XII	3.435	1.718	.8586	.644	.8462	.826995	.89615	.62347	.087451
XIII	12.036	6.019	3.01	2.256	.5632	.56607	.56867	.8249	.056079
XIV	6.459	3.618	1.809	1.356	.67218	1.0067	1.0038	.74667	.0731566
XV	4.061	2.031	1.015	.762	1.08523	1.08288	1.079	.838168	.095142
XVI	3.408	1.704	.852	.639	1.200	1.2255	1.2963	.8258	.105742
XVII	11.715	5.877	2.93	2.194	.34567	.8493	.8418	1.15278	.070742
XVIII	6.635	3.316	1.681	1.245	1.45813	1.45365	1.4698	1.1683	.096178
XIX	3.926	1.964	.875	.736	1.63322	1.59873	1.44804	1.28353	.12641
XX	3.40	1.7	.850	.637	1.8715	1.9427	1.96745	1.22261	.1374275
XXI	11.42	5.75	2.87	2.155	1.12025	1.12632	1.1202	1.50736	.0851933
XXII	6.611	3.305	1.653	1.239	2.0081	2.00163	1.93018	1.56552	.117021
XXIII	3.916	1.958	.979	.734	2.43133	2.3735	2.40169	1.66842	.1508805
XXIV	3.396	1.699	.849	.637	2.98876	3.00603	2.64431	1.692983	.1708666

Boundary Shear Forces, Critical Tractive Force, and Stream Power

The tractive force per area of boundary was calculated by using the following definition of boundary-shear force, τ_o :

$$\tau_o = \gamma d\ S_f \ . \qquad (107)$$

In previous sections, because two kinds of S_f were calculated, two kinds of τ_o corresponding S_f were calculated, too. Calculated τ_o is shown in Tables 9 and 10 for a given slope and rainfall intensity for each run. The critical tractive force, τ_c , calculated using d_{50} and Shields relation, is listed in Table 9 for each run. A third method of calculating τ_o is numerical approximation of the momentum equation using Eq. (55). Equation 55 gives the tractive force, τ_o , directly without calculating S_f or f . These values of τ_o are shown in Table 11. The values of τ_o in Table 11 which include rainfall effects are less than τ_o calculated by Li's (1972) equation but greater than the τ_o calculated assuming steady uniform flow. Using the shear stress calculated by Eq. 55, the effective tractive force $(\tau_o - \tau_c)$ and effective stream powers $(\tau_o - \tau_c)\ \bar{u}$ were determined.

Rill Measurements

At the end of each run, dimensions of rills were both measured and photographed. Trapezoidal shape was assumed for the short segment of rills, and their length, depth, bottom width, and surface width were measured and recorded. From the measurements, the volume of rills V_R was calculated for each run. Since bulk density of soil was known, total erosion was converted to bulk volume of sediment:

$$V_T = \frac{W_T}{d_b} \qquad (108)$$

in which

V_T = volume of total transported sediment (L^3) ,
W_T = weight of total transported sediment (F).

All the measurements and calculations were put into dimensionless form as simple ratios so that they would be free of units and could easily be compared with other researchers' results or applied elsewhere. The calculated ratios were: rill volume/volume of total transported sediment volume, rill surface area/total area exposed, and width/depth of rill. The results of all calculations are given in Table 12.

TABLE 11. BOUNDARY SHEAR, τ_o , AND STREAM POWER FOR EACH RUN AT THE END OF FLOW (τ_o IS CALCULATED BY EQUATION 2-55; WITH RAINFALL EFFECT IN THE OUTDOOR LABORATORY)

Run No.	$\frac{\Delta\bar{u}}{\Delta x} = \frac{d\bar{u}}{dx}$ @ 16'	τ_o (lb/ft^2) @ 16'	$\tau_o - \tau_c$ (lb/ft^2) @ 16'	$(\tau_o - \tau_c)\ \bar{u}$ (lb/ft-sec) @ 16'
I	.0111	.010724	.004624	.00081392
II	.0190	.01845	.01225	.00365295
III	.027	.0240686	.0179686	.0075434
IV	.033	.031583	.025583	.0128736
V	.0142	.022212	.016512	.0036333
VI	.025	.038316	.032616	.012095
VII	.036	.045837	.040137	.020972
VIII	.043	.050945	.045245	.027731
IX	.0180	.025163	.0200632	.005498
X	.0294	.04481	.03911	.0165525
XI	.0460	.051295	.045595	.0289405
XII	.0570	.0619066	.0571066	.0427568
XIII	.0220	.033846	.029146	.00933663
XIV	.0340	.050406	.045606	.0215228
XV	.0550	.05768	.05298	.0380365
XVI	.0660	.067906	.063906	.0528196
XVII	.0262	.04107	.03707	.0135246
XVIII	.0430	.053696	.048996	.027669
XIX	.0680	.06095	.05625	.047365
XX	.0770	.06722	.06252	.059002
XXI	.0310	.049101	.044951	.018160
XXII	.0510	.060544	.056394	.0352135
XXIII	.0800	.068225	.064075	.059025
XXIV	.095	.0762806	.0721306	.075903

TABLE 12. DATA FROM RILL MEASUREMENTS

Run No.	V_T (ft^3/hr)	V_R (ft^3/hr)	A_R (mean) (ft^2/hr)	V_R/V_T (per hr)	A_R/A_T [1/] or W_R ($A_T = 80\ ft^2$) (per hr)	V_R/ft of width ($ft^3/ft/hr$)	A_R/ft of width ($ft^2/ft/hr$)	D_R (mean) (ft/hr/ft of width)
I	.0185	.001889	14.8	.1021	.185	.0003778	2.96	.0001276
II	.0577	.0007974	18.16	.1382	.227	.001595	3.632	.00043915
III	.124	.028185	25.28	.2273	.316	.005637	5.056	.001114913
IV	.285	.07644	28.24	.2682	.353	.015288	5.648	.0027067
V	.0565	.006865	15.68	.1215	.196	.001373	3.136	.00043782
VI	.290	.04634	18.88	.1598	.236	.009268	3.776	.00245445
VII	.715	.1678	25.76	.2347	.322	.03356	5.152	.006514
VIII	1.131	.33715	28.56	.2981	.357	.067431	5.712	.0011905
IX	.1054	.0147	16.72	.1396	.209	.00294	3.344	.0008792
X	.572	.105	20.08	.1834	.251	.0210	4.016	.0052291
XI	1.373	.3692	26.40	.2689	.330	.07384	5.28	.013985
XII	2.477	.8040	29.44	.3246	.368	.1608	5.888	.02731
XIII	.124	.02192	18.88	.1768	.236	.004384	3.776	.001161
XIV	1.094	.23762	21.68	.2172	.271	.047524	4.336	.01096
XV	2.866	.8363	27.28	.2918	.341	.16726	5.456	.0306562
XVI	5.127	1.844	30.32	.3596	.379	.3688	6.064	.0508179
XVII	.177	.0386	21.44	.2182	.268	.00772	4.288	.00180037
XVIII	1.952	.5034	24.32	.2579	.304	.10068	4.864	.020699
XIX	4.355	1.516	29.68	.3482	.371	.31032	5.936	.05227763
XX	7.215	2.952	33.04	.4091	.413	.5904	6.608	.08934625
XXI	.218	.0523	23.20	.2398	.290	.01046	4.64	.0022543
XXII	2.5185	.8104	28.16	.3218	.352	.16208	5.632	.02877841
XXIII	7.1154	2.983	33.60	.4192	.420	.5966	6.720	.08878
XXIV	12.5154	6.115	37.20	.4886	.465	1.2230	7.440	.1643817

[1/] Magnitude of A_R/A_T is equal to W_R which is the mean rill width in ft/hr/ft of width.

SIMPLE RELATIONSHIPS BETWEEN THE VARIABLES

Sediment Concentration Versus Time

Figures 6 to 11 show sediment concentration as a function of time and rainfall intensity. Although there was some oscillation for the first five- to ten-minute period of each run and some variation of concentration with time, statistical analysis of data showed that the changes with time are not significant.

Sediment Concentration Versus Slope and Rainfall Intensity

The relation between slope, averaged sediment concentration, and rainfall intensity for a rainfall duration of one hour is given in Fig. 12. The same type of plotting was done in Figs. 13, 14, and 15 by separating the concentration for the first zero- to ten-minute period, the first thirty minute period, and the last thirty minute period. Figure 16 shows averaged C_s between thirty and forty minutes with varying intensity and slope. Then Figs. 12 through 16 show similarly shaped curves.

Sediment Discharge Versus Slope and Intensity

Converting sediment discharge into different units such as lb/hr., lb/hr/ft of width of lb/sec/ft of width and plot with varying slope and intensities, as seen in Figs. 17, 18, and 19, yields curves similar to those in Fig. 16. The plotting of sediment discharge versus water discharge for a given slope (Fig. 20) as would be expected shows an increase in sediment discharge for an increase in water discharge. Also the relation shows the large increases that are to be expected when the slopes are steep.

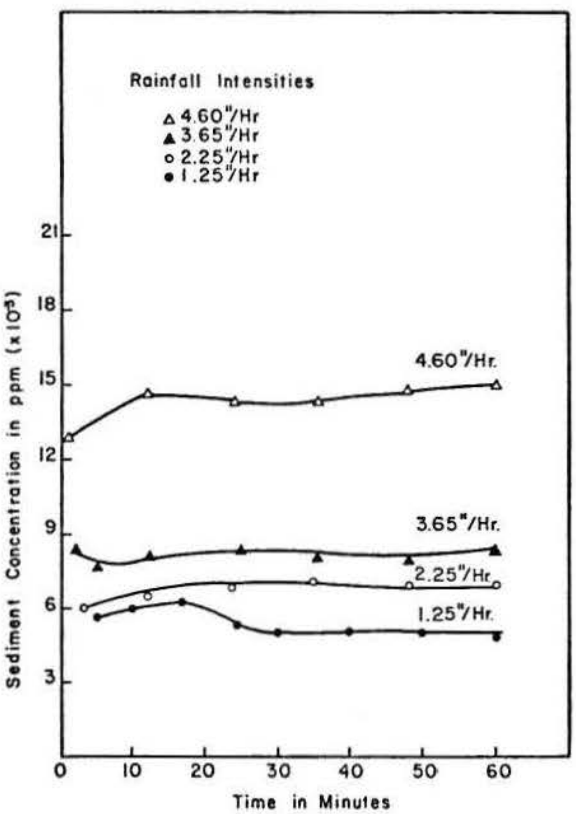

Fig. 6. Relationship between sediment concentration and time for given rainfall intensities on 5.7 percent slope.

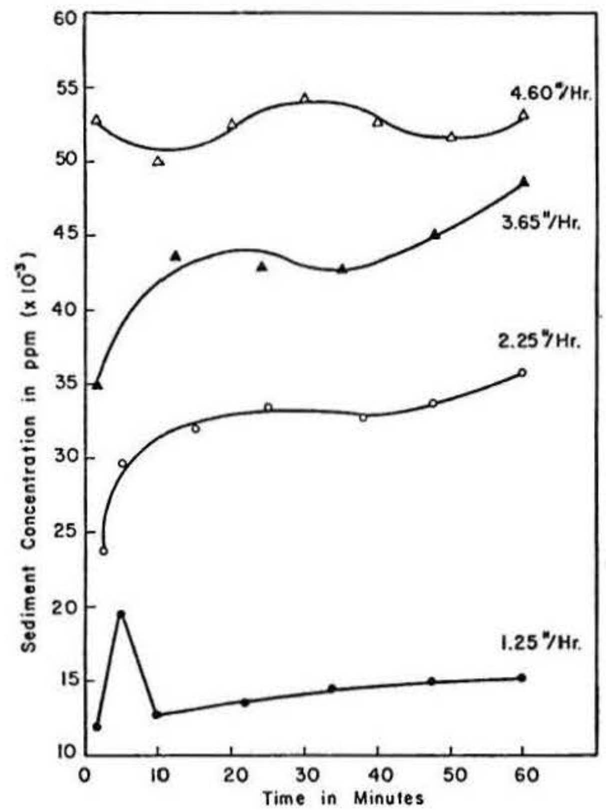

Fig. 7. Relationship between sediment concentration and time for given rainfall intensities on 10 percent slope.

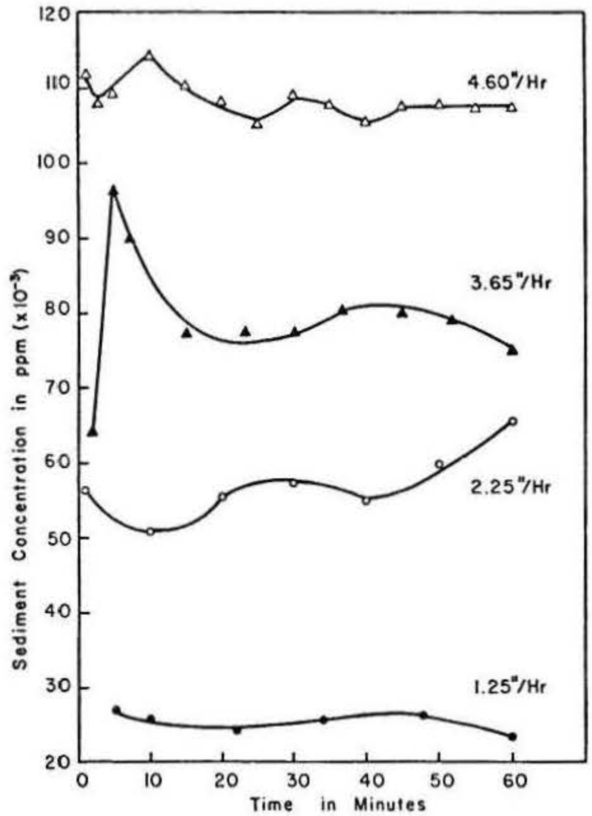

Fig. 8. Relationship between sediment concentration and time for given rainfall intensities on 15 percent slope.

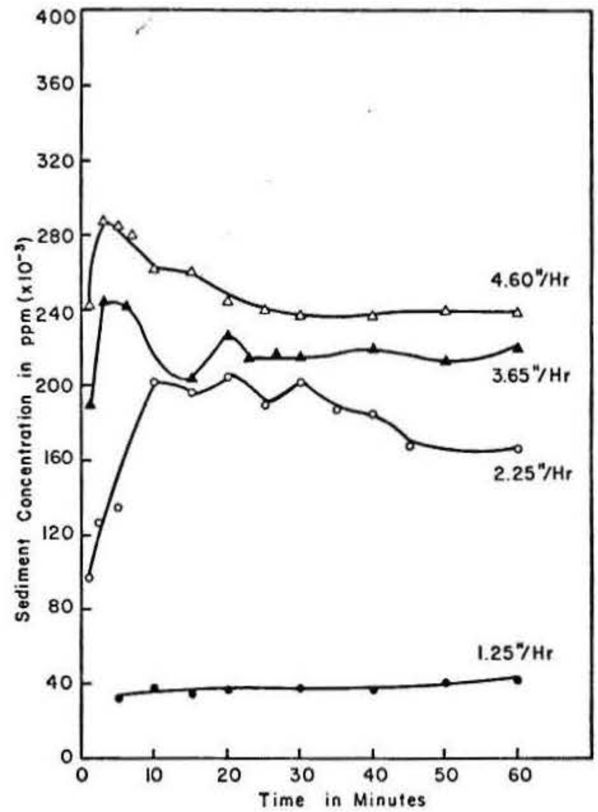

Fig. 10. Relationship between sediment concentration and time for given rainfall intensities on 30 percent slope.

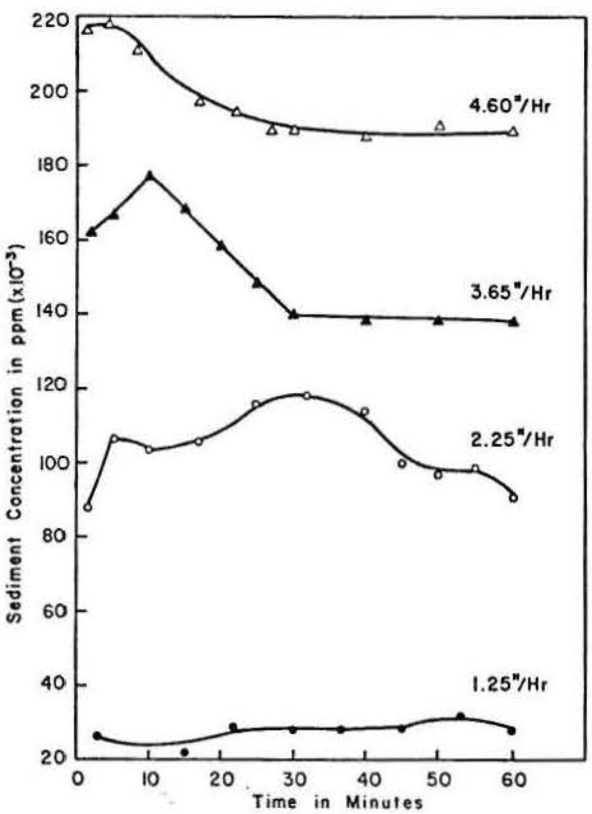

Fig. 9. Relationship between sediment concentration and time for given rainfall intensities on 20 percent slope.

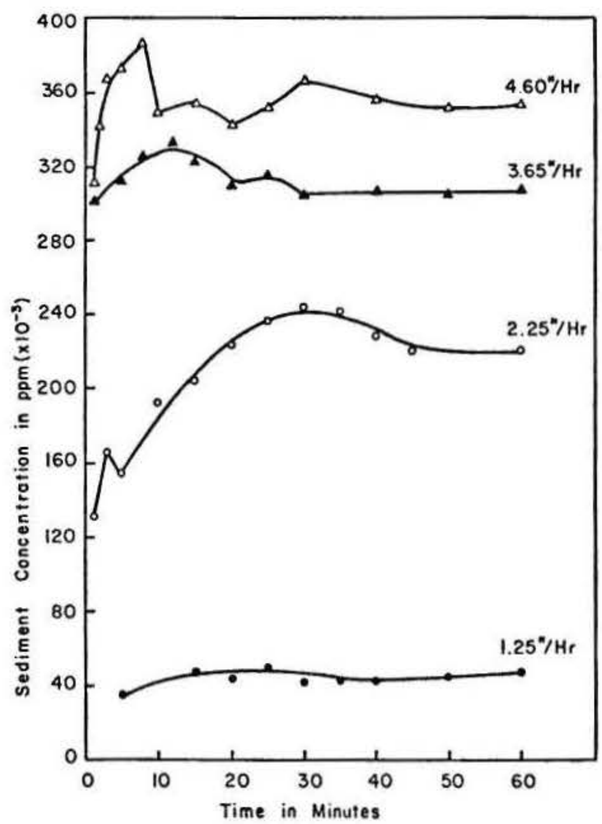

Fig. 11. Relationship between sediment concentration and time for given rainfall intensities on 40 percent slope.

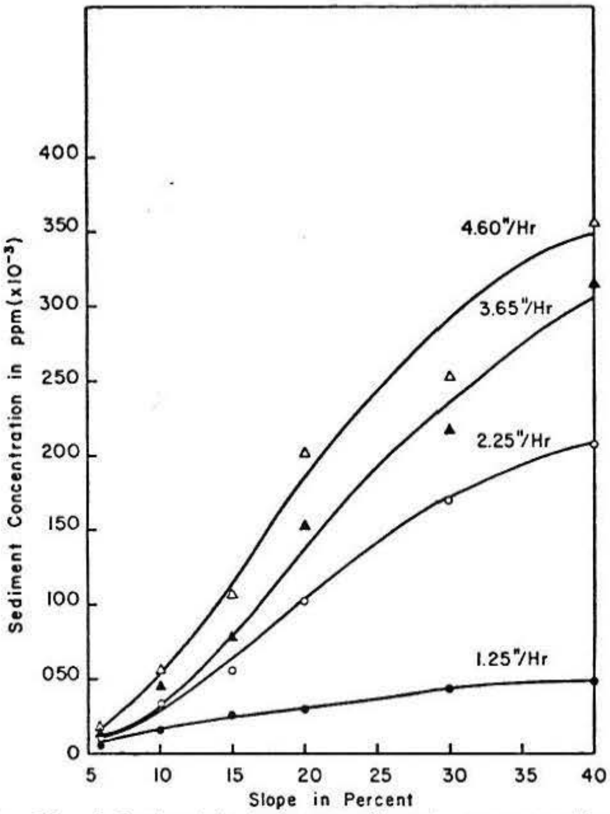

Fig. 12. Relationship between sediment concentration and slope for given rainfall intensities (average concentration values obtained after one hour run).

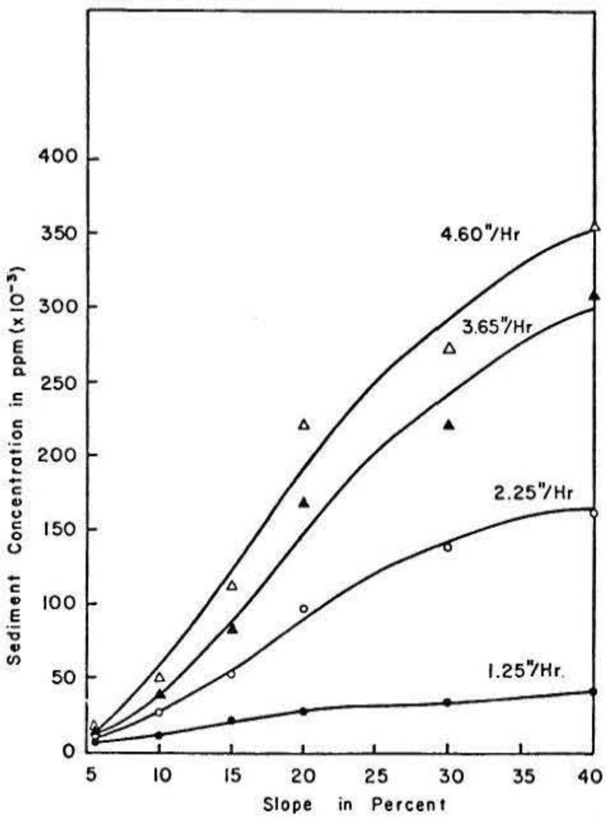

Fig. 13. Relationship between sediment concentration and slope for given rainfall intensities (average concentration values obtained between 0-10 minutes).

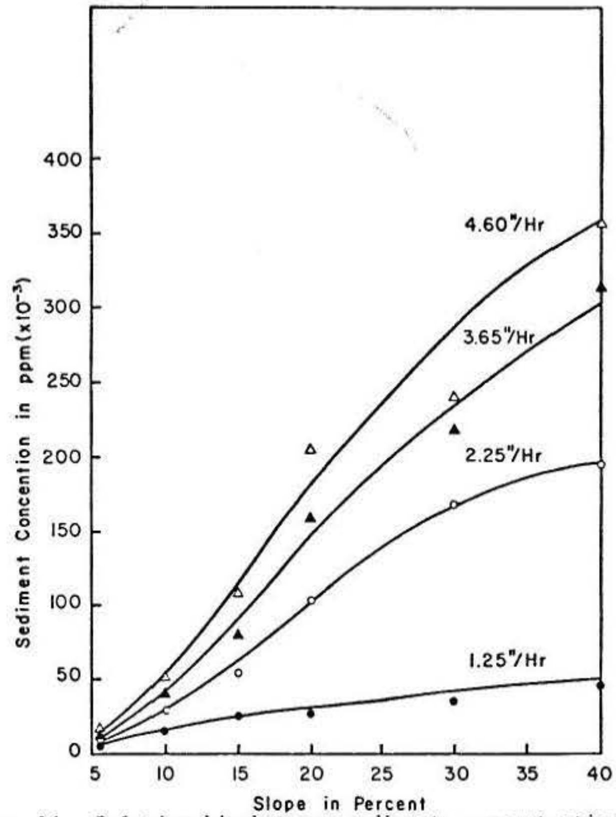

Fig. 14. Relationship between sediment concentration and slope for given rainfall intensities (average concentration values obtained after first 30 minutes).

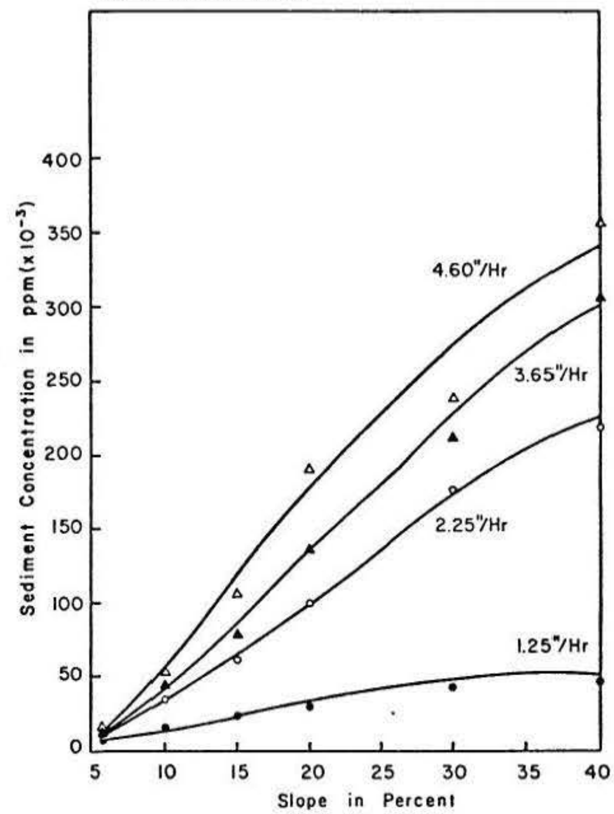

Fig. 15. Relationship between sediment concentration and slope for given rainfall intensities (average concentration values obtained between 30-60 minutes).

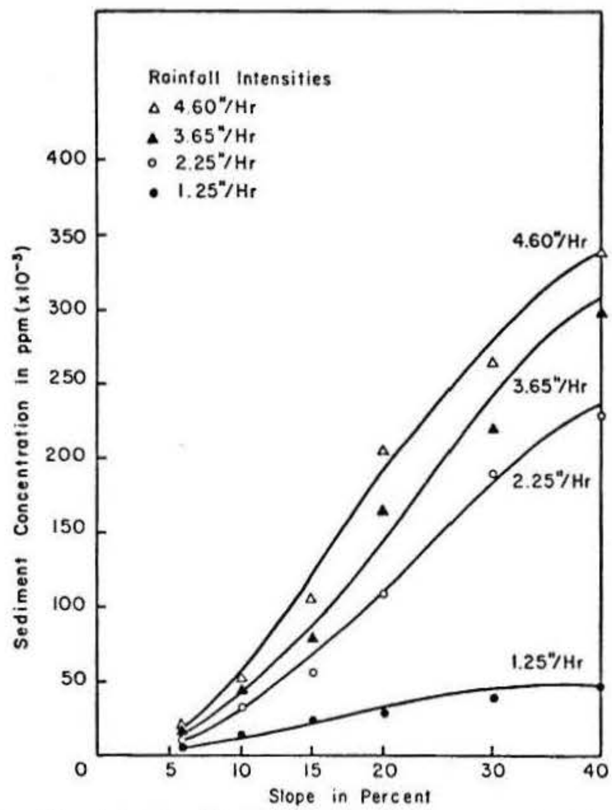

Fig. 16. Relationship between sediment concentration and slope for given rainfall intensities (average concentration values obtained between 30-40 minutes).

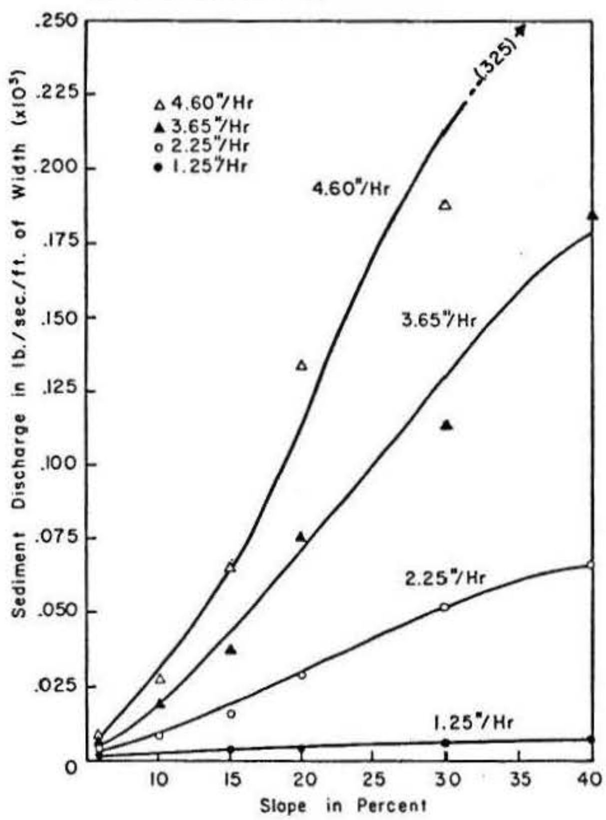

Fig. 17. Relationship between sediment discharge and slope for given rainfall intensities (q_s in lb/hr/ft of width).

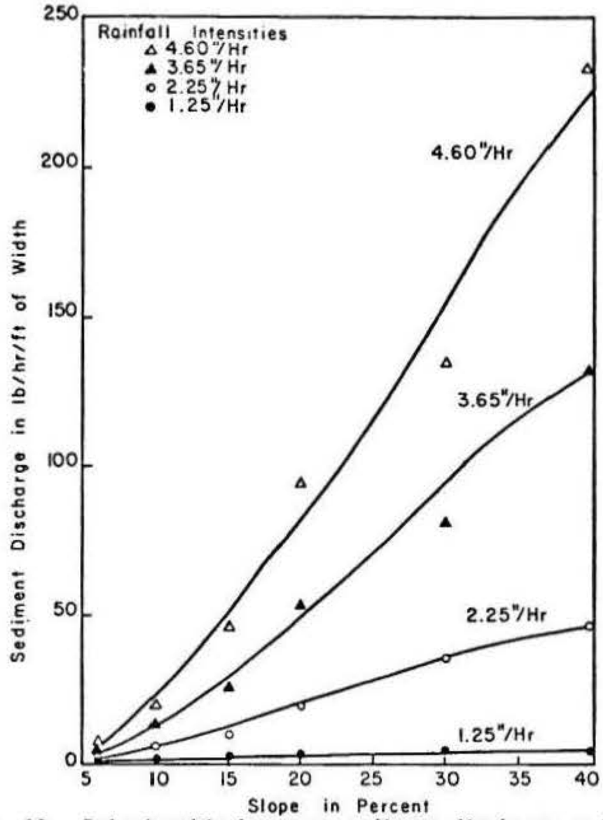

Fig. 18. Relationship between sediment discharge and slope for given rainfall intensities (q_s in lb/hr/ft of width).

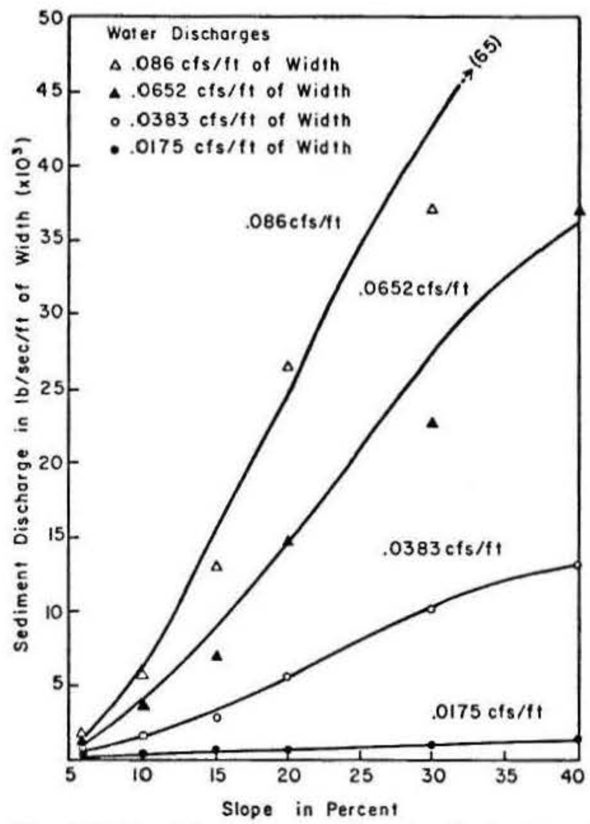

Fig. 19. Relationship between sediment discharge and slope for given water discharges (q in cfs/ft of width and q_s in lb/sec/ft of width).

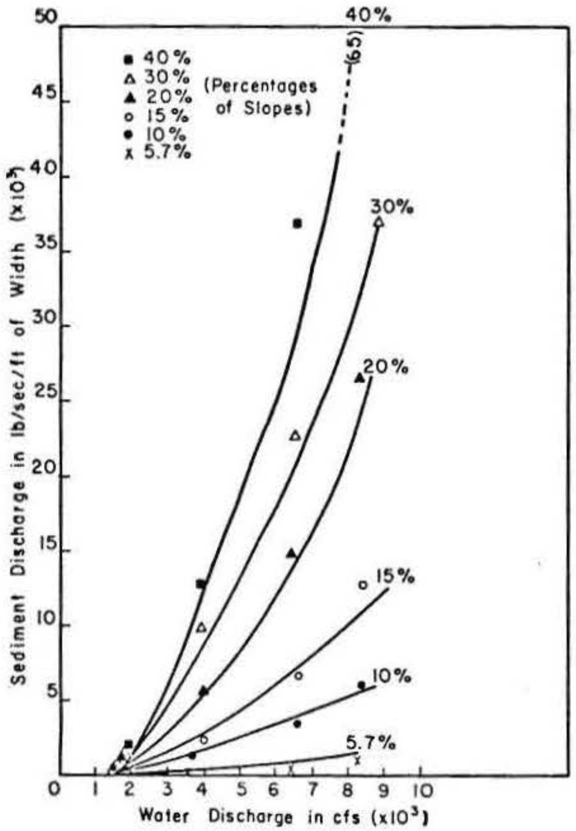

Fig. 20. Relationship between sediment discharge and water discharges on given slopes for one hour run.

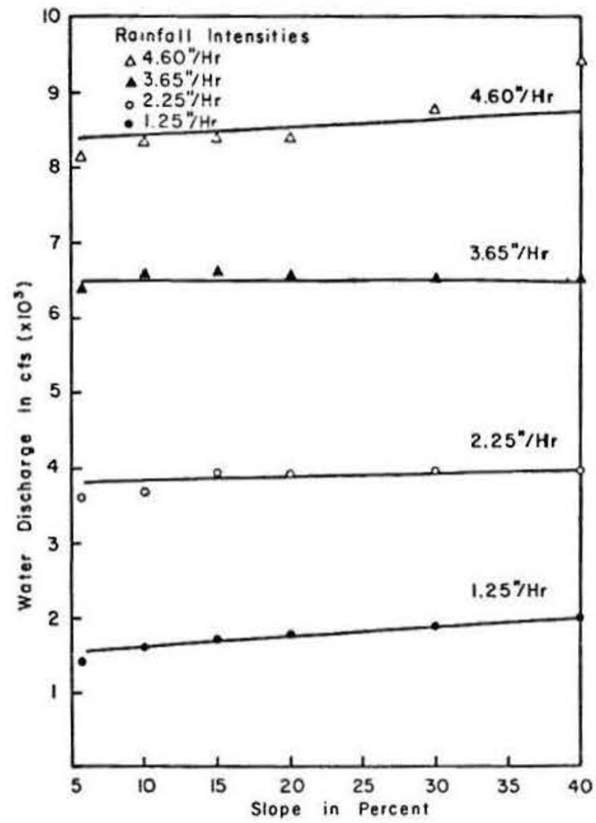

Fig. 21. Relationship between water discharge and slope for given rainfall intensities.

Local Mean Velocity and Depth Versus Overland Flow Distance, Slope and Intensity

Local mean velocity and depth versus distance were plotted in Figs. 22 to 27 for each slope length and for given intensities of rainfall.

Friction factor, f , Versus Reynolds Number, Re

For each given run and slope, the relationship between friction factor, f , as calculated by Eq. (5) , and Reynolds number, was plotted in Fig. 28. The change in f with slope distance is given in Figs. 29 through 34. These figures show that f decreased in the downstream direction and, at a given section, decreased with rainfall intensity.

Independent and Dependent Variables

Major analyses were made of data from 24 runs without vegetative cover. Sediment transport and erosion rate correlations with independent variables show steady but nonlinear relationships. Nonlinear multiple regression analysis was performed on sediment discharge, sediment concentration, water discharge, rill volume and surface area, slope, rainfall intensity, rainfall excess, velocity, depth kinematic viscosity, median diameter of sand, bulk density, and the Reynolds numbers.

For the purpose of analysis, sediment discharges, sediment concentration, erosion, median diameter of transported sediment, local mean velocity and depth of flow, rill volume and rill surface area were used individually as dependent variables. Slope, rainfall intensity, rainfall excess, median diameter of sediment (d_{50}) , depth and mean velocity of flow, water discharge, kinematic viscosity, bulk density, and length of slope (overland flow distance) were used as independent variables. Major dependent variables were sediment discharge, sediment concentration, and erosion. Whenever these major variables were used as dependent variables, the remaining variables were considered independent. When velocity, depth, and median diameter of sediment were used as dependent variables, erosion, sediment discharge, and sediment concentration were not taken into account in the analysis. The single-correlation matrix of variables used in this analysis, except rill volume and area, is shown in Table 13. Rills were analyzed separately.

One major purpose of analyzing the data generated by the experiments here was to develop equations which would provide a means of predicting sediment discharge or soil loss resulting from overland-flow erosion for practical use in the field, in the hope that such equations could utilize the information on slope and intensity of rainfall for the soil type under consideration.

In the following sections, the results of computer analysis and equations thus derived are tabulated, with brief explanations wherever necessary. The correlations obtained from the computer are presented in the same sequence in which independent variables were first considered. Some less significant intermediate sequences are omitted. The increment ΔR^2 , coefficient of determination R^2 , and change in standard error of estimate SEE can thus easily be seen. The standard error of estimate SEE is to be compared with the standard deviation of the dependent variable; thus,

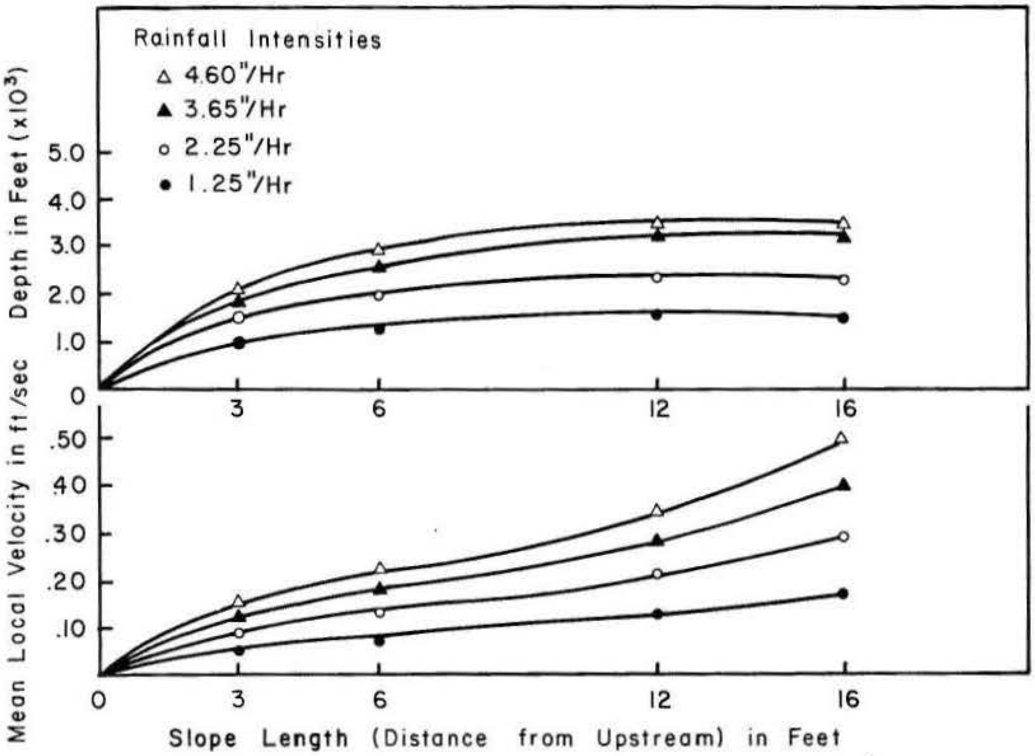

Fig. 22. Mean local velocity and depth related to slope length for given rainfall intensities on 5.7 percent slope.

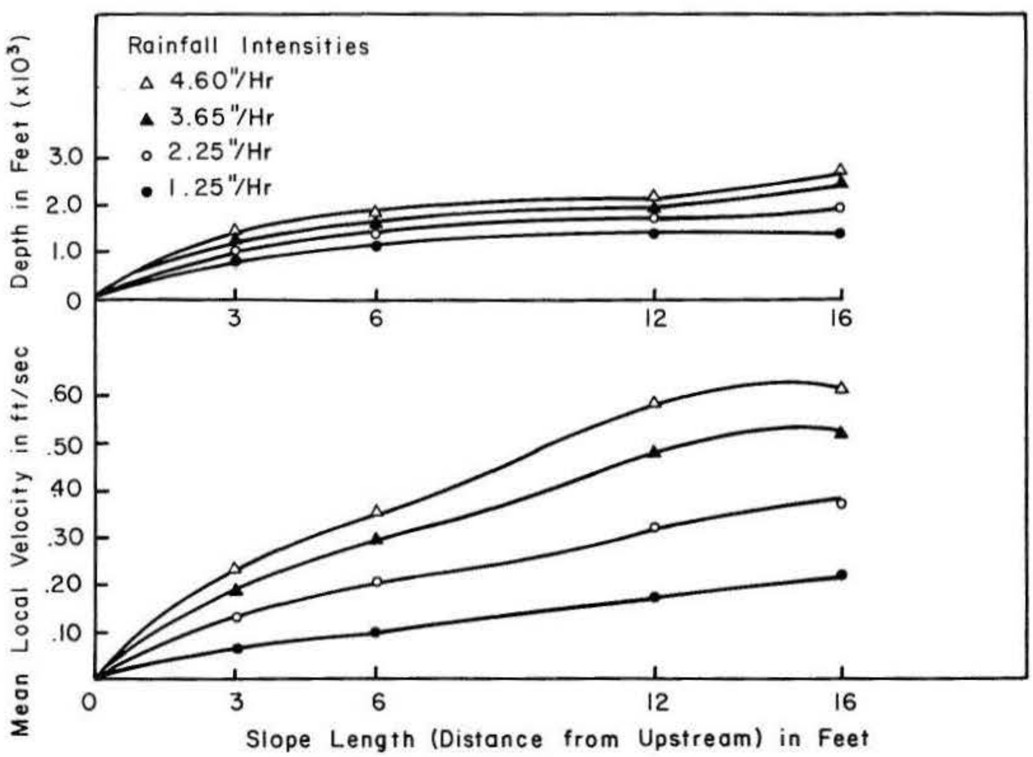

Fig. 23. Mean local velocity and depth related to slope length for given rainfall intensities on 10 percent slope.

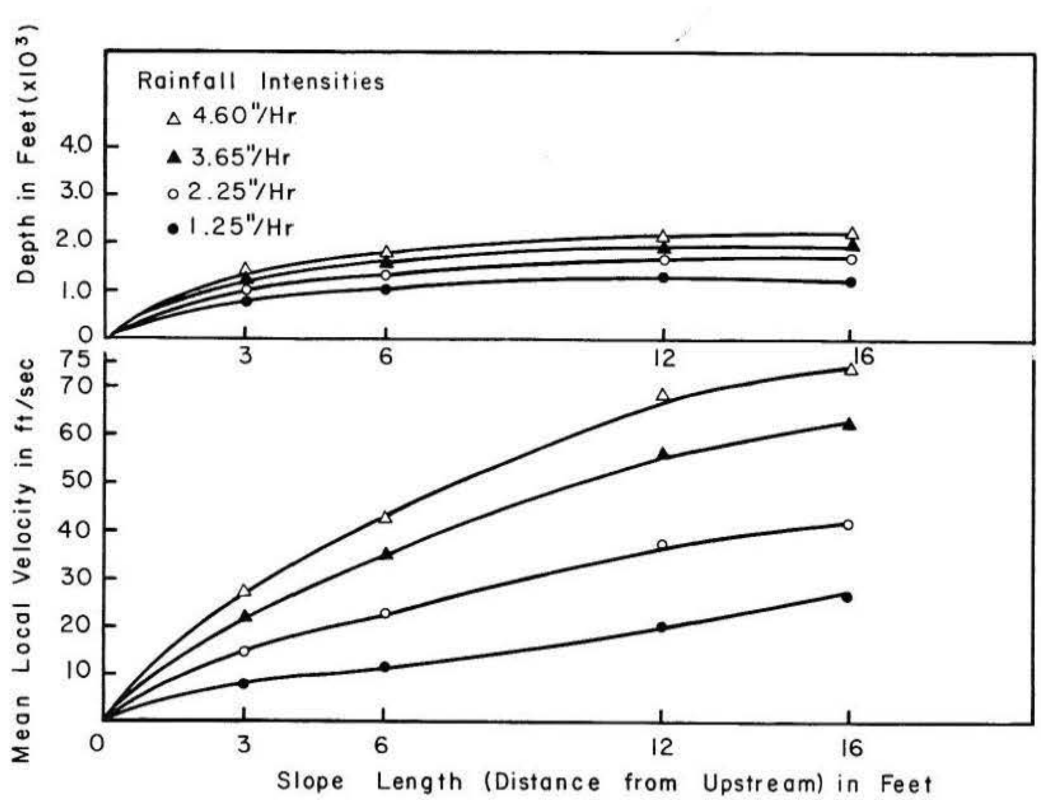

Fig. 24. Mean local velocity and depth related to slope length for given rainfall intensities on 15 percent slope.

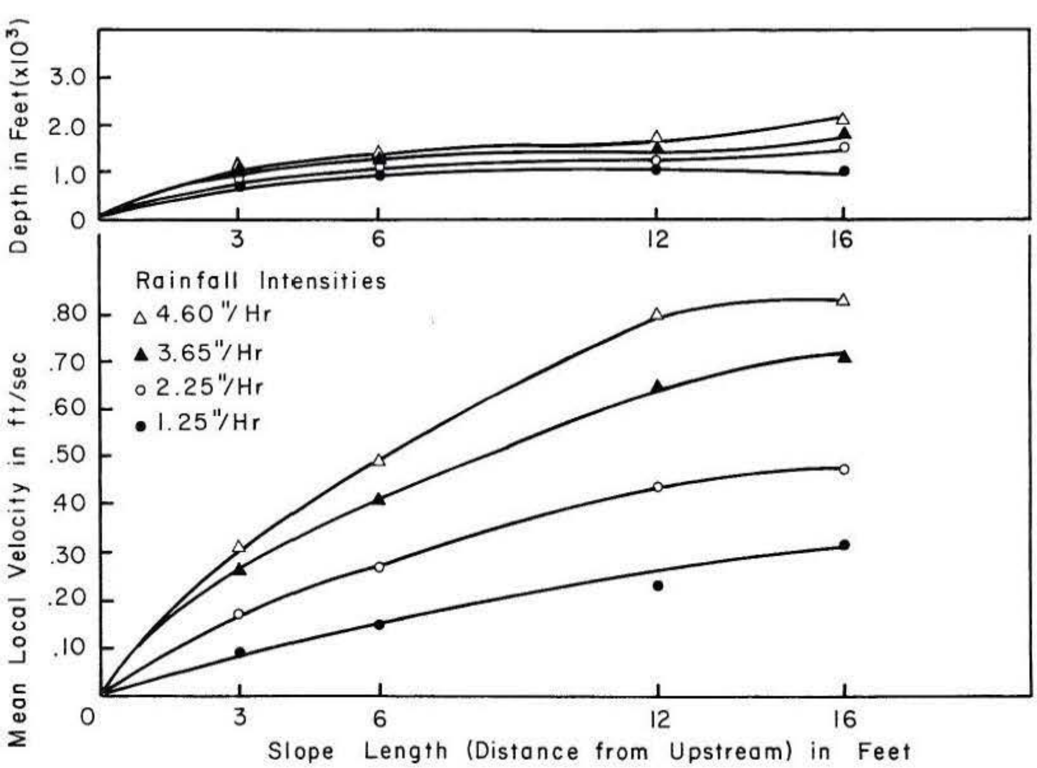

Fig. 25. Mean local velocity and depth related to slope length for given rainfall intensities on 20 percent slope.

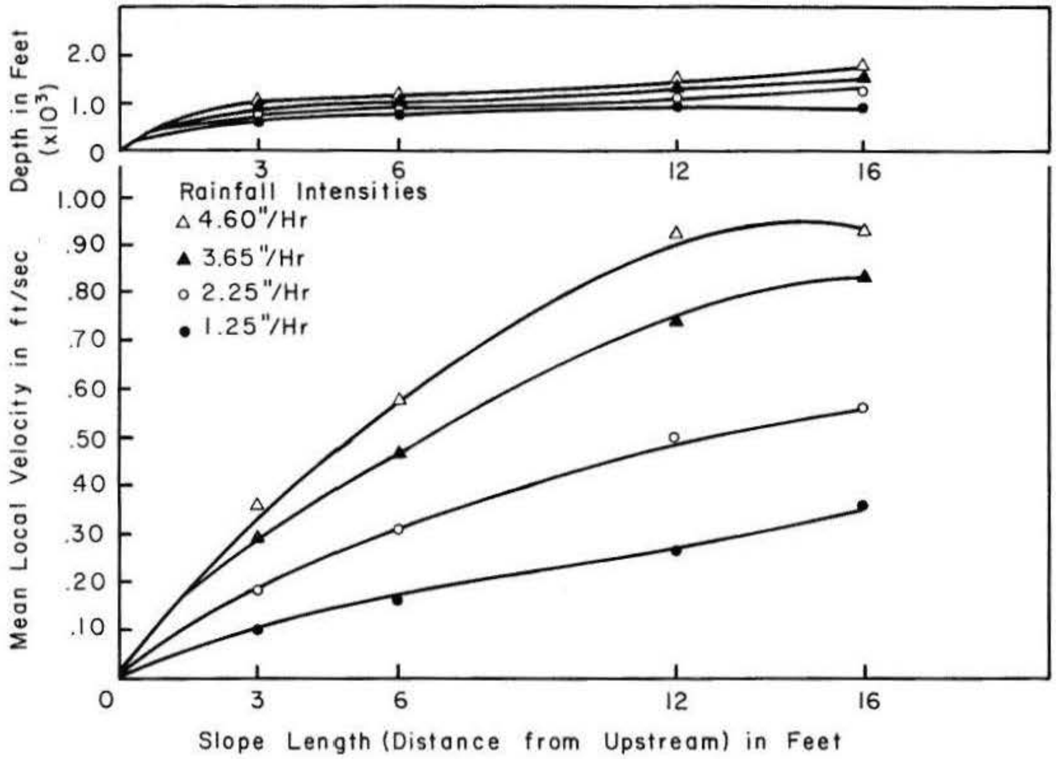

Fig. 26. Mean local velocity and depth related to slope length for given rainfall intensities on 30 percent slope.

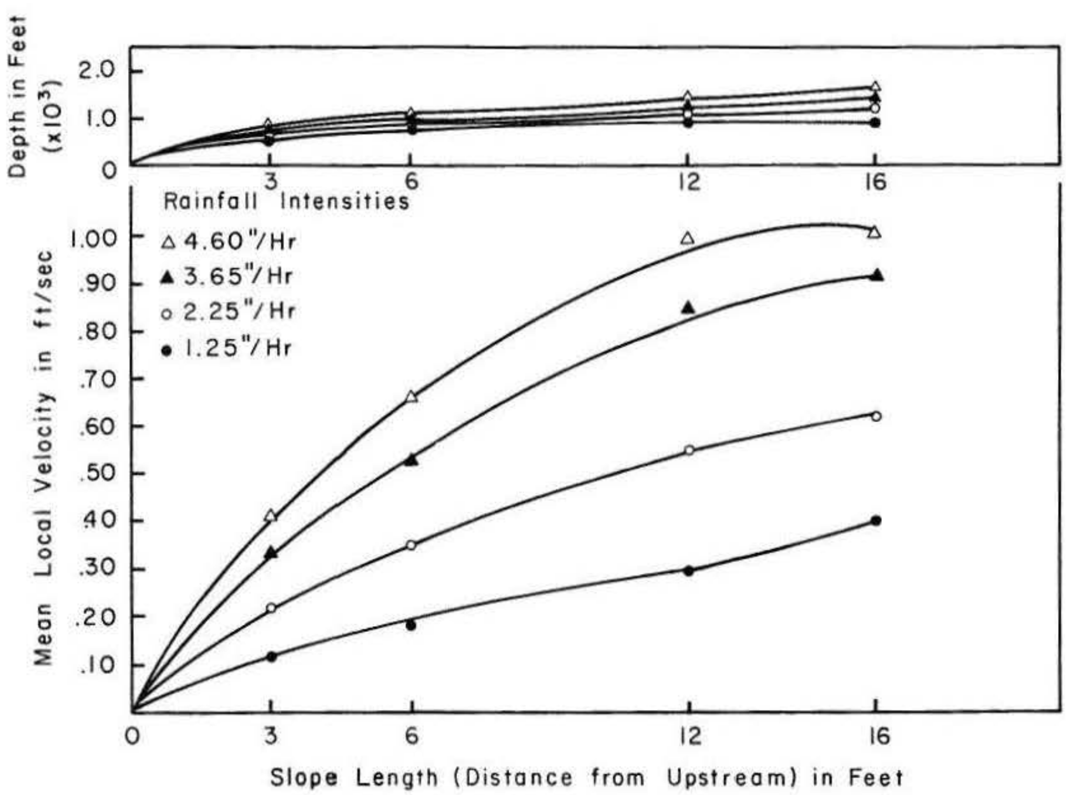

Fig. 27. Mean local velocity and depth related to slope length for given rainfall intensities on 40 percent slope.

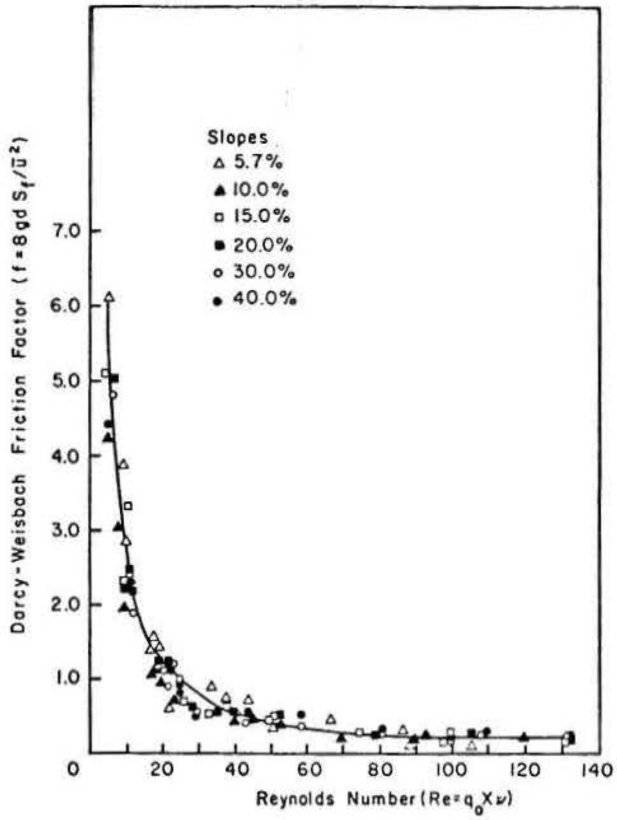

Fig. 28. Relationship between Darcy-Weisbach friction factor, f , and Reynolds number Re for given slopes.

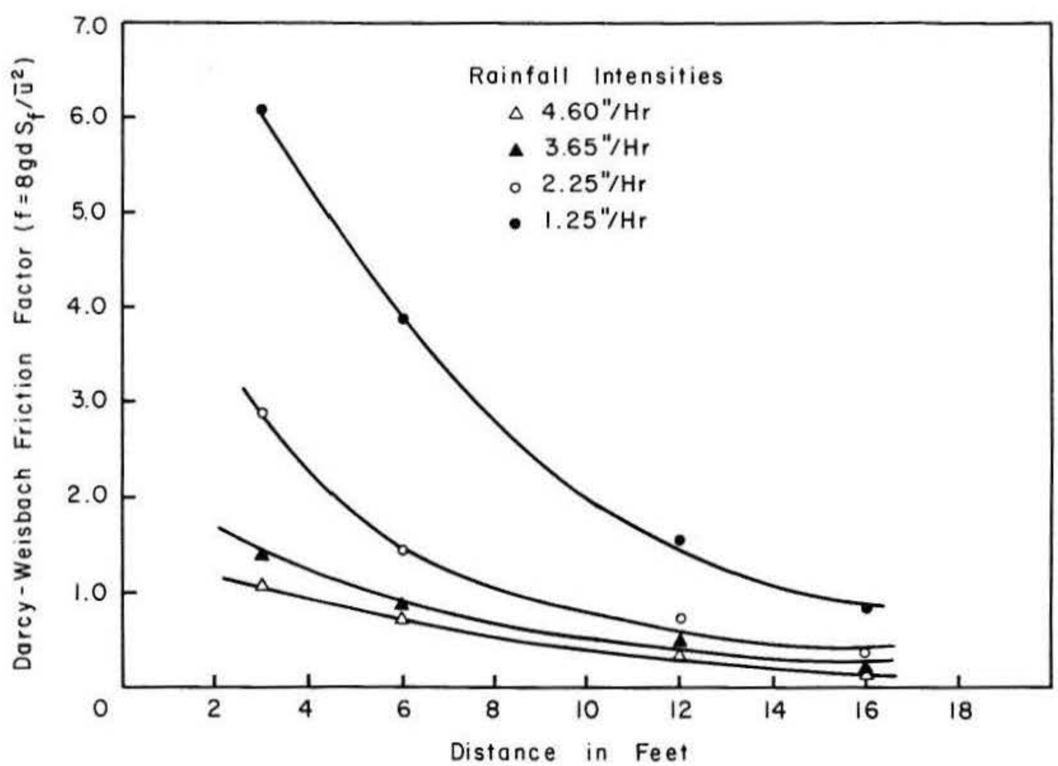

Fig. 29. Relationship between Darcy-Weisbach friction factor and distance for given rainfall intensities on 5.7 percent slope.

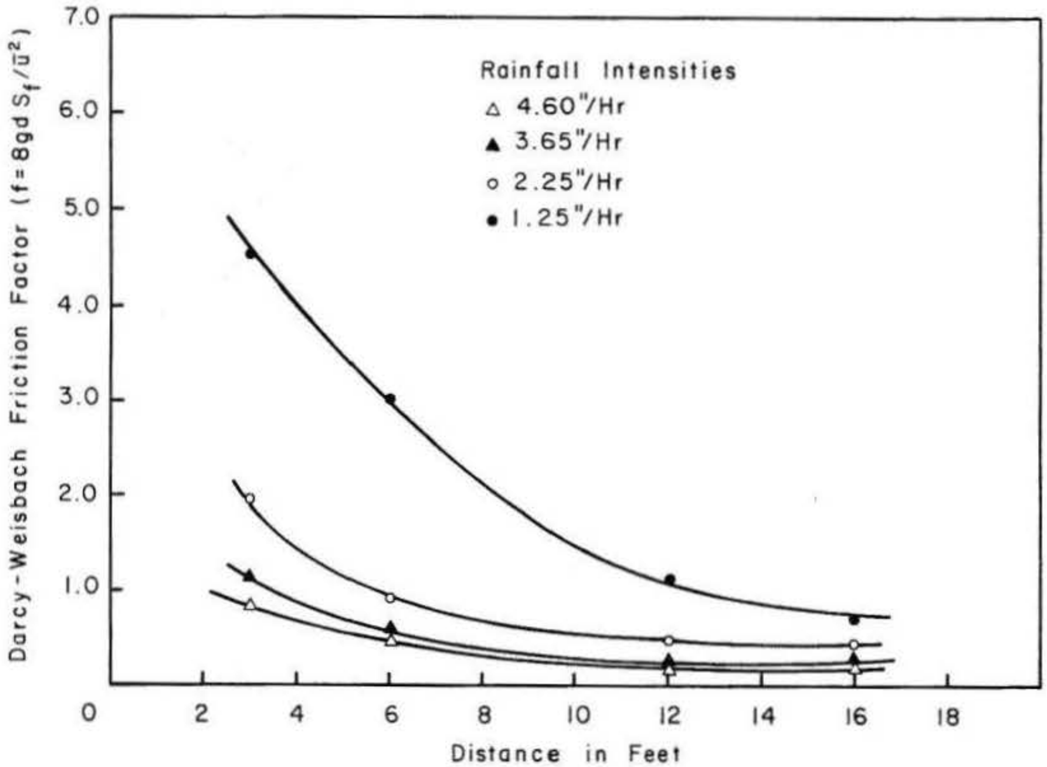

Fig. 30. Relationship between Darcy-Weisbach friction factor and distance for given rainfall intensities on 10 percent slope.

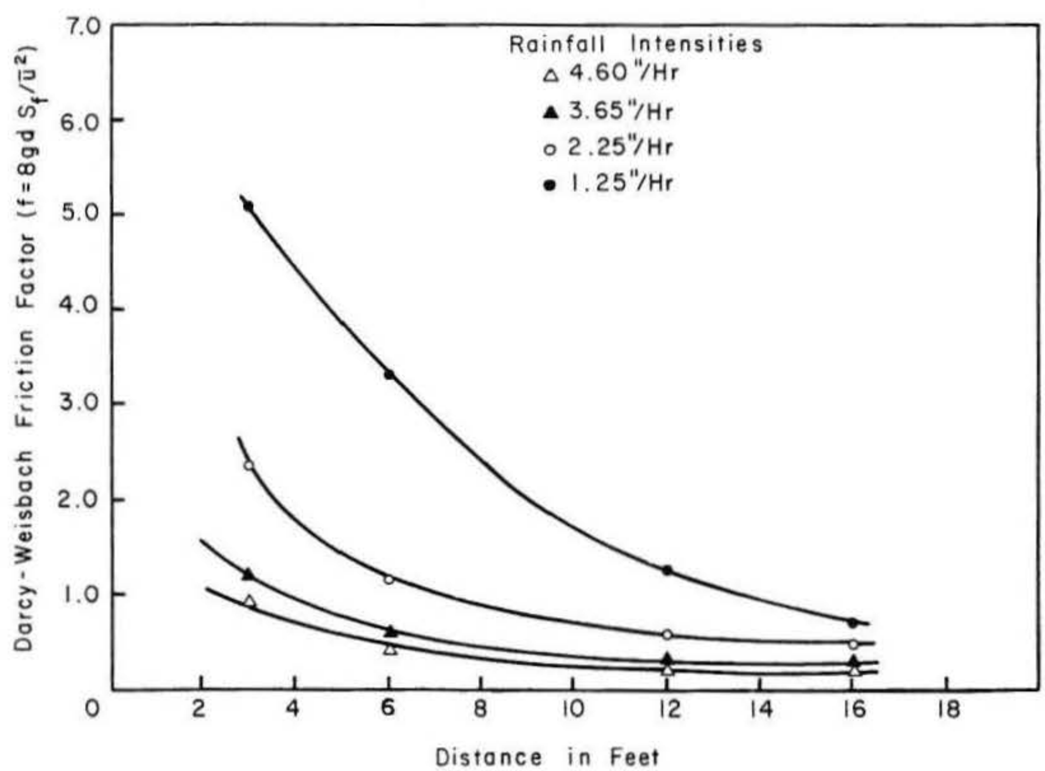

Fig. 31. Relationship between Darcy-Weisbach friction factor and distance for given rainfall intensities on 15 percent slope.

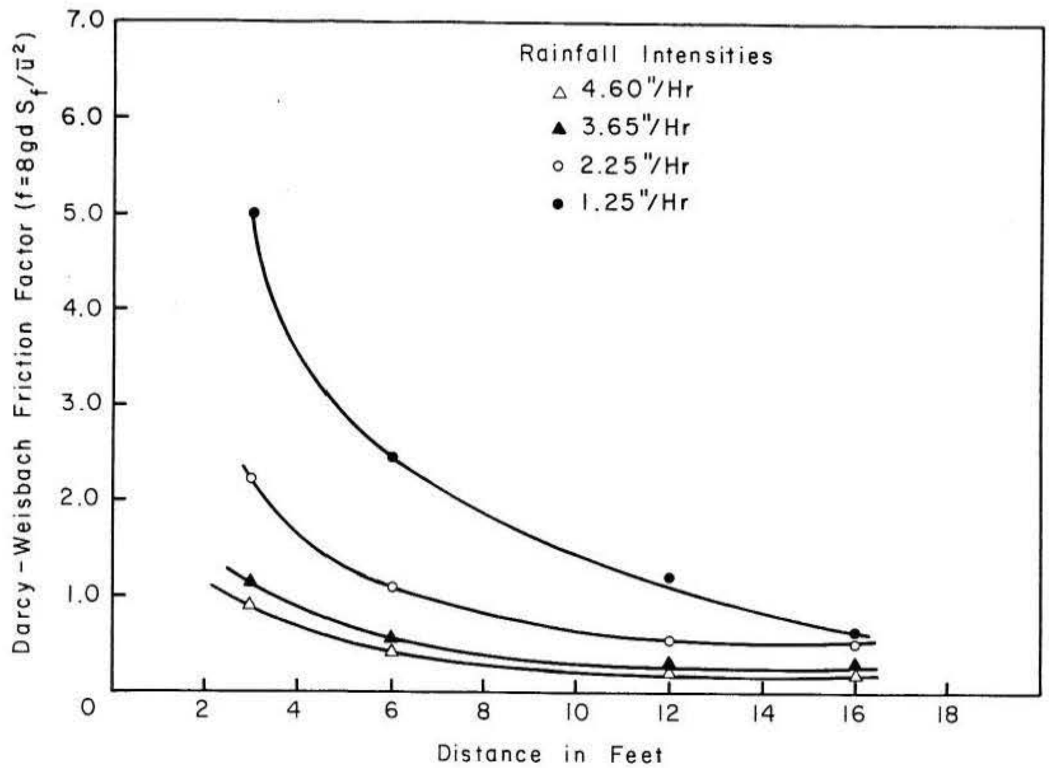

Fig. 32. Relationship between Darcy-Weisbach friction factor and distance for given rainfall intensities on 20 percent slope.

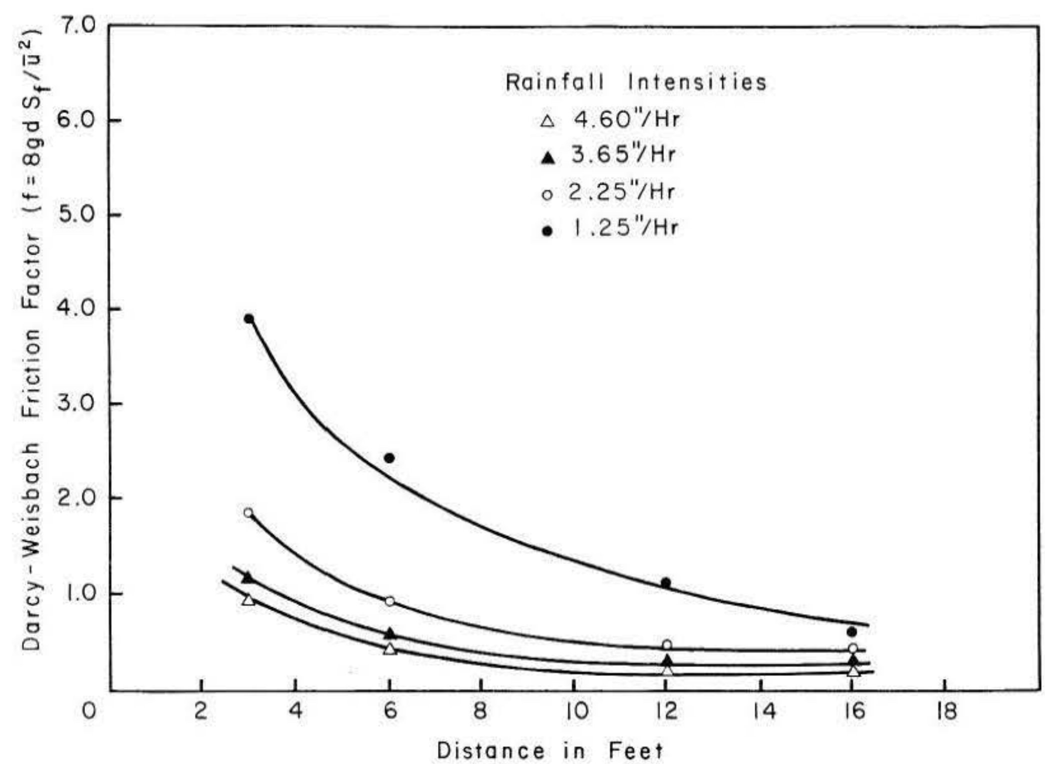

Fig. 33. Relationship between Darcy-Weisbach friction factor and distance for given rainfall intensities on 30 percent slope.

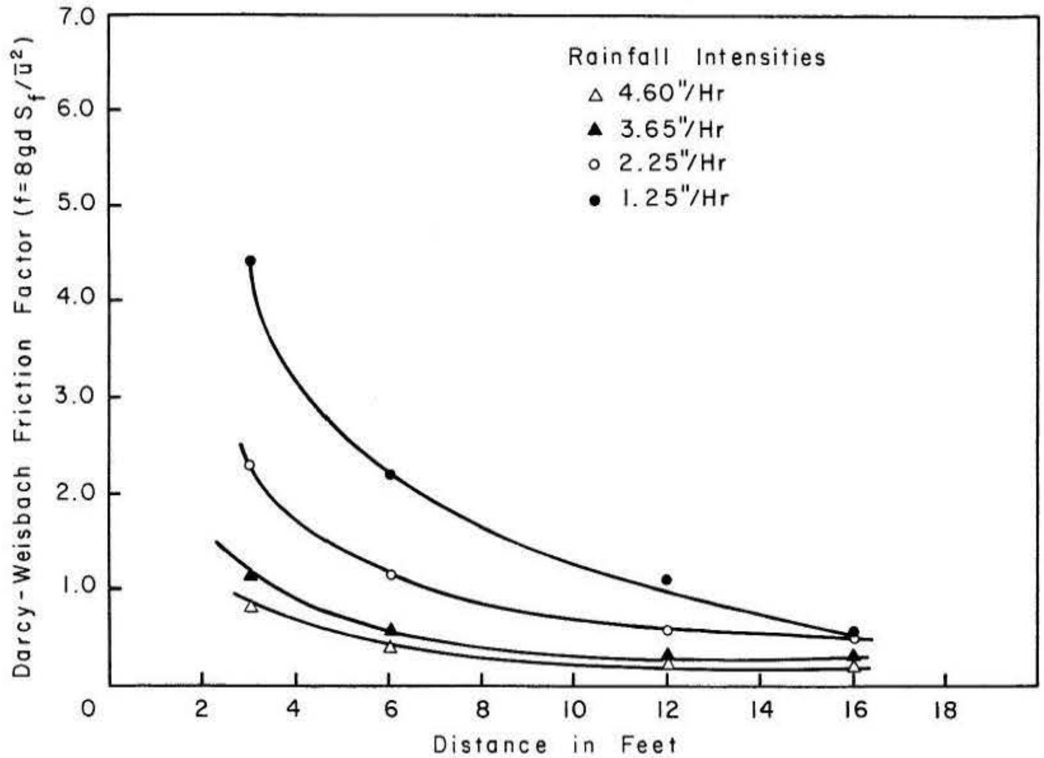

Fig. 34. Relationship between Darcy-Weisbach friction factor and distance for given rainfall intensities on 40 percent slope.

TABLE 13. CORRELATION MATRIX OF MAJOR VARIABLES USED IN STEPWISE NONLINEAR REGRESSION ANALYSIS

Variable	C_s	C_s/A	q_s	E_r	S_o	q_o
Sediment concentration (C_s)	1.000	1.000	.961	.957	.816	.565
Concentration/area (C_s/A)		1.000	.963	.960	.808	.573
Sediment discharge (q_s)			1.000	1.000	.660	.758
Erosion (E_r)				1.000	.649	.766
Slope (S_o)					1.000	.054
Rainfall excess (q_o)						1.000

Variable	q	d_{50}	r	$\bar{u}$	d	ν
Sediment concentration (C_s)	.565	-.819	.524	.891	-.192	-.470
Concentration/area (C_s/A)	.573	-.814	.532	.893	-.181	-.463
Sediment discharge (q_s)	.758	-.685	.727	.968	.060	-.324
Erosion (E_r)	.766	-.677	.735	.969	.073	-.314
Slope (S_o)	.054	-.928	-.000	.571	-.696	-.734
Rainfall excess (q_o)	1.000	-.131	.996	.849	.676	.156
Water discharge (q)	1.000	-.131	.996	.849	.676	.156
Mean diameter of transported sediment (d_{50})		1.000	-.084	-.602	.596	.738
Rainfall intensity (r)			1.000	.819	.710	.174
Mean local velocity ($\bar{u}$)				1.000	.185	-.290
Depth of flow (d)					1.000	.696
Kinematic viscosity (ν)						1.000

the smaller the SEE, the better the equation. The coefficient of determination, R^2, shows to what extent variations of dependent variables were explained by independent variables; thus, the higher the R^2, the better the equation (the range of R^2 is 0 to 1).

Sediment Concentration as a Dependent Variable

The purpose of this computer run was to test whether the sediment concentration was steady or unsteady with respect to time. A one-hour run, therefore, was divided into 6 to 13 time intervals, and instantaneous sediment concentration, C_i, was punched for each interval with corresponding slope, S_o, and intensities of rainfall, r. All values were obtained at the end of 16 feet. The result of the run showed that time did not enter into the multiple regression analysis. There is no significant change of concentration with respect to time. Since this result is significant, it is used in further analysis. Because sediment concentration was steady, sediment transport was also steady. Since sediment concentration was steady, only the averaged values of sediment concentration, C_s, and discharge, Q_s, for each run of a given slope and intensity were used throughout the analyses.

The experimental data showed also that water discharge, velocity, rainfall intensity, and rainfall excess were steady. Consequently, flow was spatially varied with respect to distance but not time. Sediment discharge and concentration varied nonlinearly with respect to distance, water discharge varied linearly with respect to constant rainfall, and infiltration varied linearly with respect to distance.

The first run of C_i as a function of S_o, r, and time gives:

Sequence of regression equations	R^2	SEE	ΔR^2	
$C_i = e^{13.888} S_o^{1.585}$	.6838	.6804	.6838	(109)
$C_i = e^{12.540} S_o^{1.225} r^{1.525}$	.9267	.3284	.2429	(110)

in which

C_i is in ppm,

S_o is in (ft/ft), and

e is the base of the natural logarithm

As seen above, time did not enter the equation at all.

The averaged sediment concentration, C_s, was related to S_o, q_o, $r/\bar{u}$, q, d_{50}, d_{50}/d_{50_o}, d_{50_o}, r, $\bar{u}$, d, ν. The variables which correlated most strongly with C_s were the mean velocity, $\bar{u}$, and slope, S_o. The equations obtained were:

Sequence of regression equations	R^2	SEE	ΔR^2	
$C_s = e^{6.926} \bar{u}^{-2.258}$	.7947	.5615	.7947	(111)
$C_s = e^{9.600} \bar{u}^{.826} S_o^{1.600}$	.9347	.3241	.1400	(112)
$C_s = e^{62.323} \bar{u}^{.558} (r/\bar{u})^{3.196} S_o^{2.330} \nu^{1.823}/d_{50}^{1.127}$	.9515	.3019	.0168	(113)

in which

C_s is in ppm,

$\bar{u}$ is in (ft/sec),

S_o is in (ft/ft),

ν is in (ft^2/sec) and

d_{50} is in millimeter (mm).

Eliminating d_{50}/d_{50_o}, $r/\bar{u}$ from the previous analysis, the equation,

$$C_s = e^{33.022} S_o^{.728} \bar{u}^{1.478} \nu^{2.934}/d_{50}^{1.096} \qquad (114)$$

was correlated with highest R^2, with R^2 equal to .9446 and SEE equal to .3188.

Using slope, S_o, and rainfall, r, with sediment concentration, C_s, the following equations were obtained:

Sequence of regression equations	R^2	SEE	ΔR^2	
$C_s = e^{13.660} S_o^{1.480}$	.6657	.7164	.6657	(115)
$C_s = e^{15.553} S_o^{1.479} r^{1.246}$	.9407	.3089	.2750	(116)

When the units of the variables were changed and analyzed, the same type of equations with the same coefficients and constants were found, as long as C_s was dimensionless.

Because certain variables such as ν, d_{50}, d_b, and X, were constant, no significant correlation between them and sediment concentration could be obtained. However, significant results were obtained when dimensionless forms were tried; for example, X and ν did not give good results. However, when they were used with a Reynolds number of $Re = q_o X/\nu$, there was a high correlation with sediment concentration. A similar result was obtained for sediment discharge for the same reasons. Dimensional analysis was used to group the variables. The Reynolds number and slope were the most important parameters throughout the analysis in correlations with sediment discharge, sediment concentration, or local mean velocity.

Because dimensional analysis of C_s gave $C_s = \phi$ (Re, S_o, roughness), a regressional analysis of C_s as a function of the Reynolds number and slope was run. The equation was:

$$C_s = e^{9.554} Re^{.963} S_o^{1.453} \qquad (117)$$

with R^2 equal to .9220 and SEE equal to .3674.

Sediment concentration, C_s, was divided by the total area of flume and the sediment concentration per unit area, C_s/A, obtained. When C_s/A was analyzed as a function of S_o, q_o, q, d_{50}, r, $\bar{u}$, d. The following sequence of equations was obtained:

Sequence of regression equations	R^2	SEE	ΔR^2	
$C_s/A = e^{2.581}\ u^{2.231}$	.7981	.5487	.7981	(118)
$C_s/A = e^{5.140}\ u^{1.600}\ S_o^{.791}$	.9302	.3302	.1321	(119)
$C_s/A = e^{30.848}\ u^{1.548}\ S_o^{.956}\ \nu^{2.252}$	.9355	.3253	.0053	(120)
$C_s/A = e^{37.19}\ u^{1.475}\ S_o^{.678}\ \nu^{2.957}/d_{50}^{1.153}$	.9409	.3194	.0054 .	(121)

In Eq. (119), R^2, did not increase significantly when more variables than u and S_o were added. The variables $\bar{u}$ and S_o, therefore, are of considerable importance.

Using $r/\bar{u}$, ν and d_{50} along with S_o and u gave the relation:

$$C_s/A = e^{57.669}\ S_o^{2.250}\ (r/\bar{u})^{3.136}\ u^{.572}\ \nu^{.868}/d_{50}^{1.184} \tag{122}$$

with R^2 equal to .9477 and SEE equal to .3088. Using only S_o and r in the prediction equation for C_s/A gave R^2 equal to .94. This is significant inasmuch as they are often the only information available.

Sequence of regression equations	R^2	SEE	ΔR^2	
$C_s/A = e^{9.200}\ S_o^{1.144}$	.6532	.7192	.6532	(123)
$C_s/A = e^{11.095}\ S_o^{1.445}\ r^{1.246}$	.9363	.3156	.2831	(124)

Sediment Discharge as a Dependent Variable

As shown in Table 9, sediment discharge was first calculated in terms of pound per second per foot of width, then converted into different units such as pound per hour, pound per hour per foot of width, pound per second, ton per hour per acre. Sediment discharge was also converted in terms of surface erosion loss in feet per hour, in. per hour, and in. per second. Surface erosion, it will be remembered, was defined as removal of the surface layer of soil in terms of a length unit.

In Table 13, the correlation matrix, R, shows individual correlations between the variables when sediment discharge, q_s, (in terms of pound per second per foot of width) is the dependent variable; slope, S_o; rainfall intensity, r; rainfall excess, q_o; rainfall-velocity ration; $r/\bar{u}$, water discharge, q; mean diameter of transported sediment, d_{50}; transported-original-sediment-diameter ratio, d_{50}/d_{50_o}; mean local velocity, $\bar{u}$; depth of flow, d; and kinematic viscosity, ν; were the independent variables. As can be seen from this table, the mean velocity, $\bar{u}$, was the variable that correlated most closely with sediment discharge, q_s. Rainfall excess and water discharge were the next highly correlated variables.

As discussed previously, some variables did not correlate significantly, because they were constants in these experiments. If these variables did vary during the experiments, some of them, such as original median sediment diameter, d_{50}, kinematic viscosity, ν, and length of slope, X, would be significant for sediment discharge.

The following sequence of equations was obtained from stepwise regression analysis, where variables were individually selected.

Sequence of regression equations	R^2	SEE	ΔR^2	
$q_s = (1/e^{10.56})\ u^{3.625}$	.9372	.4589	.9372	(125)
(where $\bar{u}$ is in inches per second)				
$q_s = (1/e^{9.181})\ u^{3.284}\ S_o^{.428}$	.9544	.4000	.0172	(126)
$q_s = e^{72.670}\ u^{1.506}\ S_o^{3.217}\ (r/\bar{u})^{5.644}$	.9719	.3394	.0175,	(127)

in which

r and $\bar{u}$ are in in. per second, and
d_{50} is in mm.

The analysis above shows that mean velocity contributes almost 94 percent of the variation in sediment discharge. The sediment concentration analysis gave similar results. Sediment concentration, C_s, represents the total sediment discharge, q_s, because the entire overland flow was sampled for sediment concentration at each sampling time.

When the ratio of $r/\bar{u}$ was eliminated and d/d_{50} substituted, the results of the computer analysis were

$$q_s = e^{14.074}\ S_o^{2.585}\ u^{.695}\ d^{4.096}/d_{50}^{1.179}\ , \tag{128}$$

in which R^2 is equal to .9622 and SEE is equal to .3834.

Sediment discharge as a function of slope, S_o, and water discharge, q, yielded

Sequence of regression equations	R^2	SEE	ΔR^2	
$q_s = e^{5.719}\ q^{2.129}$	.5747	1.1945	.5747	(129)
$q_s = e^{8.280}\ q^{2.035}\ S_o^{1.664}$	.9588	.3805	.3841	(130)

in which

- q is represented in terms of in. per second of runoff,
- S_o is represented in terms of percentage and,
- q_s is represented in terms of pounds per second per foot of width.

When q is used in terms of Cfs/ft of width, a similar equation with a different constant is obtained:

$$q_s = e^{11.727}\ q^{2.035}\ S_o^{1.664}\ , \tag{131}$$

in which R^2 is equal to .9588 and SEE is equal to .3805.

The following correlations were obtained when sediment discharge was related to rainfall excess, q_o, and slope, S_o:

Sequence of regression equations	R^2	SEE	ΔR^2	
$q_s = e^{7.667}\, q_o^{2.130}$	.5747	1.1945	.5747	(132)
$q_s = e^{10.504}\, q_o^{2.035}\, S_o^{1.664}$	.9588	.3805	.3841	(133)

in which

q_s is represented in terms of pounds per hour and,
q_o is represented in terms of feet per hour.

Rainfall excess is the exact representation of water discharge because water discharge is equal to rainfall excess times constant slope length ($q = q_o X$).

Sediment discharge in terms of feet per hour was related to rainfall intensity, r, in terms of feet per hour and slope, S_o.

Sequence of regression equation	R^2	SEE	ΔR^2	
$q_s = e^{8.04}\, r^{2.552}$	.5280	1.2584	.5280	(134)
$q_s = e^{11.226}\, r^{2.552}\, S_o^{1.770}$	.9635	.3581	.4355	(135)

Mean local velocity, $\bar{u}$, depth of flow, d, and kinematic viscosity, ν, are correlated with sediment discharge q_s:

Sequence of regression equations	R^2	SEE	ΔR^2	
$q_s = (1/e^{10.564})\, \bar{u}^{3.625}$	.9372	.4589	.9372	(136)
$q_s = (1/e^{13.247})\, \bar{u}^{3.711}/d^{.650}$	.9521	.4104	.0149	(137)
$q_s = (1/e^{36.018})\, \bar{u}^{3.955}\, \nu^{4.634}/d^{1.260}$	.9596	.3860	.0075	(138)

in which

q_s is represented in terms of pounds per second,
$\bar{u}$ is represented in terms of in. per second and,
d is represented in terms of in. per second.

Sediment discharge was analyzed as a function of velocity, $\bar{u}$, the Reynolds number, Re, slope, S_o, depth, d, rainfall excess, q_o, and water discharge, q. The correlations are:

Sequence of regression equations	R^2	SEE	ΔR^2	
$q_s = (1/e^{3.166})\, \bar{u}^{3.625}$	.9372	.4589	.9372	(139)
$q_s = e^{1.239}\, \bar{u}^{4.674}/Re^{.878}$	.9554	.3959	.0282	(140)

in which

$\bar{u}$ is represented in terms of feet per second and,
q_s is represented in terms of pounds per second per foot of width.

Sediment discharge as a function of $\bar{u}$ and q gives:

$$q_s = (1/e^{7.250})\, \bar{u}^{4.360}/q^{.650}, \qquad (141)$$

in which R^2 is equal to .5747 and SEE is equal to 1.1945. The results are exactly the same as those for Eq. (129) except that the constants are different as will always be true if sediment discharge or other variables are expressed in different units for different times. Analysis gives similar correlations with different constants.

Sediment discharge was related to the Reynolds number, Re, and slope, S_o, for the same reason as was sediment concentration analysis. The results are:

Sequence of regression equations	R^2	SEE	ΔR^2	
$q_s = (1/e^{15.295})\, Re^{2.300}$	.6625	1.0641	.6625	(142)
$q_s = (1/e^{11.645})\, Re^{2.054}\, S_o^{1.460}$	.9517	.4119	.2892,	(143)

in which q_s is represented in terms of pounds per second per foot of width. Equation (143) presents the most simple and practical relation. Important factors such as X and ν did not enter into the correlations because they were constant, dimensionless parameters. Re and S_o related to q_s and X; ν therefore entered into the equation.

Sediment discharge was related to tractive force and stream power under the previously assumed models of $q_s = K_n (\tau_o - \tau_c)^n$ and $q_s = K_m ((\tau_o - \tau_c)\, \bar{u})^m$. To find constants, K_n and K_m, and coefficients, n and m, of these models, τ_o needs to be determined. As mentioned before, τ_o was calculated in three ways: (1) uniform flow assumption, (2) using Eq. (43), which was obtained by Li (1972) from statistical analysis, and (3) solving the momentum equation by numerical approximation for τ_o (Eq. 55). The three-way determination of τ_o will result in different values of the constants and coefficients in the models. Moreover, if m and n are assumed to be equal to unity, the models will be linear. For a linear model with τ_o of uniform flow, the relations obtained from computer analysis are:

Linear regression equations	R^2	SEE	ΔR^2	
$q_s = 1.0\, (\tau_o - \tau_c)$	.9222	.0055	.9222	(144)
$q_s = .71274\, (\tau_o - \tau_c)\, \bar{u}$	.9663	.0036	.0441.	(145)

For nonlinear model, with τ_o of uniform flow, the relations are:

Nonlinear regression equations	R^2	SEE	ΔR^2	
$q_s = e^{1.513}\, (\tau_o - \tau_c)^{1.480}$	.8694	.6620	.8694	(146)
$q_s = (1/e^{.327})((\tau_o - \tau_c)\, \bar{u})^{1.089}$	.9598	.4189	.0904.	(147)

If τ_o is calculated using Eq. 43, the following linear and nonlinear model relations are obtained from computer analysis:

Linear regression equations	R^2	SEE	ΔR^2	
$q_s = .19907\, (\tau_o - \tau_c)$	.7377	.0102	.7377	(148)
$q_s = .28052\, (\tau_o - \tau_c)\, \bar{u}$	.9281	.0058	.1904	(149)
$q_s = e^{2.05256}\, (\tau_o - \tau_c)^{2.784}$	.8659	.6339	.8659	(150)
$q_s = e^{.12249}\, ((\tau_o - \tau_c)\, \bar{u})^{1.667}$	.9476	.4216	.0817.	(151)

If τ_o is calculated using the momentum equation (Eq. 55), the following equations are obtained from computer analysis:

Linear regression equations	R^2	SEE	ΔR^2	
$q_s = .33932\ (\tau_o - \tau_c)$	.6184	.01942	.6184	(152)
$q_s = .5357\ (\tau_o - \tau_c)\ \bar{u}$	.8517	.0076	.2433.	(153)
$q_s = e^{2.716}\ (\tau_o - \tau_c)^{2.506}$	.8094	.7997	.8094	(154)
$q_s = e^{.7441}\ ((\tau_o - \tau_c)\ \bar{u})^{1.584}$	.9195	.5196	.1101.	(155)

The analysis showed that nonlinear models yield better correlation than linear models except for the uniform flow assumption. Further, using the more complex methods of computing τ_o (methods 2 and 3) gave no better correlations.

Averaged Surface Erosion Depths as Dependent Variables

Surface erosion, E_r, expressed in terms of feet and in. of surface depth per second per hour, was correlated with given independent variables in the same kind of nonlinear multiple regression analysis. Surface erosion, E_r, it should be noted, is another way of expressing sediment discharge.

The erosion rate was analyzed using the independent variables of slope, S_o; rainfall excess, q_o; rainfall intensity-mean velocity ratio, $r/\bar{u}$; water discharge, q; median diameter of transported sediment-original sediment ratio, d_{50}/d_{50_o}; rainfall intensity, r; mean velocity, $\bar{u}$; depth, d; and kinematic viscosity, ν. All the variables are in terms of feet per hour except d_{50}, which is in mm; d, which is in in.; and viscosity, which is in ft^2 per second. Correlations were obtained from the computer in the following sequence:

Sequence of equations	R^2	SEE	ΔR^2	
$Er = (1/e^{31.735})\ u^{3.593}$	.9388	.4488	.9388	(156)
$Er = e^{17.154}\ u^{3.500}\ \nu^{4.754}/d_{50}^{1.235}\ d^{.615}$	.9608	.3865	.0220,	(157)

in which E_r is measured in feet of eroded soil surface depth per hour. Mean velocity is the first variable entered; d_{50}, ν, and d follow the velocity in the correlation but did not increase R^2 significantly (only abour 2 percent). Although rainfall excess, water discharge, and slope are important factors in erosion, they do not enter into the correlation when velocity is used because velocity has a correlation with them. This means that velocity takes care of the influence of q, q_o, and S_o on correlation.

When $(r/\bar{u})$ was eliminated from the above analysis and the variables were converted into units of in. per second, except for d_{50}, which is in mm, ν, which is in ft^2 per second, and d, which is in feet, almost the same type of relation was obtained except that q entered the equation after $\bar{u}$, d_{50} and ν instead of after d. The equation is

$$E_r = e^{31.412}\ \bar{u}^{-4.115}\ \nu^{4.754}/d_{50}^{1.235}\ q^{.615}, \qquad (158)$$

in which R^2 equals .9608 and SEE equals .3865. If Eq. (61) is compared with Eq. (62), the only difference between the two is that q is selected by the computer instead of d, with the same coefficient as before because both have the same partial correlation coefficient. Therefore, the computer picks one of them with the same effectiveness it did in the correlation of erosion. Thus, one of them may be written for the other.

When $(r/\bar{u})$, $\bar{u}$, d and ν were eliminated, diferent equations were obtained. Erosion, E_r, was correlated to S_o, q_o, q, d_{50}/d_{50_o}, and r in terms of feet per hour, except that d_{50} is in mm and S_o and d_{50}/d_{50_o} are dimensionless. Because $\bar{u}$ was not in the analysis, the first variable entered into the correlation was q_o, with the following sequences:

Sequence of regression equations	R^2	SEE	ΔR^2	
$Er = (1/e^{1.254})\ q_o^{2.130}$	.5866	1.1663	.5866	(159)
$Er = e^{1.506}\ q_o^{2.038}\ S_o^{1.618}$	.9571	.3845	.3705	(160)
$Er = (1/e^{.022})\ q_o^{2.013}\ S_o^{1.338}/d_{50}^{.920}$	.9588	.3860	.0017.	(161)

When the second variable, S_o, entered into the correlation, it increased the result by 37 percent. The last variable entered was d_{50}; it did not change R^2 significantly.

When the above variables were converted into units of in. per second, the same equations with the same coefficients were obtained. Of course the constants were different.

Sequence of regression equations	R^2	SEE	ΔR^2	
$Er = e^{7.429}\ q_o^{2.038}\ S_o^{1.618}$	.9571	.3845	.9571	(162)
$Er = e^{5.754}\ q_o^{2.013}\ S_o^{1.338}/d_{50}^{.920}$	.9588	.3860	.0017	(163)

Erosion, E_r, as a function of only slope, S_o, and water discharge, q, gave the following sequence of regression equations:

Sequence of regression equations	R^2	SEE	ΔR^2	
$Er = (1/e^{1.254})\ q^{2.130}$	.5860	1.1663	.5860	(164)
$Er = e^{1.506}\ q^{2.038}\ S_o^{1.618}$	.9571	.3845	.3705,	(165)

in which

E_r is in feet of eroded soil surface per hour,
q is in feet per hour (depth of runoff), and
S_o is in percent.

Equations (159) and (160) are exactly the same as Eqs. (164) and (165) because q is an exact representation of q_o.

The variables, although in different units, give the same type of correlation, except for the constant, as follows:

$$E_r = e^{1.778}\ q^{2.038}\ S_o^{1.618}, \qquad (166)$$

in which

E_r is in in. of eroded soil per second,

q is in in. per second, and

R^2 equals .9571 and SEE equals .3845.

Thus, sediment discharge, q_s, sediment concentration, C_s, and erosion, E_r, produce similar correlations when independent variables are used.

Median Transported Sediment Diameter, d_{50}, as Dependent Variable

Median transported sediment diameter, d_{50}, for each run was related to slope, S_o, and intensity of rainfall, r. The correlations are:

Sequence of regression equations	R^2	SEE	ΔR^2	
$d_{50} = 1/e^{1.617} S_o^{.306}$	.8612	.0840	.8612	(167)
$d_{50} = 1/e^{1.673} S_o^{.306} r^{.037}$	.8683	.0838	.0071,	(168)

in which

d_{50} is in mm, and

r is in feet per hour.

The slope was the first to enter the equation and produced a high negative correlation. In this run, r, when entered, was not significant at all. Negative correlation of d_{50} with slope could be explained by the fact that finer sediments are washed down faster than coarser sediments on a steeper slope because of the lack of cohesiveness of the particles. Different units of r only change the value of the constant as follows:

$$d_{50} = 1/e^{1.880} S_o^{.306} r^{.037}, \qquad (169)$$

with R^2 equal to .8683 and SEE equal to .0838, and with r in in. per second.

A computer analysis to obtain a relation for d_{50} as a function of the remaining independent variables resulted in

$$d_{50} = e^{8.148} r^{.045} \nu^{.768}/(C_s/A)^{.078} S_o^{.145}, \qquad (170)$$

with R^2 equal to .8908 and SEE equal to .0812, with r in in. per second.

Mean Velocity of Overland Flow as a Dependent Variable

The results of statistical analysis up to this point show that velocity is one of the variables most highly correlated to sediment discharge, concentration, and erosion. But variables are correlated with velocity; that is, although velocity was assumed to be an independent variable with regard to sedimentation, it, in turn, is dependent upon slope, rainfall intensity or excess, and surface roughness. An analysis of such variables will, therefore, help in determining which variables correlated with velocity correlated significantly with sediment discharge, sediment concentration, and erosion.

So far this distance, X, has not been included as a variable in the analysis. Now the distance, X, is entered into the analysis by using measured velocities at distances of 3, 6, 12 and 16 feet, so that velocity appears as a function of distance as well as of other independent variables. Velocity as a function of slope, S_o, rainfall excess, q_o, depth of flow, d, kinematic viscosity, ν, and distance, X, gives the following sequence of regression equations:

Sequence of regression equations	R^2	SEE	ΔR^2	
$\bar{u} = e^{5.220} q_o^{.663}$	.4054	.5081	.4054	(171)
$\bar{u} = e^{4.160} q_o^{.663} X^{.592}$	.6714	.3805	.2660	(172)
$\bar{u} = (1/e^{5.782}) q_o^{1.156} X^{1.236}/d^{1.902} S_o^{.484}$	.8548	.2567	.1834	(173)
$\bar{u} = (1/e^{24.733}) q_o^{1.188} X^{1.238}/d^{1.910} S_o^{.596} \nu^{1.691}$	.8641	.2502	.0093	(174)

in which

$\bar{u}$ is in feet per second at a given distance,

q_o is in feet per second,

d is in feet.

The most significant variables are q_o and X. The slope gives negative correlation because d enters into the equation before S_o, so that slope and d are related with each other in negative correlation.

When d is eliminated from the above analysis, the result is:

Sequence of regression equations	R^2	SEE	ΔR^2	
$\bar{u} = e^{5.220} q_o^{.663}$	.4054	.5081	.4054	(175)
$\bar{u} = e^{4.160} q_o^{.663} X^{.592}$	.6714	.3805	.2660	(176)
$\bar{u} = e^{4.625} q_o^{.641} X^{.592} S_o^{.375}$	.8138	.3082	.1424	(177)
$\bar{u} = (1/e^{13.98}) q_o^{.641} X^{.592} S_o^{.375}/\nu^{1.664}$	.8228	.2886	.0090	(178)

Equations (177) and (178) are similar to Eq. (36), derived analytically, except for the constant and the coefficients, which differ slightly. When d is removed from analysis, the slope is positively correlated with velocity.

Finally, as with C_s and q_s, velocity, $\bar{u}$, was also run through the computer as a function of Re and S_o. Reynolds number, Re, was the most highly correlated independent variable, accounting for 70.4 percent of the variation in this analysis. The correlations are:

Sequence of regression equations	R^2	SEE	ΔR^2	
$\bar{u} = (1/e^{3.37691}) Re^{.651}$	.7042	.3584	.7042	(179)
$\bar{u} = (1/e^{2.69687}) Re^{.627} S_o^{.336}$	.8177	.2834	.1135	(180)

In subsequent sections the calculated velocities in Eq. (180) will be compared with measured velocities.

Depth of Flow as Dependent Variable

Depth as a function of X , q_o , S_o and ν gives the following equations:

Sequence of regression equations	R^2	SEE	ΔR^2	
$d = (1/e^{7.502})/S_o^{.438}$	.5395	.2683	.5395	(181)
$d = (1/e^{8.110})\ X^{.340}/S_o^{.438}$	.7811	.1865	.2416	(182)
$d = (1/e^{5.472})\ X^{.540}\ q_o^{.271}/S_o^{.452}$	.9685	.0712	.1874	(183)

Kinematic viscosity, ν , did not enter into regression. Depth of flow is related to slope, as opposed to velocity, in negative correlation. When slope becomes steeper, flow changes from subcritical to supercritical.

Depth as a function of Reynolds number, Re , and slope, S_o , was correlated first with S_o , before Re becomes negative correlation. The equations are:

Sequence of regression equations	R^2	SEE	ΔR^2	
$d = (1/e^{7.502})/S_o^{.438}$	.5394	.2683	.5394	(184)
$d = (1/e^{8.537})\ Re^{.304}/S_o^{.473}$	.9632	.0768	.4237	(185)

Throughout all of the analyses, ν had no significance because it was constant. Velocity, rainfall excess, slope, and Reynolds number are the important variables, those significantly correlated to sediment discharge, sediment concentration, and erosion. Although length of slope, X , is an important factor affecting sediment discharge and erosion, it could not be tested in this analysis because it had almost a constant value during all runs excpet for a slight change with slope. This is one of the limitations inherent in the study which future research should eliminate.

RILL ANALYSIS

Rill erosion starts by channeling flow through microchannels smaller than rills. If channels can be obliterated by tillage they are called rills; if they cannot be, they are called gullies. Thus, a rill is an advanced stage of sheet erosion, whereas a "gully" is an advanced stage of rill. The rate of rill erosion depends mainly on rainfall intensity, slope of surface, properties of soil, and surface conditions (roughness, vegetation, tillage, etc.). Predicting rill and gully development is not easy because the factors affecting rill and gully development are not well defined (Schwab, et al., 1966).

In this section the values and the ratios obtained from rill observations were analyzed by computer in terms of given independent variables. In the following analyses, rainfall intensity, r , and rainfall excess, q_o , are expressed in terms of ft/sec; water discharge, q , is expressed in terms of cfs/ft of width; Re and S_o are dimensionless; rill area/total area ratio, A_R/A_T , and total volume/rill volume ratio, V_R/V_T , are dimensionless; averaged depth of gully, D_R , is expressed in terms of ft/hr/ft of width; and volume of gully, V_R , is expressed in terms of ft^3/hr/ft of width.

Rill/Surface Area Ratio as a Dependent Variable

The surface area of rills for each run divided by the total area of flume surface gives the rill/area ratio, A_R/A_T . This ratio is analyzed in terms of surface slope, rainfall intensity, rainfall excess, water discharge, and Reynolds number.

Neglecting q_o , q , and Re , the A_R/A_T ratio as a function of r and S_o gives:

Sequence of regression equations	R^2	SEE	ΔR^2	
$A_R/A_T = (1/e^{1.597})\ r^{.415}$	.7052	.1398	.7052	(186)
$A_R/A_T = (1/e^{1.269})\ r^{.415}\ S_o^{.183}$	.9400	.0645	.2348	(187)

Thus, rainfall intensity explains 70.5 percent of all variations in the rill area ratio.

Eliminating r , q , and Re , the ratio A_R/A_T as a function of q_o and S_o gives:

Sequence of regression equations	R^2	SEE	ΔR^2	
$A_R/A_T = e^{2.146}\ q_o^{.340}$	.7418	.1308	.7418	(188)
$A_R/A_T = e^{2.352}\ q_o^{.331}\ S_o^{.165}$	.9341	.0676	.1923	(189)

The ratio A_R/A_T as a function of q and S_o yields:

Sequence of regression equations	R^2	SEE	ΔR^2	
$A_R/A_T = e^{1.204}\ q^{.340}$	.7418	.1308	.7418	(190)
$A_R/A_T = e^{1.435}\ q^{.331}\ S_o^{.165}$	.9341	.0676	.1923	(191)

The A_R/A_T ratio as a function of slope and Reynolds number yields the following dimensionless form of correlation:

Sequence of regression equations	R^2	SEE	ΔR^2	
$A_R/A_T = (1/e^{2.686})\ Re^{.356}$	.7975	.1158	.7975	(192)
$A_R/A_T = (1/e^{2.345})\ Re^{.338}\ S_o^{.14357}$	.9406	.0142	.1431	(193)

The Reynolds number is the variable most correlated to A_R/A_T , with almost 80 percent of the variations explained by it. Water discharge gives the same correlation as rainfall excess with a dependent variable, excluding the constant. Therefore, q was eliminated from further analyses.

Averaged Rill Depth as a Dependent Variable

Depths of rills measured at the end of each run were averaged as representative of each run. These averaged values were correlated to the independent variables of rainfall intenstiy, slope, rainfall excess, and Reynolds number. The results of the analysis of rill depth as a function of given variables have been combined and given simultaneously.

Rill depth, D_R, was first related to r and S_o, then to q_o and S_o, and finally to Re and S_o. The slope was kept in the analysis for each trial, while the other independent variables were changed. The sequence of correlations obtained from these analyses is as follows:

Sequence of regression equations	R^2	SEE	ΔR^2	
$D_R = (1/e^{7.639})\ r^{2.748}$	.5179	1.3829	.5179	(194)
$D_R = (1/e^{4.106})\ r^{2.748}\ S_o^{1.964}$	.9720	.3414	.4541	(195)
$D_R = e^{17.598}\ q_o^{2.296}$	.5654	1.3131	.5654	(196)
$D_R = e^{19.894}\ q_o^{2.191}\ S_o^{1.850}$	.9674	.3683	.4020	(197)
$D_R = (1/e^{15.184})\ Re^{2.440}$	.6256	1.2187	.6256	(198)
$D_R = (1/e^{11.188}L\ Re^{2.219}\ S_o^{1.708}$	.9637	.3883	.3381	(199)

Rill Volume, V_R and Rill Volume/Total Erosion Volume Ratio, V_R/V_T, as Dependent Variables

Rill volume was then related to slope, rainfall intensity, rainfall excess, and Reynolds number, and the independent variables were correlated to the rill/erosion ratio, V_R/V_T, in the same way previously mentioned in this section. The analysis of V_R with these variables yields correlations as follows:

Sequence of regression equations	R^2	SEE	ΔR^2	
$V_R = (1/e^{6.464})\ r^{3.163}$	.5494	1.4939	.5494	(200)
$V_R = (1/e^{2.602})\ r^{3.163}\ S_o^{2.147}$	.9838	.2900	.4144	(201)
$V_R = e^{22.517}\ q_o^{2.636}$	.5968	1.4131	.5969	(202)
$V_R = e^{25.018}\ q_o^{2.522}\ S_o^{2.016}$	.9789	.3305	.3821	(203)
$V_R = (1/e^{15.096})\ Re^{2.800}$	.6580	1.3015	.6580	(204)
$V_R = (1/e^{10.765})\ Re^{2.557}\ S_o^{1.851}$	.9763	.3510	.3183	(205)

The rill/erosion ratio, V_R/V_T, as a function of given independent variables yields:

Sequence of regression equations	R^2	SEE	ΔR^2	
$V_R/V_T = (1/e^{2.015})\ r^{.610}$	.5790	.2711	.5790	(206)
$V_R/V_T = (1/e^{1.337})\ r^{.610}\ S_o^{.376}$	.9579	.0877	.3789	(207)
$V_R/V_T = e^{3.552}\ q_o^{.506}$	.6242	.2561	.6242	(208)
$V_R/V_T = e^{3.988}\ q_o^{.486}\ S_o^{.351}$	.9532	.0925	.3290	(209)
$V_R/V_T = (1/e^{3.674})\ Re^{.538}$	.6904	.2325	.6904	(210)
$V_R/V_T = (1/e^{2.927})\ Re^{.496}\ S_o^{.319}$	.9585	.0871	.2681	(211)

The Reynolds number is, once again, one of the most important parameters in predicting rill geometry. Rainfall intensity, or rainfall excess, or water discharge and slope are the second and third most important parameters. The dimensionless form of the correlations is important in comparing this study with any other study. Therefore, special emphasis is given to the equations that are in dimensionless form, especially those including Reynolds number and slope.

DISCUSSION OF RESULTS

In this section, figures are explained and discussed briefly, and selected prediction equations are explained with application and comparison. Predicted values versus measured values are plotted and compared for sediment discharges, mean local velocity, and gully geometry. Finally, field application of the erosion-loss-prediction equation is explained, with its limitations and advantages.

ANALYTICAL RESULTS

Longitudinal Mean Local Velocity Profile

Equation (36), suggested by a simplification of the Navier-Stokes equation for parallel flow, indicates velocity could be approximated by parabolic curve. It was found that Eq. (36) and regression Eq. (178) derived from data are comparable. Therefore, Newton's law of viscosity is applicable for spatially varied, steady overland flow under rainfall with low Reynolds number. It appears that the parabolic vertical velocity profile is a good approximation of overland flow under rainfall.

Sediment Transport Equations

Sediment-transport equations developed by dimensional analysis, computer analysis of data, and model assumptions are similar in general form. They are also comparable for their terms in a physical sense. Equation (89) is a dimensionless form of sediment-transport equation as a function of Reynolds number, slope, porosity, and roughness characteristics. Equation (143) is the prediction equation of sediment discharge developed from regression analysis of data in terms of Reynolds number and slope. A comparison of the two equations shows that terms included in the equations are identical except that porosity and roughness were entered as a constant in Eq. (143). Equations (74) and (155) represent a model, and an equation obtained from a model, respectively, for sediment transport in terms of stream power. Although terms of Eq. (143) look different from terms of Eq. (155), their physical significance is similar.

Equation (143) contains slope, viscosity, and Reynolds number, which includes rainfall excess and flow length or water discharge. Equation (155) contains mean velocity and tractive force which includes depth of flow, viscosity, and slope. Thus, both Eq. (143) and Eq. (155) include water discharge, viscosity, and slope.

The results of dimensional analysis, regression analysis of data, and assumed model, then, are found to be similar.

FIGURES AND SIGNIFICANT RELATED VARIABLES

This section highlights the significance of figures and variables related to sediment transport. Their significance lies in showing a single correlation between dependent and independent variables, which in turn shows the general trend of relationships. Data plotted in these figures were also analyzed in multiple correlation, from which regression equations were selected.

Sediment Concentration Versus Time

Figures 6 to 11 show the change of instantaneous sediment concentration, C_i , with time on 5.7- to 40-percent slopes with a given rainfall intensity. Averaged values of C_i were calculated for the entire 60 minites, the first 30 minutes, and the last 30 minutes for all runs. There were no significant differences between the three averaging methods, and the average concentration as calculated from the 60-minute record was used in all computations.

A statistical analysis was also performed on the concentration-versus-time data. For all runs C_i was found to be independent of time. In some of the figures C_i varied with t for short periods of time. These variations were believed to be the result of the formation of rills but no comprehensive study of rills was done. Also, in many of the runs steady-state conditions were not reached during the first few minutes.

Slope and Intensity of Rainfall

Figures 12 to 19 show the relationship between sediment yield in different units on different slopes for given intensity of rainfall. These figures have essentially the same meaning, since it was only sediment transport that was expressed in different units; therefore, the shapes of the figures are similar. Sediment yield (erosion loss) increased slightly with slope, almost in a straight line at the lesser intensity of 1.25 in. per hour, but increasing rapidly at the higher intensities of 2.25, 3.65 and 4.60 in. per hour. Rainfall intensity of 1.25 in. per hour may be very near critical rainfall (that intensity which starts erosion) for the type of soil studied in this experiment. Therefore, increases in slope do not materially increase erosion loss with this intensity of rainfall. Erosion loss increased relatively more slowly with slopes up to 15 than with slopes between 15 and 35. After slope of 35, erosion loss seems to be less again.

Among the most important factors affecting erosion loss are steepness and length of slope. The present study (Eq. 131) found the rate of erosion to change with 1.66 power of slope steepness.

Water Discharge

Figure 20 shows that sediment discharge increased slowly with increasing water discharge on slopes of 5.7 to 15 percent but increased rapidly on slopes of 20 to 40 percent. Figure 21 shows that water discharge was constant and steady with respect to slope.

Mean Local Velocity, Depth of Flow Versus Length of Slope

Figures 22 to 27 show the relation between length of slope and mean velocity, or mean depth, for given slope and intensity of rainfall. Velocity increased nonlinearly with increment of slope length. Depth of flow increased more with slope length on smaller slopes than on larger slopes. Mean velocity of overland flow increased with .59 power of slope length and .375 power of slope steepness, according to data analysis, and .666 power of slope length and .333 power of slope steepness, according to the analytical analysis using the parabolic vertical velocity assumption. Thus, those assumptions are justified by data analysis. Because of the steep but short segment of slope and very shallow depth of water, the flow can be said to be greatly influenced by viscosity; therefore, flow is laminar.

Flow Properties, Reynolds Number, and Froude Number

As shown in Table 8, Reynolds numbers are very small (less that 130), while Froude numbers are high (0.6 to 5.4). According to these Froude numbers, most of the flows were supercritical; it is an unusual phenomenon to find supercritical laminar flow in practice, yet according to the Reynolds number and critical Reynolds number given by Chen and Chow (1968), the flow of the present study falls into this supercritical-laminar-flow class. Although this flow is continuously disturbed by raindrops, it is not a turbulent flow, because 1) the Reynolds number is low and 2) perturbations of flow by the raindrops die out as soon as raindrop impact is diminished. This flow probably represents the beginning of a laminar-sublayer of an undeveloped turbulent flow; it will be termed in this study agitated supercritical laminar flow.

Figure 28 shows a relationship between Re and f . Figures 30 to 34 show a relationship between f and distance, X , for given rainfall intensities on given slopes. Friction factors, which are taken from Table 9, are exponentially decreasing with Reynolds number and distance, especially under higher intensities of rainfall.

PREDICTION EQUATIONS

In the following sections, prediction equations, derived both from the computer analysis of data and from analysis, are presented for velocity, sediment discharge and concentration, and gully geometry. Selected prediction equations are listed in Table 14. The discussion compares theory and measured values with predicted values. One of the most important objectives, of course, is to show how to predict soil loss from overland flow; therefore, special consideration is given to predicting sediment discharge. Because mean velocity of overland flow as an independent variable is one of the basic factors affecting sediment discharge, more attention is given to velocity than to other independent variables, so that the phenomenon can be better understood.

Velocity is important not only in sediment transport but also in boundary shear and stream power, factors which determine the rate of sediment discharge. Although tractive force, velocity, and stream power are important, it is very difficult to measure or evaluate them for overland flow generated by rainfall. Therefore, regression equations with slope, water discharge, rainfall excess, and Reynolds number, which are easier to measure, are useful to predict sediment discharge. Moreover, velocity and shear stress are related to the variables above. Thus, the slope, the Reynolds number (which includes rainfall excess), and the distance are the dominant parameters for any prediction equation presented in these sections.

Mean Velocity of Overland Flow

With the assumption of $S_f = S_o$, mean velocities were calculated using analytical Eq. (36). Predicted values were plotted against measured mean velocities at given distances, slopes, and rainfall intensities, as shown in Table 15 and Figs. 35 and 36. In the figures, the difference between the perfect line (the line with a 45° axis) and the actual line shows that predicted values are less than measured values. These differences come from the assumption of $S_f = S_o$, because S_f is always greater than S_o for spatially varied flow, especially under rainfall impact. According to Eq. (36), the greater the S_f , the higher the velocity. So, although there are discrepancies, Eq. (36) gives fairly good approximations. If S_f were evaluated, much better results could be obtained. The correlation between measured values (Table 10) and predicted values (Table 36) is very high, with R^2 equal to .9885.

The second prediction equation used was regression Eq. (180); from it mean local velocities of overland flow were calculated and then plotted at given distances, slopes, and intensities, as shown in Table 16 and Figs. 37 and 38. Comparison of the predicted values shown in Table 37 with the measured values shown in Table 10 indicates that predicted values are slightly less than measured values except for velocities at 16 feet, which are almost the same. These differences, shown in Figs. 37 and 38, come from regression Eq. (180). This could explain only 82 percent of the variation of velocities, having R^2 of .8177, and thus leaving 18 percent still unexplained. Although predicted values of velocities differ from their measured values, the correlation among them, with R^2 equal to .9880, is very high.

Equation (178), derived from data analysis, was not used to predict velocity because of its similarity to Eq. (180); however, it does show near agreement with coefficients of Eq. (36), derived analytically (see Table 14). This comparison helps to clarify the mathematical model of overland flow-velocity variation under rainfall.

Computing mean velocity using Eq. (36) as a mathematical model of overland flow means assuming laminar and parallel flow for short increments of distance. In a future study, a mathematical model should be derived for turbulence flow as well.

Sediment Concentration and Erosion Depth

Sediment concentration, sediment discharge, and erosion depth all have the same physical significance in relating independent variables, because sediment concentration is a dimensionless form of sediment discharge and erosion depth is the conversion of sediment weight into depth of surface. Therefore, selected equations for predicting discharge (but not sediment concentration and erosion depth) were used here, since all three are simply different ways of representing erosion loss.

Sediment Discharge

The sediment transport model, Eq. (74), whose coefficients and constant were determined by data analysis in Eq. (155), was used to predict sediment discharges for each run, which were then plotted against measured values. Next, sediment discharges were predicted and plotted using Eq. (143). Predicted values and measured values comparing the two methods are listed in Table 17. The plots of predicted versus measured values are shown in Figures 39 and 40. Both tables and figures show that predicted values of sediment discharges are less than measured values. A comparison of predicted values obtained by Eqs. (143) and (155) with measured values of sediment transport gives a high correlation, having R^2 equal to .983 and R^2 equal to .97, respectively. Although correlation between predicted and measured values is very high, there are certain limitations in the use of these equations. First, Eq. (155) depends on the calculation of τ_o , which is based on velocity measurements; the effect of velocity changes on τ_o is thus very significant. Therefore, the evaluation of τ_o , as well as measurement of velocities, is important. Secondly, Eq. (143) was obtained from the analysis of data collected on the model experiment under simulated rainfall. It is not known how well simulated rainfall represents the natural rainfall of a particular region, or how much erosion due to laminar overland flow from disturbed sandy soil over uniform slope represents erosion over undisturbed natural soil. Moreover, the length of slope did not vary during the experiment, although its effect on erosion is quite significant.

In spite of the fact that limitations are important, the models are good enough to enable us to understand the mechanism of soil erosion and to approximate soil loss under similar conditions. Throughout the data analysis, the Reynolds number, slope, and velocity were important factors affecting erosion and sediment discharges, especially the Reynolds number, which is defined as $Re = q_o X/\nu$ and includes rainfall excess, distance, and kinematic viscosity. As an earlier section shows, the whole problem in sediment transport by overland flow, especially that generated by rainfall, is to find a way to determine either τ_o or S_f and f . Therefore τ_o is calculated directly from momentum equation without S_f and f . The advantage of Eq. (143) is that it is simple, easy and dimensionless, which makes it useful in comparing the data of other researchers.

The other equations in Table 14 were not tested for predicting sediment discharge, because they are similar to these two equations, but were selected so that they could be compared with each other. In particular the model assumed by Meyer and Wischmeier (1969), Eq. (72), has almost the same coefficients as Eq. (131), which was obtained by the regression analysis of data, except that coefficient of water discharge, q , differs, because Eq. (72) is in a more general form than Eq. (131).

Rill Geometry

One of the important but poorly defined subjects in erosion study is rill-and-gully geometry. There is very little exact theoretical basis for predicting rill-and-gully geometry.

Data analysis shows that rainfall and slope are the most important variables affecting rills. Because Reynolds number includes rainfall, prediction equations with Reynolds number and slope are preferred, as before.

The relative rill surface area over total area for each run was predicted by using Eq. (193), and relative rill erosion, which means volume of rill over total volume of erosion, was predicted by Eq. (211). The predicted values for each run are listed in Table 18. The remaining selected equations in Table 14, which differ from each other only slightly, are given as possible prediction equations for different forms of rill geometry. They can be used in the same manner and for the same purpose as others which have been explained.

Comparison of measured values in Table 10 with predicted values in Table 18 shows very close agreement. Correlation between predicted and measured values is very high, with R^2 equal to .985. Both tables show that erosion loss from gullies ranges from 10 percent to 48 percent, and similarly, that relative rill surface area ranges from 18 percent to 45 percent for our experiment.

FIELD APPLICATION OF RESULTS

An objective of this study was to seek a way to develop a soil loss prediction equation that could be used in the field for a single storm, one that was simple, accurate, and supported by basic concepts of hydraulics and theory. Since selected equations in Table 14 meet these criteria any one of them could serve these purposes.

Equation (143) can be used as a first approximation of soil loss resulting from overland flow generated by a single storm. The equation can be used whenever conditions are similar or when certain modifications of the constants are made. The reasons for selecting this equation are that (1) the terms in the equation can be determined easily and without any major errors or easily obtained from meteorological stations, (2) anyone with a basic idea of hydraulics can use this equation to estimate soil loss, (3) the equation is not time-consuming, and (4) it is therefore economical to use. Moreover, this equation yields results comparable with those from the models accepted in the literature and from dimensional analysis. Knowing the Reynolds number, in including discharge, rainfall, and length of slope, decreases the possibility of major error in determining S_f , f , or τ_o .

There are, however, some limitations to its use. For instance, in the present study the equation for predicting sediment discharge was based upon data obtained only for (1) sandy disturbed soil, (2) simulated rainfall with a limited range of rainfall intensities, (3) bare, smooth surface, and (4) short distance of slope.

TABLE 14. SELECTED PREDICTION EQUATIONS WHICH ARE OBTAINED FROM NONLINEAR REGRESSION ANALYSIS AND ANALYTICAL ANALYSIS

No.	Equations	R^2	SEE	Origin[1]	Dependent variable unit[6]
1	$\bar{u} = (\frac{g}{3\nu})^{1/3} S_f^{1/3} q_o^{2/3} X^{2/3} = (\frac{g}{3\nu})^{.333} S_f^{.333} q_o^{.666} X^{.666}$			(40) ANALY.[2]	ft/sec
2	$\bar{u} = (1/e^{13.98} \nu^{1.664}) S_o^{.37526} q_o^{.64132} X^{.59211}$	.8228	.2836	(178) REG.[3]	ft/sec
3	$\bar{u} = (1/e^{2.69687}) Re^{.627} S_o^{.33598}$	.8177	.2834	(180) REG.	ft/sec
4	$C_s = e^{9.59952} \bar{u}^{.82628} S_o^{1.59977}$	.9347	.3241	(112) REG.	ppm
5	$C_s = e^{9.55318} Re^{.96315} S_o^{1.45277}$	.9224	.3674	(117) REG.	ppm
6	$q_s^* = C_s = \phi(Re, S_o, P, d_{50}/d)$			(88) ANALY.	
7	$q_s = (1/e^{9.181}) \bar{u}^{3.28437} S_o^{.42756}$	.9544	.400	(126) REG.	lb/sec/ft of width
8	$q_s = S_{TF} q^{5/3} S_o^{5/3} = S_{TF} q^{1.666} S_o^{1.666}$			(168) MODL.[4]	lb/sec/ft of width
9	$q_s = e^{11.7269} q^{2.03475} S_o^{1.66374}$	.9588	.3805	(131) REG.	lb/sec/ft of width
10	$q_s = e^{10.50448} q_o^{2.03475} S_o^{1.66374}$	.9588	.3805	(133) REG.	lb/sec/ft of width
11	$q_s = (1/e^{11.64517}) Re^{2.05403} S_o^{1.46002}$	.9517	.4119	(143) REG.	lb/sec/ft of width
12	$q_s = e^{.7441} ((\tau_o - \tau_c)\bar{u})^{1.5836}$	.9195	.5196	(155) MODL-REG.[5]	lb/sec/ft of width
13	$A_R/A_T = e^{2.35186} q_o^{.33062} S_o^{.16547}$	.9341	.0676	(189) REG.	ft^2/ft^2
14	$A_R/A_T = (1/e^{2.344968}) Re^{.33758} S_o^{.14357}$	.9406	.0142	(193) REG.	ft^2/ft^2
15	$V_R = e^{25.01813} q_o^{2.52194} S_o^{2.01617}$	.9789	.3305	(203) REG.	ft^3/hr/ft of width
16	$V_R = (1/e^{10.76525}) Re^{2.55688} S_o^{1.85121}$	.9763	.3510	(205) REG.	ft^3/hr/ft of width
17	$V_R/V_T = e^{3.98813} q_o^{48628} S_o^{.35128}$	.9532	.0925	(209) REG.	ft^3/ft^3
18	$V_R/V_T = (1/e^{2.92708}) Re^{.49654} S_o^{.31906}$	.9585	.0871	(211) REG.	ft^3/ft^3

[1] Equation number and how derived.

[2] Analytically derived equation.

[3] Regression equation.

[4] Model from literature.

[5] Assumed model which its coefficients were found by data analysis.

[6] Units which values are predicted.

Note: Units of independent variables are: S_f and S_o are in ft/ft, q_o is in ft/sec, q is in cfs/ft of width, X is in ft, e is natural logarithm base, ν is ft^2/sec, Re is dimensionless.

TABLE 15. PREDICTED MEAN LOCAL VELOCITIES OF OVERLAND FLOW GENERATED BY RAINFALL AT A GIVEN DISTANCE FOR EACH RUN FROM ANALYTICALLY OBTAINED EQUATION

(EQUATION 36: $\overline{u} = (\frac{g}{3\nu})^{1/3} S_o^{1/3} q_o^{2/3} X^{2/3}$)

Run No.	Predicted velocities, $\overline{u}$'s in ft/sec @ 3'	@ 6'	@ 12'	@ 16'
I	.050735	.08054	.127845	.15487
II	.091793	.145713	.231305	.280206
III	.134649	.213743	.3342	.411027
IV	.15940	.25304	.401674	.486593
V	.064719	.102735	.163082	.19756
VI	.112788	.17904	.284208	.34429
VII	.165225	.2622785	.41634	.50436
VIII	.195229	.30991	.49195	.59595
IX	.078657	.12486	.1982	.240107
X	.129392	.205397	.3260471	.394978
XI	.194136	.30817	.4891917	.5926135
XII	.232115	.368459	.584893	.708547
XIII	.090995	.144446	.229294	.27777
XIV	.143923	.22846	.362663	.43933
XV	.218144	.34628	.549689	.66590
XVI	.256789	.4076276	.6470685	.7838676
XVII	.106105	.16843	.267367	.323892
XVIII	.16986	.269638	.4280235	.5185135
XIX	.254009	.4032	.640063	.77538
XX	.2944	.46735	.74187	.8987
XXI	.1183187	.187819	.29814	.361176
XXII	.187458	.29757	.472365	.57223
XXIII	.280306	.44496	.70632	.85565
XXIV	.3242968	.514789	.8171769	.98994

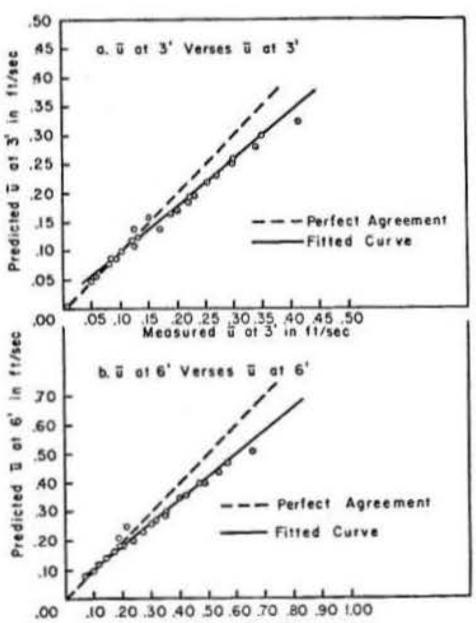

Fig. 35. Predicted velocity versus measured velocity at 3' and 6' ($\overline{u} = (g/3\nu)^{1/3} S_o^{1/3} q_o^{2/3} X^{2/3}$).

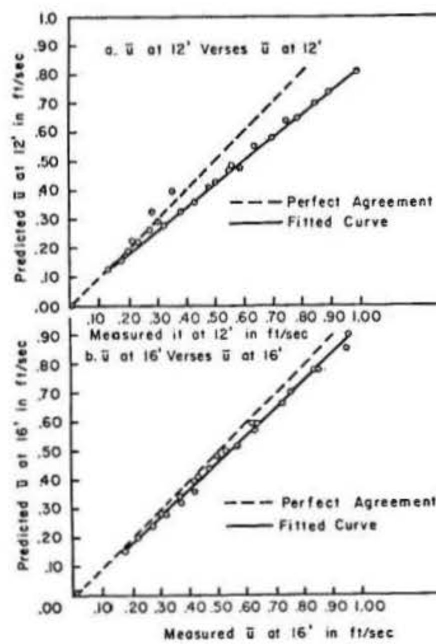

Fig. 36. Predicted velocity versus measured velocity at 12' and 16' ($\overline{u} = (g/3\nu)^{1/3} S_o^{1/3} q_o^{2/3} X^{2/3}$).

TABLE 16. PREDICTED MEAN LOCAL VELOCITIES OF OVERLAND FLOW GENERATED BY RAINFALL AT A GIVEN DISTANCE FOR EACH RUN FROM REGRESSION EQUATION

$$\text{(EQUATION 180: } \bar{u} = (1/e^{2.69687})\ Re^{.6270}\ S_o^{.33598})$$

Run No.	Predicted $\bar{u}$'s in ft/sec @ 3'	@ 6'	@ 12'	@ 16'
I	.062179	.09603	.1483	.1776
II	.1052133	.162486	.25094	.2998
III	.15065	.23262	.35924	.42984
IV	.17731	.27382	.42291	.50602
V	.07756	.11978	.18499	.22048
VI	.13027	.20118	.31069	.37178
VII	.18640	.28787	.4445	.5324
VIII	.218041	.33675	.52007	.62288
IX	.09604	.14832	.22894	.2742
X	.1481	.22877	.3530	.42312
XI	.2228	.34406	.5317	.63668
XII	.2656	.41013	.6336	.75868
XIII	.11250	.1737	.2683	.32146
XIV	.16621	.25676	.39655	.4749
XV	.25483	.3935	.60777	.72784
XVI	.29397	.4540	.70112	.8397
XVII	.131126	.2021	.3127	.37483
XVIII	.20116	.31076	.47584	.5745
XIX	.29828	.6406	.7647	.85188
XX	.337365	.52103	.80463	.9637
XXI	.14676	.22576	.34895	.41752
XXII	.22209	.34298	.52968	.6344
XXIII	.32908	.50822	.78477	.94006
XXIV	.37186	.57417	.88694	1.06225

TABLE 17. MEASURED AND PREDICTED SEDIMENT DISCHARGES BY EQUATION (143) AND EQUATION (155) RESPECTIVELY

$$\text{(EQUATION (143): } q_s = (1/e^{11.64517}\ Re^{2.05403}\ S_o^{1.46002}))$$

$$\text{(EQUATION (155): } q_s = e^{.7441}\ ((\tau_o - \tau_c)\ \bar{u})^{1.5836})$$

Run No.	Measured q_s (lb/sec/ft of width)	Predicted q_s by Equation 4-47 (lb/sec/ft of width)	Predicted q_s by Equation 4-59 (lb/sec/ft of width)
I	.000096	.0000748	.00002682
II	.00300	.0004177	.00028941
III	.000646	.0013523	.00091326
IV	.001482	.0023078	.0021299
V	.000294	.0001905	.000287033
VI	.001508	.001121	.00192952
VII	.00372	.003413	.00461508
VIII	.00548	.00564	.00718439
IX	.000548	.0004409	.000553332
X	.002974	.001902	.00317199
XI	.007138	.007088	.00768714
XII	.01288	.012408	.01426633
XIII	.000644	.0008189	.00128039
XIV	.005686	.0030232	.00480844
XV	.014904	.012038	.01185276
XVI	.02666	.019047	.01994071
XVII	.000922	.0015584	.00230314
XVIII	.01015	.006508	.00715895
XIX	.022648	.023032	.01677803
XX	.03752	.03476	.02376312
XXI	.00134	.0024687	.0036737
XXII	.013096	.009749	.01048956
XXIII	.0370	.035356	.0237778
XXIV	.06508	.05276	.03541768

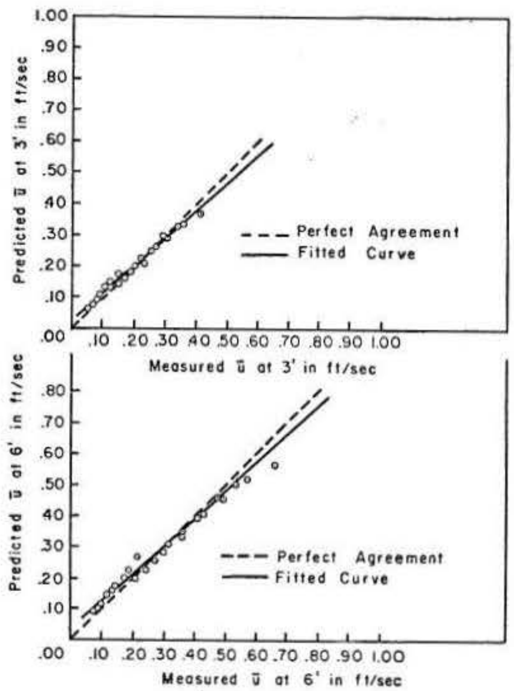

Fig. 37. Predicted velocity versus measured velocity at 3' and 6' ($\bar{u} = (1/e^{2.697})\ Re^{.627}\ S_o^{.336}$).

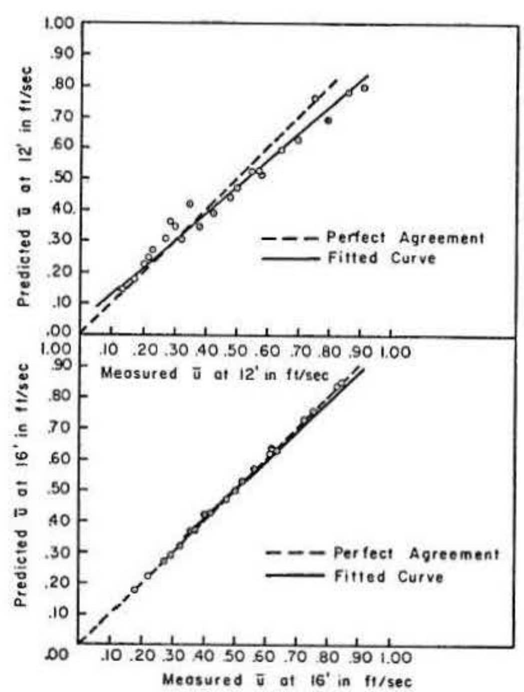

Fig. 38. Predicted velocity versus measured velocity at 12' and 16' ($\bar{u} = (1/e^{2.697})\ Re^{.627}\ S_o^{.336}$).

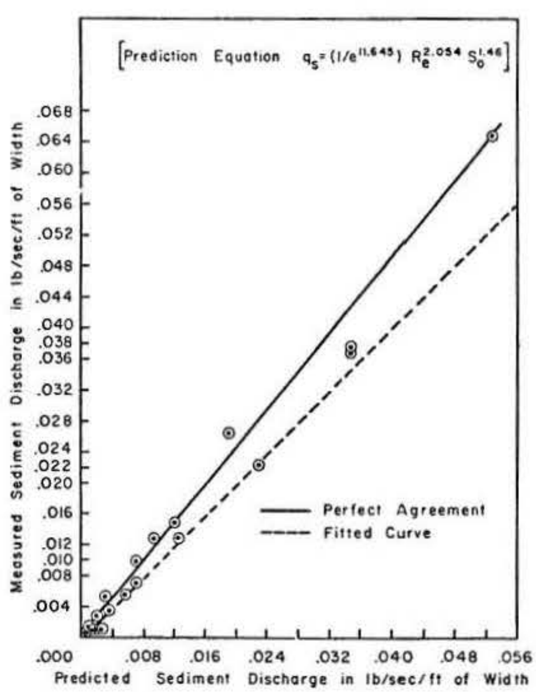

Fig. 39. Relationship between measured and predicted sediment discharges (prediction equation: $q_s = (1/e^{11.645})\ S_o^{1.46}$).

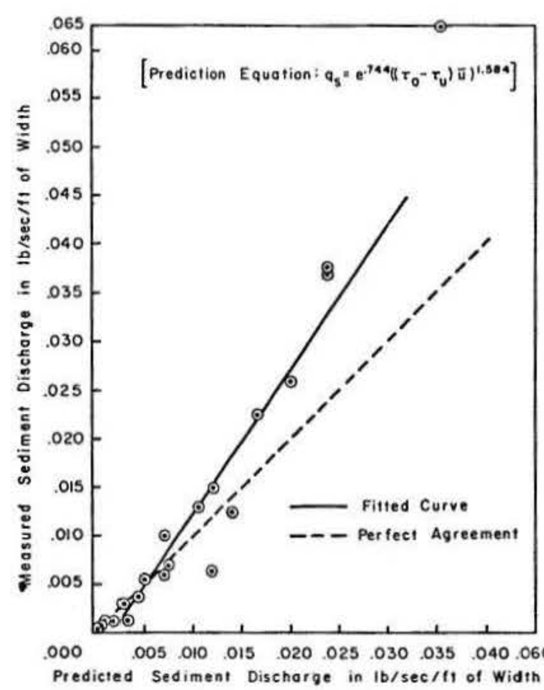

Fig. 40. Relationship between measured and predicted sediment discharges (prediction equation: $q_s = e^{.744}\ ((\tau_o - \tau_c)\ \bar{u})^{1.584}$).

TABLE 18. PREDICTION OF RILL GEOMETRY

(EQUATION (193): $A_R/A_T = (1/e^{2.344968})\ Re^{.33759}\ S_o^{.14357})$

(EQUATION (209): $V_R/V_T = (1/e^{2.92708})\ Re^{.49654}\ S_o^{.31906})$

Run No.	A_R/A_T (predicted by Equation (211)	V_R/V_T (predicted by Equation (193)
I	.17887	.0991
II	.23709	.14999
III	.287852	.19953
IV	.3143	.227046
V	.19678	.12116
VI	.26069	.18325
VII	.3163	.243522
VIII	.34418	.27575
IX	.21795	.14711
X	.2753	.20743
XI	.34304	.286675
XII	.3770	.329365
XIII	.2349	.16942
XIV	.28983	.23078
XV	.36473	.32362
XVI	.393904	.36241
XVII	.25132	.1955
XVIII	.3163	.27415
XIX	.3910	.3745
XX	.41785	.4129
XXI	.26365	.216377
XXII	.33006	.3011
XXIII	.4080	.411122
XXIV	.43564	.45291

CONCLUSION

The main objectives of this research were to study the mechanics of soil erosion from overland flow generated by simulated rainfall, to study the most important factors affecting soil erosion, and to develop a soil-loss prediction equation.

Experiments were conducted and data collected for sediment concentration, surface velocity of overland flow, water discharge, water temperature, infiltration rate, bulk density of surface soil, slope, intensity of rainfall, and rill geometry. The eroded sediments collected were dried, weighed, and sieved for grain-size distribution.

The results and conclusions of this study involve the limitations of the use of (1) sandy distrubed soil, (2) Reynolds number to 130, (3) intensity of simulated rainfall ranging from 1.25 in. to 4.60 in. per hour, (4) slopes ranging from 5.7 to 40 percent, (5) flume dimensions of 4'x5'x16', and (6) steady, spatially varied flow under constant uniform rainfall and infiltration.

The major conclusions are summarized below:

1. Longitudinal mean local velocity of spatially varied, steady overland flow can be predicted in terms of viscosity, gravitational acceleration, friction slope, rainfall excess, and length of run. The derived equation is:

$$\bar{u} = \left(\frac{g}{3\nu}\right)^{.333} S_f^{.333}\ q_o^{.666}\ X^{.666}$$

The regression equation obtained from data analysis is:

$$\bar{u} = \left(1/e^{13.98}\ \nu^{1.664}\right) S_o^{.375}\ q_o^{.64}\ X^{.59}\ .$$

The derived and regression equations were comparable. Hence, it was concluded that a parabolic vertical velocity profile and Newton's law of viscosity were applicable for spatially varied, steady overland flow under rainfall with a low Reynolds number.

2. The boundary shear stress, τ_o, can be approximated from the momentum equation of overland flow under rainfall by the numerical method.

3. The dimensionless form of the sediment-transport equation was found to be a function of Reynolds number, slope, porosity, and roughness characteristics, as follows:

$$C_s = \emptyset\left(Re,\ S_o,\ P,\ \frac{d_{50}}{d}\right)\ .$$

4. Reynolds number and slope were found to be the most important parameters in sediment transport. The prediction equation developed from the regression of data is:

$$q_s = \left(1/e^{11.65}\right) Re^{2.05}\ S_o^{1.46}\ .$$

Sediment discharge increased with the square of Reynolds number, Re , and an almost 3/2-power of the slope.

5. It was concluded that stream power, $\tau_o\,\bar{u}$, gives better prediction of sediment discharge than

boundary shear, τ_o , alone. The model derived from regression analysis of the data is:

$$q_s = e^{.744} \left(\left(\tau_o - \tau_c\right) \bar{u} \right)^{1.584} .$$

6. Analysis indicates that sediment discharge increases the square of water discharge, q , and 5/3 power of the slope. This model was comparable to that used by Meyer and Wischmeier (1969).

The regression equation is:

$$q_s = e^{11.727} q^{2.035} S_o^{1.664} ;$$

Meyer and Wischmeier's model is:

$$q_s = S_{TF} q^{5/3} S_o^{5/3} = S_{TF} q^{1.666} S_o^{1.666} .$$

7. It was concluded that velocity, slope and rainfall intensity were the most important factors affecting soil erosion and sediment transport. Velocity was found to be important not only in sediment transport, but also in determining the boundary shear and the stream power of the flow. Although tractive force is an important factor in the overland flow phenomena, it has proved very difficult to measure in the field or in the laboratory. Therefore, regression equations with easily measurable quantities, such as slope, water discharge, rainfall excess, and fluid viscosity, were preferred for predicting sediment discharge. Slope and Reynolds number, $Re = \frac{q_o X}{\nu}$, became the dominant parameters for the sediment-transport prediction equations.

8. Sediment discharge increased by 3.625 (7/2) power of the mean local velocity of overland flow and almost the square of rainfall excess (2.13). Velocity increased with 2/3 power of the Reynolds number, rainfall excess, and water discharge.

9. Reynolds number, rainfall excess, and water discharge each had the same significance and influence on mean velocity of overland flow and on sediment transport from overland flow.

10. The relative surface area of rills was changed by approximately 1/e power of rainfall excess, water discharge, and Reynolds number, and .16 power of slope.

11. The relative volume of rills was changed by 1/2 power of rainfall excess and water discharge, .54 power of Reynolds number, and approximately 1/3 power of slope.

12. The volume or rills was increased by 2.52 power of rainfall excess and water discharge, and 2.64 power of Reynolds number and square of slope.

FUTURE STUDY

In the future, similar research should be carried on with different types of undisturbed soil and with varying length of slope and larger intensities of simulated rainfall approximating more closely natural rainfall. Roughness properties of different soil types and the resistance they offer to overland flow under rainfall should be studied more comprehensively. Roughness of soil surface should be defined and a representative index of roughness found. With better facilities, conditions, and methods, an attempt should be made to measure more τ_o and velocities with respect to distance. Also, S_f and f should be evaluated from τ_o and the velocity change; then S_f and f should be related to rainfall intensity, slope, and roughness characteristics of the soil.

Better criteria for defining the laminar and turbulence flow under rainfall over mobile bed should be found. Further, analytical analysis should be done and experiments made on turbulence flow; when results should be compared with the results of data analysis and laminar flow. The overall conclusions should be checked by field study or field data, and the final developed erosion-loss prediction equation should be applied to situations in the field.

Both theoretical framework and equations should be developed for most general conditions of overland-flow erosion under rainfall. In addition to concepts from hydraulics and fluid mechanics, concepts from stochastic statistics should, wherever necessary, be used.

To test the effect of vegetation on soil erosion, a different type and density of vegetation should be used on various slopes under varying rainfall. The hydraulic properties of vegetation on roughness and velocity should be studied. The prediction equation should include the roughness characteristics of soil and the effects of vegetation.

Because it is impossible to have sheet erosion alone, rill and gully erosion should be studied simultaneously. After flow concentration, small microchannels (rills) start developing, and these rills begin forming gullies. The mechanics of rill and gully formation and all associated erosion should be studied and understood.

APPENDIX

EFFECT OF VEGETAL COVER ON EROSION LOSS

Four runs were made with a 40 percent slope partially covered with winter wheat (approximately 40 percent of the area). Data collected from these runs included sediment concentration, sediment discharge, and water discharge. It was found that this type and amount of cover reduced erosion between 38 percent and 78 percent with rainfall intensities of 1.25 to 4.60 in. per hour. The effect of the vegetal cover as an erosion-retarding agent decreased as rainfall intensity increased. Data from these runs was used only for qualitative comparison (see Tables A-1 and A-2).

Vegetal cover affects erosion loss in two ways: (1) it dissipates raindrop impact energy and intercepts rainfall, and (2) it reduces the area exposed to erosion. Moreover, it reduces erosion loss in indirect ways; for instance, the roots tend to bind soil particles and the stems to hide eroded particles. If soil particles are uniformly distributed, the hiding factor is unity, as Einstein (1950) suggested. However, vegetal cover will increase the hiding factor even if the particles are uniform.

If the soil surface is covered by vegetation, raindrops will first strike the vegetation and then will start flowing downhill; therefore, both splash erosion from the impact and the turbulence effect of the raindrops will be reduced significantly. Vegetal cover increases resistance to overland flow and depth of flow; boundary shear may also increase with depth. Though it would appear that increasing boundary shear would increase erosion loss, it does not. Boundary shear alone is not a good criterion for erosion loss, since an increase in boundary shear is accompanied by a decrease in velocity and may be accompanied by a decrease in stream power; velocity used with boundary shear is a better criterion. Moreover, since less area is exposed to shear effect in the presence of vegetal cover than from a bare area, net erosion loss is less.

Figure A-1 shows that increasing rainfall intensity reduces the erosion-retardation effect of vegetal cover by decreasing the relative effect of vegetal cover on impact energy, flow resistance, and flow velocity. Vegetal cover decreases erosion, but the rate of decrease depends on the type and density of the vegetal cover as well as the intensity of rainfall.

Figure A-2 shows averaged sediment concentration, C_s, from vegetated surface and bare surface at 40 percent slope with varying intensities of rainfall.

TABLE A-1. DATA FROM VEGETATED SURFACE RUNS

Slope (%)	Rainfall Intensity (in/hr)	C_s (ppm)	q_s (lb/sec/ft)	q (cfs)	q (cfs/ft)	q_o (ft/sec)	Temp (C°)	$\nu \times 10^5$ (L^2/t)	Re (q/ν)
40	1.25	9399.3	.000094	.00080	.0016	.00001	18	1.39	11.15
40	2.25	83464.98	.003148	.00306	.000601	.000038	18	1.39	42.0
40	3.65	165815.6	.00829	.0040	.00080	.000050	18	1.39	57.2
40	4.60	2237600.5	.02236	.0080	.0016	.00010	18	1.39	11.5

TABLE A-2. COMPARISON BETWEEN VEGETATION AND BARE SOIL

Slope (%)	Rainfall Intensity (in/hr)	C_s, vegetated soil (ppm)	C_s, bare soil (ppm)	Difference ΔC_s	Erosion decreased (%)
40	1.25	9399.30	44149	34749.7	78.71
40	2.25	83464.98	207585	124120	59.79
40	3.65	165815.6	313749	147933.4	47.15
40	4.60	223760.5	355885	132124.5	37.126

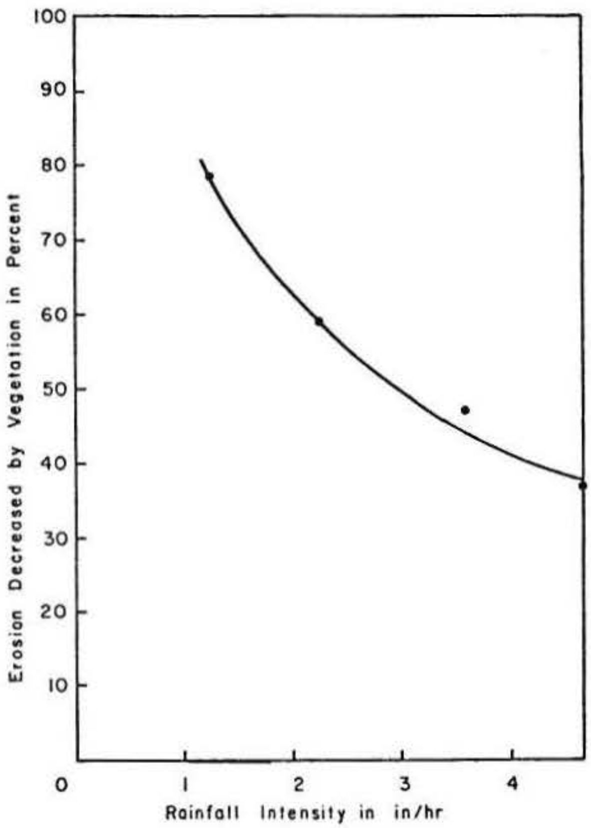

Fig. A-1. Relationship between percentage of erosion decreased by vegetation and rainfall intensity on 40 percent slope (40 percent surface is covered with 3-4 inch high winter wheat.

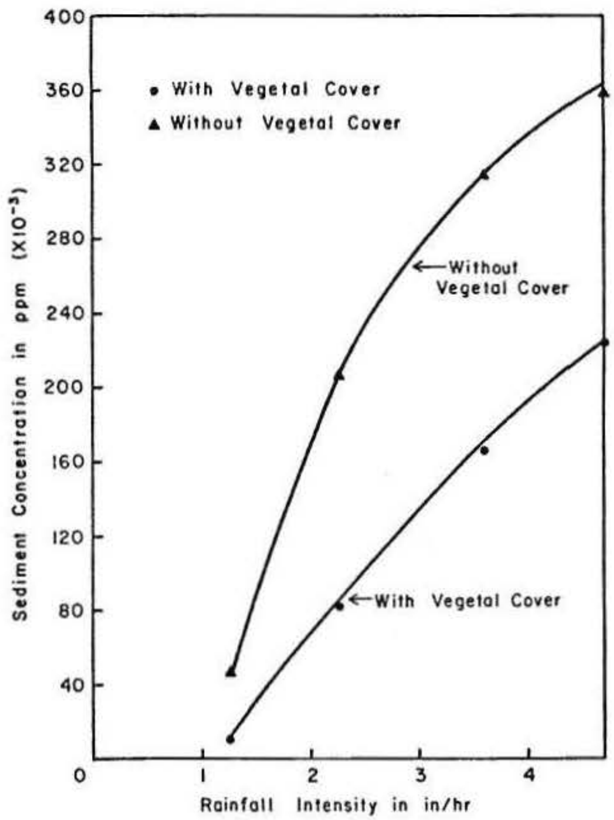

Fig. A-2. Relationship between sediment concentration and rainfall intensity (with and without vegetal cover on 40 percent slope).

REFERENCES

Albertson, M. L., Barton, J. R., and Simons, D. B., 1965, Fluid mechanics for engineers, Fifth Printing: Prentice-Hall, Inc., N. J., 564 p.

Bagnold, R. A., 1966, An approach to the sediment transport problem from general physics: Geological Survey Professional Paper 422-I, 37 p.

Baver, L. D., 1965, Soil physics, Third Ed., Fifth Printing: John Wiley and Sons, Inc., New York, London, Sydney, 489 p.

Behlke, C. E., 1957, The mechanics of overland flow: Ph.D. dissertation, Stanford University.

Borst, H. L., and Woolburn, R., 1940, Rain simulator studies of effect of slope on erosion and runoff: U.S.D.A. Soil Conservation Service, SCS-TP-36, 30 p.

Chen, C. L., 1962, An analysis of overland flow: Ph.D. dissertation, Michigan State University, East Lansing, Mich.

Chen, C. L., and Chow, V. T., 1968, Hydrodynamics of mathematically simulated surface runoff: Civil Engineering Studies, Hydraulic Engineering Series No. 18, Dept. of Civil Engineering, University of Illinois, Urbana, Ill., 132 p.

Chen, C. L., and Hansen, V. E., 1966, Theory and characteristics of overland flow: Trans. Am. Soc. of Agricultural Engineers, Vol. 9, No. 1, pp. 20-26.

Chow, V. T., and Harbaugh, T. E., 1965, Raindrop production for laboratory watershed experimentation: J. Geophysical Research, Vol. 70, No. 24, pp. 6111-6119.

Colby, B. R., 1964, Discharge of sands and mean-velocity relationships in sand-bed streams: U.S. Geol. Survey Prof. Paper 462-A.

Du Boys, P., 1879, Études du régime du Phône et l'action exercee' par les eaux sur un lit a fond de graviers indefiniment affouillable: Annales des ponts et Chaussees, Ser. 5, 18, 141-95 (Cited by Raudkivi, A. J., 1967, Loose boundary hydraulics: Pergammon Press, New York, London, Sydney, 330 p.).

Duley, F. L., and Hays, O. E., 1932, The effect of the degree of slope on runoff and soil erosion: J. Agricultural Research, Vol. 45, No. 6, pp. 349-360.

Einstein, H. A., 1950, The bed-load function for sediment transportation in open channel flows: U.S. Dept. of Agriculture, Soil Conservation Service, Washington, D. C., Tech. Bulletin No. 1026.

Ellison, W. D., 1944, Studies of raindrop erosion: Agricultural Engineering, Vol. 25, No. 4, pp. 131-136, and Vol. 25, No. 5, pp. 181-182.

Ellison, W. D., 1945, Some effects of randrops and surface-flow on soil erosion and infiltration: Trans., Am. Geophys. Union, Vol. 26, No. 3, pp. 415-429.

Ellison, W. D., 1947, Soil erosion studies: Agricultural Engineering, Vol. 28, pp. 145-146, 197-201, 245-248, 297-300, 349-351, 402-405, 442-444.

Emmett, W. W., 1970, The hydraulics of overland flow on hillslopes: U.S. Geol. Survey Prof. Paper 662-A, 68 p.

Favre, H., 1933, Contribution à l'étude des courants liquides (Contribution to the study of flow of liquid), Dunod, Paris, (Cited by Ven Te Chow, Open Channel Hydraulics: McGraw-Hill Book Company, Inc., New York, 1959, p. 327).

Grace, R. A., and Eagleson, P. S., 1965, Similarity criteria in the surface runoff process: M.I.T. Dept. of Civil Engineering, Hydrodynamics Lab. Rept. 77.

Grace, R. A., and Eagleson, P. S., 1966, The modeling of overland flow: J. Water Resources Research, Vol. 2, No. 3, pp. 393-403.

Graf, Walter Hans, 1971, Hydraulics of sediment transport: McGraw-Hill Book Co., Inc., New York, 513 p.

Henderson, F. M., and Wooding, R. A., 1964, Overland flow and groundwater flow from a steady rainfall of finite duration: J. Geophysical Research, Vol. 69, No. 8, pp. 1531-1540.

Hinds, J. 1926, Side channel spillways; Hydraulic theory, economic factors, and experimental determination of losses: Trans., Am. Soc. of Civil Engineers, Vol. 89, pp. 881-927.

Holland, M. E., 1969, Colorado State University experimental rainfall-runoff facility: Colorado State University Experiment Station, Ft. Collins, Colorado, CER 69-70 MEH 21, 81 p.

Horner, W. W., and Jens, S. W., 1942, Surface runoff determination from rainfall without using coefficients: Trans., Am. Soc. of Civil Engineers, Vol. 107, pp. 1039-1117.

Horton, R. E., 1938, Interpretation and application of runoff plot experiments with reference to soil erosion problems: Proceedings, Soil Science Society of America, Vol. 3, pp. 340-349.

Huff, D. D., and Kruger, P., 1967, The chemical and physical parameters in a hydrologic transport model for radioactive aerosol: Proceedings, the International Hydrology Symposium, Ft. Collins, Colorado, Vol. 1, Paper No. 17, pp. 128-135.

Izzard, C. F., and Augustine, M. T., 1943, Preliminary report on analysis of runoff resulting from simulated rainfall on a paved plot: Trans., Am. Geophys. Union, Vol. 24, pp. 500-509.

Izzard, C. F., 1944, The surface-profile of overland flow: Trans., Am. Geophys. Union, Pt. VI, pp. 559, 968.

Kalinske, A. A., 1947, Movement of sediment as bed in rivers: Trans., Am. Geophys. Union, Vol. 28, pp. 615-620.

Keulegan, G. H., 1944, Spatially variable discharge over a sloping plane: Trans., Am. Geophys. Union, Pt. VI, pp. 956-959.

Kilinc, MustaFa Yilmaz, 1972, Mechanics of soil erosion from overland flow generated by simulated rainfall. Colorado State University. Hydrology Paper No. , p., illus.

Kisisel, I. T., 1971, An experimental investigation of the effect of rainfall on the turbulence characteristics of shallow flow: Ph.D. dissertation, Purdue University, Lafayette, Ind.

Langhaar, H. L., 1967, Dimensional analysis and theory of models: 8th Printing, John Wiley and Sons, Inc., New York, London, Sydney, 166 p.

Laursen, E. M., 1958, The total sediment load of stream: J. Hydraulics Division, Proceedings of the Am. Soc. of Civil Engineers, Vol. 84, No. HY1.

Laws, J. O., 1941, Measurements of the fall velocity of waterdrops and raindrops: Trans., Am. Geophys. Union, Vol. 22, pp. 709-721.

Laws, J. O., and Parsons, D. A., 1943, Relation of raindrop-size to intensity: Trans., Am. Geophys. Union, Vol. 24, pp. 452-460.

Li, R. M., 1972, Effect of rainfall on sheet flow: M. S. Thesis, Colorado State University, Ft. Collins, Colorado.

Liggett, J. A., 1959, Unsteady open channel flow with lateral inflow. Tech. Rept. 2, Dept. of Civil Engineering, Stanford University.

MacDougall, C. H., 1934, Bed-sediment transportation in open channels: Trans., Am. Geophys. Union, Vol. 15, pp. 491-495.

Meyer, L. D., and Monke, E. J., 1965, Mechanics of soil erosion by rainfall and overland flow: Trans. of the Am. Soc. of Agricultural Engineers, Vol. 8, No. 4, pp. 572-577, 580.

Meyer, L. D., 1971, Soil erosion by water on upland areas: River Mechanics, Vol. 2, Edited and published by H. W. Shen, P.O. Box 606, Ft. Collins, Colorado, USA, 80521, Chap. 27, 25 p.

Meyer, L. D., and Wischmeier, W. H., 1969, Mathematical simulation of the process of soil erosion by water: Trans. of the Am. Soc. of Agricultural Engineers, Vol. 12, pp. 754-758, 762.

Meyer-Peter, E., and Muller, R., 1948, Formulae for bed-load transport: Proc. 2nd Meeting IAHR, Stockholm, pp. 39-64.

Morgali, J. R., 1963, Hydraulic behavior of small drainage basins: Dept. of Civil Engineering, Stanford University, Stanford, Calif., Technical Report No. 3.

Musgrave, G. W., 1947, The quantitative evaluation of factors in water erosion, a first approximation: J. Soil and Water Conservation, Vol. 2, pp. 133-138.

Neal, J. H., 1937, The effect of the degree of slope and rainfall characteristics on runoff and soil erosion: Missouri Agr. Exp. Sta. Research Bull. 280.

Nordin, C. F., and Richardson, E. V., 1971, Instrumentation and measuring techniques: River Mechanics, Vol. 1, Edited and published by H. W. Shen, P. O. Box 606, Ft. Collins, Colorado, USA, 80521, Chap. 14, 38 p.

Parson, D. A., 1949, Depths of overland flow: Soil Conservation Service, Technical Paper 82.

Ree, W. O., 1939, Some experiments on shallow flows over a grassed slope: Trans., Am. Geophys. Union, Vol. 20, pp. 653-656.

Ree, W. O., 1949, Hydraulic charactersitics of vegetation for vegetated waterways: Agricultural Engineering, Vol. 31, pp. 184-187, 189.

Robertson, A. F., et al., 1964, Runoff from impervious surfaces under conditions of simulated rainfall: Trans. of the Am. Soc. of Agricultural Engineers, Vol. 9, No. 3, pp. 343-346.

Schoklitsch, A., 1934, Der Geschiebetrieb und Geschiebefracht: Wasserkraft und Wasserwirtschaft, p. 37, (Cited by Raudkivi, A. J., 1967, Loose boundary hydraulics: Pergamon Press, New York, London, Sydney, 330 p.).

Schwab, G. O., et al., 1966, Soil and water conservation engineering: Second Ed., John Wiley and Sons, Inc., New York, London, Sydney, 683 p.

Smerdon, E. T., and Beasley, R. P., 1961, Critical tractive forces in cohesive soils: Agricultural Engineering, Vol. 42, No. 1, pp. 26-29.

Smith, D. D., and Wischmeier, W. H., 1962, Rainfall erosion: Advances in Agronomy, Academic Press, Inc., New York, Vol. 14, pp. 109-148.

Soil Conservation Society of America, 1952, Soil and water conservation glossary: J. Soil and Water Conservation, Vol. 7, No. 3, pp. 144-146.

Task Committee on Preparation of sedimentation Manual, Committee on Sedimentation, 1965, Sediment transportation mechanics; Nature of sedimentation problems: J. Hydraulics Division, Proceedings of the Am. Soc. of Civil Engineers, Vol. 91, No. HY2, pp. 251-266.

Wischmeier, Walter H., 1959, A rainfall erosion index for a universal soil loss equation: Proceedings, Soil Science Society of America, Vol. 23, pp. 246-249.

Woo, D. C., 1956, Study of overland flow: Ph.D. dissertation, University of Michigan, Mich.

Wooding, R. A., 1965, A hydraulic model for the catchment-stream, problem I. Kinematic wave theory: J. Hydrology, Vol. 3, pp. 254-267.

Woolhiser, D. A., and Liggett, J. A., 1967, Unsteady, one-dimensional flow over a plane - the rising hydrograph: J. Water Resources Research, Vol. 3, No. 3, pp. 753-771.

Woolhiser, D. A., 1969, Overland flow on a converging surface: Trans. of the Am. Soc. of Agricultural Engineers, Vol. 12, No. 4, pp. 460-462.

Yoon, Y. N., and Wensel, H. G., 1971, Mechanics of sheet flow under simulated rainfall: J. Hydraulics Division, Proceedings of the Am. Soc. of Civil Engineers, Vol. 97, No. HY9, pp. 1367-1401.

Yu, Y. S., and McNown, J. S., 1963, Runoff from impervious surfaces: U.S. Army Engineer Waterways Experiment Station, Corps of Engineers, Contract Rept. No. 2-66.

Zingg, A. W., 1940, Degree and length of land slope as it affects soil loss in runoff: Agricultural Engineering, Vol. 21, pp. 59-64.

KEY WORDS: Soil erosion, sedimentation, overland flow, sheet erosion.

ABSTRACT: Six different slopes and four different rainfall intensities were used. Momentum and continuity equations for steady, spatially varied overland flow were derived; boundary shear stress calculated and longitudinal mean-velocity equation derived and tested. Dimensional analysis was performed on all the variables, and data were analyzed by computer. Sediment transport models from dimensional analysis, data analysis, and analytical approaches were similar. Equations suitable for predicting sediment yield in the laboratory, or as first approximations in the field, were developed. Velocity, slope, and rainfall intensity were the important variables. Slope and Reynolds number proved dominant parameters.

KEY WORDS: Soil erosion, sedimentation, overland flow, sheet erosion.

ABSTRACT: Six different slopes and four different rainfall intensities were used. Momentum and continuity equations for steady, spatially varied overland flow were derived; boundary shear stress calculated and longitudinal mean-velocity equation derived and tested. Dimensional analysis was performed on all the variables, and data were analyzed by computer. Sediment transport models from dimensional analysis, data analysis, and analytical approaches were similar. Equations suitable for predicting sediment yield in the laboratory, or as first approximations in the field, were developed. Velocity, slope, and rainfall intensity were the important variables. Slope and Reynolds number proved dominant parameters.

KEY WORDS: Soil erosion, sedimentation, overland flow, sheet erosion.

ABSTRACT: Six different slopes and four different rainfall intensities were used. Momentum and continuity equations for steady, spatially varied overland flow were derived; boundary shear stress calculated and longitudinal mean-velocity equation derived and tested. Dimensional analysis was performed on all the variables, and data were analyzed by computer. Sediment transport models from dimensional analysis, data analysis, and analytical approaches were similar. Equations suitable for predicting sediment yield in the laboratory, or as first approximations in the field, were developed. Velocity, slope, and rainfall intensity were the important variables. Slope and Reynolds number proved dominant parameters.

KEY WORDS: Soil erosion, sedimentation, overland flow, sheet erosion.

ABSTRACT: Six different slopes and four different rainfall intensities were used. Momentum and continuity equations for steady, spatially varied overland flow were derived; boundary shear stress calculated and longitudinal mean-velocity equation derived and tested. Dimensional analysis was performed on all the variables, and data were analyzed by computer. Sediment transport models from dimensional analysis, data analysis, and analytical approaches were similar. Equations suitable for predicting sediment yield in the laboratory, or as first approximations in the field, were developed. Velocity, slope, and rainfall intensity were the important variables. Slope and Reynolds number proved dominant parameters.

Mechanics of Soil Erosion From Overland Flow
Generated by Simulated Rainfall

Mustafa Yilmaz Kilinc
Hydrology Paper #63
Colorado State University

Mechanics of Soil Erosion From Overland Flow
Generated by Simulated Rainfall

Mustafa Yilmaz Kilinc
Hydrology Paper #63
Colorado State University

Mechanics of Soil Erosion From Overland Flow
Generated by Simulated Rainfall

Mustafa Yilmaz Kilinc
Hydrology Paper #63
Colorado State University

Mechanics of Soil Erosion From Overland Flow
Generated by Simulated Rainfall

Mustafa Yilmaz Kilinc
Hydrology Paper #63
Colorado State University

LIST OF PREVIOUS 25 PAPERS

No. 38 Evaluation of the Effect of Impoundment on Water Quality in Cheney Reservoir, by J. C. Ward and S. Karaki, March 1970.

No. 39 The Kinematic Cascade as a Hydrologic Model, by David F. Kibler and David A. Woolhiser, February 1970.

No. 40 Application of Run-Lengths to Hydrologic Series, by Jaime Saldarriaga and Vujica Yevjevich, April 1970.

No. 41 Numerical Simulation of Dispersion in Groundwater Aquifers, by Donald Lee Reddell and Daniel K. Sunada, June 1970.

No. 42 Theoretical Probability Distribution for Flood Peaks, by Emir Zelenhasic, December 1970.

No. 43 Flood Routing Through Storm Drains, Part I, Solution of Problems of Unsteady Free Surface Flow in a Storm Drain, by V. Yevjevich and A. H. Barnes, November 1970.

No. 44 Flood Routing Through Storm Drains, Part II, Physical Facilities and Experiments, by V. Yevjevich and A. H. Barnes, November 1970.

No. 45 Flood Routing Through Storm Drains, Part III, Evaluation of Geometric and Hydraulic Parameters, by V. Yevjevich and A. H. Barnes, November 1970.

No. 46 Flood Routing Through Storm Drains, Part IV, Numerical Computer Methods of Solution, by V. Yevjevich and A. H. Barnes, November 1970.

No. 47 Mathematical Simulation of Infiltrating Watersheds, by Roger E. Smith and David A. Woolhiser, January 1971.

No. 48 Models for Subsurface Drainage, by W. E. Hedstrom, A. T. Corey and H. R. Duke, February 1971.

No. 49 Infiltration Affected by Flow of Air, by David B. McWhorter, May 1971.

No. 50 Probabilities of Observed Droughts, by Jaime Millan and Vujica Yevjevich, June 1971.

No. 51 Amplification Criterion of Gradually Varied, Single Peaked Waves, by John Peter Jolly and Vujica Yevjevich, December 1971.

No. 52 Stochastic Structure of Water Use Time Series, by Jose D. Salas-La Cruz and Vujica Yevjevich, June 1972.

No. 53 Agricultural Response to Hydrologic Drought, by V. J. Bidwell, July 1972.

No. 54 Loss of Information by Discretizing Hydrologic Series, by Mogens Dyhr-Nielsen, October 1972.

No. 55 Drought Impact on Regional Economy, by Jaime Millan, October 1972.

No. 56 Structural Analysis of Hydrologic Time Series, by Vujica Yevjevich, November 1972.

No. 57 Range Analysis for Storage Problems of Periodic-Stochastic Processes, by Jose Salas-La Cruz, November 1972.

No. 58 Applicability of Canonical Correlation in Hydrology, by Padoong Torranin, December 1972.

No. 59 Transposition of Storms, by Vijay Kumar Gupta, December 1972.

No. 60 Response of Karst Aquifers to Recharge, by Walter G. Knisel, December 1972.

No. 61 Drainage Design Based Upon Aeration, by Harold R. Duke, June 1973.

No. 62 Techniques for Modeling Reservoir Salinity, by John Hendrick, August 1973.